*Manuscript
Click here to download Manuscript: Text.docx Click here to view linked References

Discovery of first-in-class multi-target adenosine A_{2A} receptor antagonists-carbonic anhydrase IX and XII inhibitors. 8-Amino-6-aryl-2-phenyl-1,2,4-triazolo[4,3-a]pyrazin-3-one derivatives as new potential antitumor agents

Costanza Ceni,[a] Daniela Catarzi,[a] Flavia Varano,[a] Diego Dal Ben,[b] Gabriella Marucci,[b] Michela Buccioni,[b] Rosaria Volpini,[b] Andrea Angeli,[a] Alessio Nocentini,[a,c] Paola Gratteri,[a] Claudiu T. Supuran,[a] Vittoria Colotta[a*]

[a]*Dipartimento di Neuroscienze, Psicologia, Area del Farmaco e Salute del Bambino, Sezione di Farmaceutica e Nutraceutica, Università degli Studi di Firenze, Via Ugo Schiff, 6, 50019 Sesto Fiorentino, Italy.*

[b]*Scuola di Scienze del Farmaco e dei Prodotti della Salute, Università degli Studi di Camerino, Via S. Agostino 1, 62032 Camerino (MC), Italy.*

[c]*Dipartimento di Neuroscienze, Psicologia, Area del Farmaco e Salute del Bambino, Sezione di Farmaceutica e Nutraceutica, Laboratorio di Molecular Modeling, Cheminformatics & QSAR, Università degli Studi di Firenze, Via Ugo Schiff, 6, 50019 Sesto Fiorentino, Italy.*

Key words: multi-target agents, 1,2,4-triazolo[4,3-*a*]pyrazin-3-one, adenosine A_{2A} receptor antagonists, carbonic anhydrase inhibitors, anticancer agents

Abstract

This paper describes identification of the first-in-class multi-target adenosine A_{2A} receptor antagonists-carbonic anhydrase (CA) IX and XII inhibitors, as new potential antitumor agents. To obtain the multi-acting ligands, the 8-amino-2,6-diphenyltriazolo[4,3-a]pyrazin-3-one, a potent adenosine hA_{2A} receptor (AR) antagonist, was taken as lead compound. To address activity against the tumor-associated CA isoforms, it was modified by introduction of different substituents (OH, COOH, CONHOH,SO_2NH_2) on the 6-phenyl ring or on a phenyl pendant connected to the former through different spacers. Among the new triazolopyrazines **1-23**, the most active were those featuring the sulfonamide residue. Derivative **20**, featuring a 4-sulfonamidophenyl residue attached through a $CONH(CH_2)_2CONH$ spacer at the para-position of the 6-phenyl ring, showed the best combination of activity at the three targets. In fact, it inhibited both the tumor-associated hCA IX and XII isozymes at nanomolar concentration (K_i= 5.0 and 27.0 nM), and also displayed a quite good affinity for the hA_{2A} AR (K_i= 108 nM). Compound **14**, bearing the 4-sulfonamidophenyl residue linked at the para-position of the 6-phenyl ring by a CONH spacer, was remarkable because both its hA_{2A} AR affinity and hCA XII inhibitory potency were in the low nanomolar range (K_i= 6.4 and 6.2 nM, respectively). Molecular docking studies highlighted the interaction mode of selected triazolopyrazines in the hA_{2A} AR recognition pocket and in the active site of hCA II, IX and XII isoforms.

1. Introduction

The multi-target approach has become an increasingly pursued strategy for the cure of different pathologies. In fact, a single-target therapy can be inadequate to obtain a satisfying therapeutic effect in complex diseases linked to the dysfunction of several biological targets [1]. The multi-target approach can be achieved either through combination of several drugs, administered in association or present in the same formulation, or by combining in the same molecule the capability to interact with the targets of interest. This latter strategy makes it possible to overcome various drawbacks, such as possible differences regarding pharmacokinetics of each component and the drug-drug interactions.

The design of multi-targeted drugs as anticancer agents has attracted much attention since several aberrant endogenous molecules and pathways can concur in the development and progression of cancer. Thus, simultaneous intervention on two or more targets can be useful for solving limited efficiencies, poor safety and, importantly, resistance profiles of a single-targeted drug [1].

In the last two decades, several studies have pointed out that the adenosine A_{2A} receptor and the carbonic anhydrase (CA) IX and XII isoforms can be useful targets for antineoplastic drugs [2-9].

Under physiological conditions, extracellular adenosine concentration is in the nanomolar order but it rises to the micromolar range when inflammation and hypoxia occur [2,3]. Hypoxic conditions are typical of many types of solid tumors and lead to the production of ATP, a danger signal released from surrounding cells, both cancer and healthy, following metabolic stress [10]. ATP is rapidly dephosphorylated by the ecto-nucleotidases CD39 and CD73, which are upregulated by hypoxia. CD73 transforms AMP into adenosine that elicits its effects through activation of four G-protein-coupled receptors, classified as A_1, A_{2A}, A_{2B} and A_3 subtypes [3]. A_1 and A_3 adenosine receptor (AR) are coupled with Gi, Gq and Go proteins, while A_{2A} and A_{2B} subtypes with Gs or Golf. AR activation increases (A_1, A_3) or decreases (A_{2A} and A_{2B}) cAMP intracellular levels but it also modulates other intracellular pathways implicated in cell growth and proliferation. All AR

subtypes have been shown to modulate adenosine actions in cancer, with A_1, A_{2A}, A_{2B} ARs being promoters of cell growth while the A_3 AR is an inhibitor [3,10,11]. In this context, the role of the A_{2A} AR subtype is notable. This receptor is expressed both in the central nervous systems and peripheral organs, and it is also present in blood vessel, platelets and in immune system cells. It has been demonstrated that A_{2A} AR is upregulated [10] in some tumors and its activation directly increases growth and proliferation of the cells [2,12]. However, the most relevant A_{2A} AR-mediated effect of adenosine is inhibition of the immune system [2,4]. The prolonged and sustained A_{2A} AR activation on immune and inflammatory cells, such as T and natural killer lymphocytes, dendritic cells, monocytes and macrophages, switches the role of the nucleoside from protective to deleterious. Adenosine, in fact, inhibits the response of the immune cells, thus depressing their defensive roles and promoting the tumor's escape. A_{2A} AR activation also potentiate the function of other cells in the tumor microenvironment, such as the endothelial cells which, through stimulation of angiogenesis, sustain tumor growth and metastasis [2].

On this basis, much research has been carried out in animal models to assess the therapeutic potential of human (h) A_{2A} AR antagonists, which have shown a remarkable activity in restoring antitumor immunity. Thus, some entered clinical trials [4,5,13] to be evaluated as single drugs or in combination with immunological anticancer drugs.

Hypoxia in the tumor microenvironment, besides being one of the leading causes triggering adenosine A_{2A} AR-mediated immunoescaping, also makes the role of the hCA IX and XII isoforms relevant in the progression of tumors and metastases [6-9]. hCAs are ubiquitous metalloenzymes differing in tissue distribution, subcellular localization and catalytic activity. Almost 15 hCA isoforms are known, and 12 isoforms are catalytically active. They contain the zinc ion in the catalytic site and are involved in the regulation of physiological functions connected to carbon dioxide hydration and its equilibrium with bicarbonate. hCA activity affects pH regulation, ion transport, secretion of electrolytes and many metabolic processes, such as lipogenesis and gluconeogenesis. hCA IX and XII isoforms are membrane-bound enzymes whose

expression is significantly increased in hypoxic tumors [6-9]. Hypoxia switches metabolism toward glycolysis, producing high levels of acidic species, such as lactic acid, carbon dioxide and protons. The consequent intracellular acidification is not compatible with metabolic processes of normal cells but tumor cells activate pumps and ion-exchangers to extrude the acidic species and maintain a slightly alkaline intracellular pH. Overexpression of the CAIX and XII isoforms significantly contribute to this process: the bicarbonate ion, deriving from carbon dioxide hydration, enters the cell through an active transport, thus alkalizing the inner pH, while the proton increases acidosis of the extracellular medium. These conditions are known to favor the onset and development of solid tumors. Thus, selective inhibition of the tumor-associated hCAs IX and XII proved to be a promising strategy to counteract cancer [6,9,14].

On this basis, and due to our involvement in the research field of AR ligands[12,15-24] and hCA inhibitors [25-26], we thought it interesting to focus on the development of new compounds able to behave as combined hA_{2A} AR antagonists and hCAs IX/XII inhibitors because the blockade of both the hA_{2A} AR- and hCA-activated pathways could lead to a synergistic effect. To design the new compounds, we exploited our experience which has lead us to identify many potent antagonists of the hA_{2A} AR [12,15,17-24] belonging to different classes. Among them, the triazolo[4,3-*a*]pyrazine series was selected [18,22,24] and the 8-amino-2,6-diphenyl-1,2,4-triazolo[4,3-a]pyrazin-3-one **A** [18], a potent hA_{2A} AR antagonist, was taken as lead compound. To obtain the new hybrid ligands (**1-23**, Fig. 1), in the first phase of the work simple substituents, such as OH, COOH, CONHOH and SO_2NH_2, were inserted directly or by small chains on the 6-phenyl ring (**1-6**) of **A**. Then, the above cited groups were introduced on a lateral phenyl pendant, linked to the 6-phenyl ring through an amide chain (**7-15**) or through other spacers of different length and flexibility (**16-23**). These small substituents used to decorate the new compounds were chosen because they usually confer good hCA inhibitory activities [14,27] as they are able to interact with the zinc ion in the catalytic site, either directly or through a water molecule.

Fig. 1. From the hA_{2A} AR antagonist **A** to the new multi-target 8-amino-6-aryl-2-phenyl-1,2,4-triazolo[4,3-*a*]pyrazin-3-ones **1-23**.

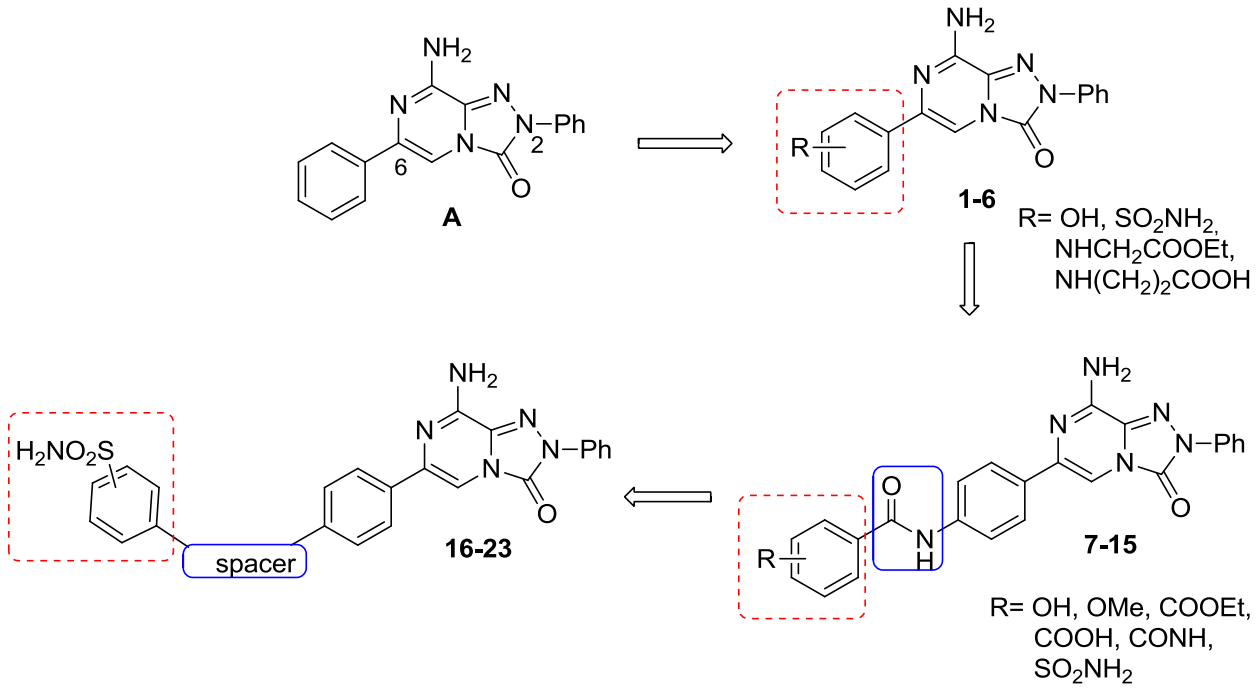

2. Results and Discussion

2.1. Chemistry

The target derivatives were synthesized as shown in Schemes 1-6. The 8-amino-2-phenyl-1,2,4-triazolopyrazin-3-one derivatives **1-3**, featuring a hydroxy group, respectively, at the 2-, 3- and 4-position of the 6-phenyl ring, were prepared as previously described by us [18,22], following the procedure described for **4** (Scheme 1). Briefly, the ethyl 1-phenyl-5-oxo-1,2,4-triazole-3-carboxylate [28] **24** was reacted with 4-(2-bromoacetyl)benzenesulfonamide **25 [**29] to give the N^4-alkylated triazole derivative **26**. The latter was cyclized by heating with ammonium acetate to provide the 1,2,4-triazolo[4,3-a]pyrazine-3,8-dione derivative **27**. Then, to protect its sulfonamide residue, **27** was reacted with dimethylformamide dimethylacetal and the resulting derivative **28** was heated in a sealed tube with phosphorus oxychloride to afford the corresponding 8-chloro derivative **29**. When this compound was heated in a saturated ethanolic solution of ammonia, the desired 8-

amino-triazolopyrazine **4** was obtained, together with the unexpected 8-dimethylamino derivative **4a**.

Scheme 1[a]

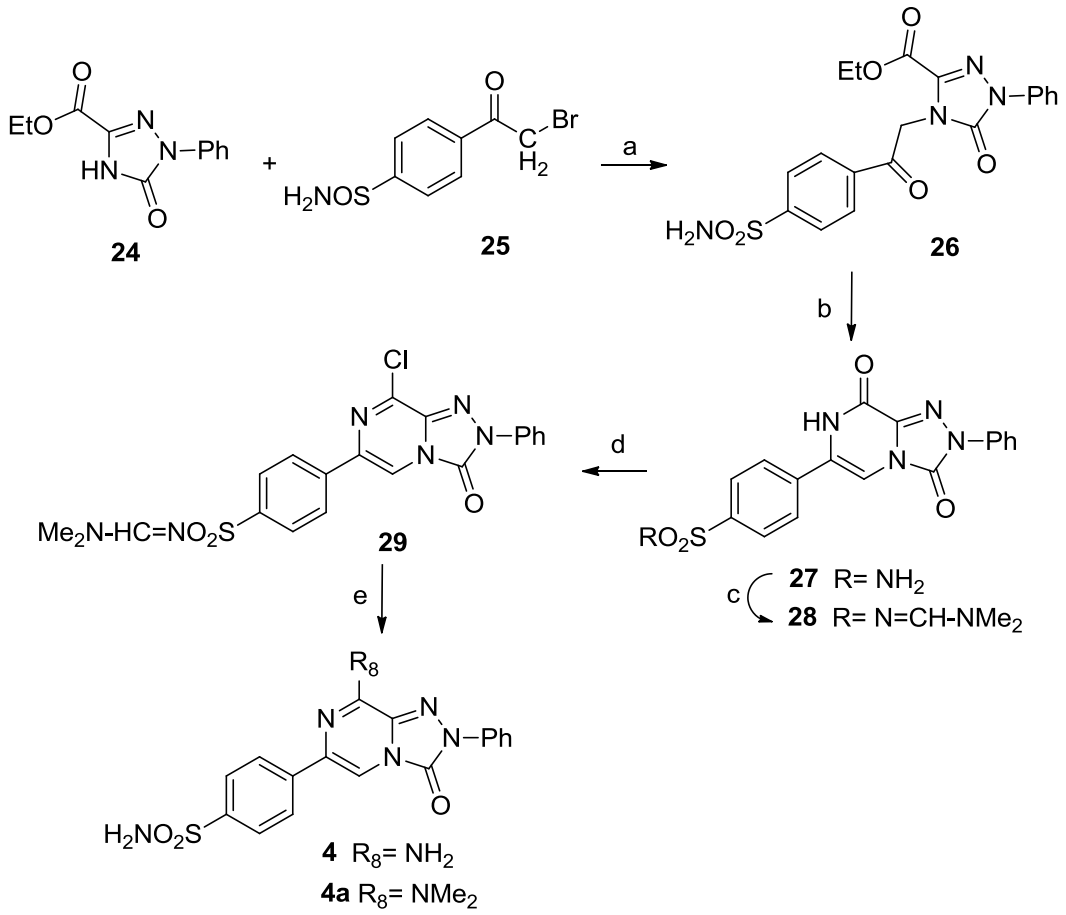

[a]Reagents and conditions: (a) K_2CO_3, DMF/MeCN, rt; (b) NH_4OAc, 140 °C sealed tube; (c) $N(Me)_2C(OMe)_2$, DMF, 0 °C-rt; (d) $POCl_3$, sealed tube, 160 °C; (e) NH_3 gas/absolute EtOH, sealed tube, 120 °C.

The triazolopyrazines **5-21**, featuring substituents connected by different linkers to the para position of 6-phenyl ring, were synthesized as depicted in Schemes 2-5. Scheme 2 describes the synthesis of compounds **5** and **6**, bearing small carboxylic chains, that were prepared by reacting the 6-(4-aminophenyl)-2-phenyltriazolopyrazine **30 [**22] with ethyl 2-bromoacetate and succinic anhydride,

respectively. Hydrolysis of the ester **5** afforded the relative carboxylic acid **5a** which proved to be unstable when purified by recrystallization or by silica gel column. Indeed, the compound **5a** was not biologically tested because its low level of purity.

Schema 2[a]

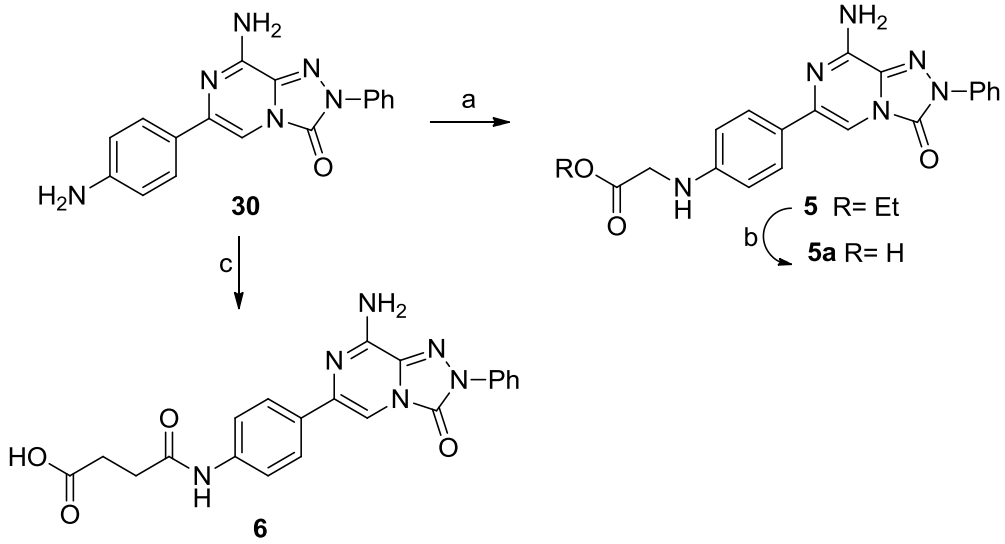

[a]Reagents and conditions: (a) ethyl 2-bromoacetate, Et_3N, THF, mw, 120 °C; (b) 1M NaOH, EtOH, reflux; (c) succinic anhydride, THF, reflux.

Compounds **7-13** were prepared allowing to react the para-amino substituent of compound **30 [**22] with suitably substituted benzoic acids, in the presence of carboxylic group activators (Scheme 3). The treatment of compound **30** with methoxy-substituted benzoic acids gave rise to the triazolopyrazines **7** and **8**, that were demethylated with a BBr_3 solution, thus providing the desired phenolic compounds **9** and **10**. Reaction of **30** with 4-(ethoxycarbonyl)benzoic acid [30] afforded derivative **11** which was hydrolyzed to give the relative acid **12**. This compound, besides being a target derivative, was also employed to prepare the hydroxamic acid **13**. By reacting compound **12**

with O-benzylhydroxylamine, the corresponding N-hydroxybenzylcarboxamido derivative **31** was obtained. Its subsequent debenzylation with a BBr_3 solution afforded compound **13**.

Scheme 3

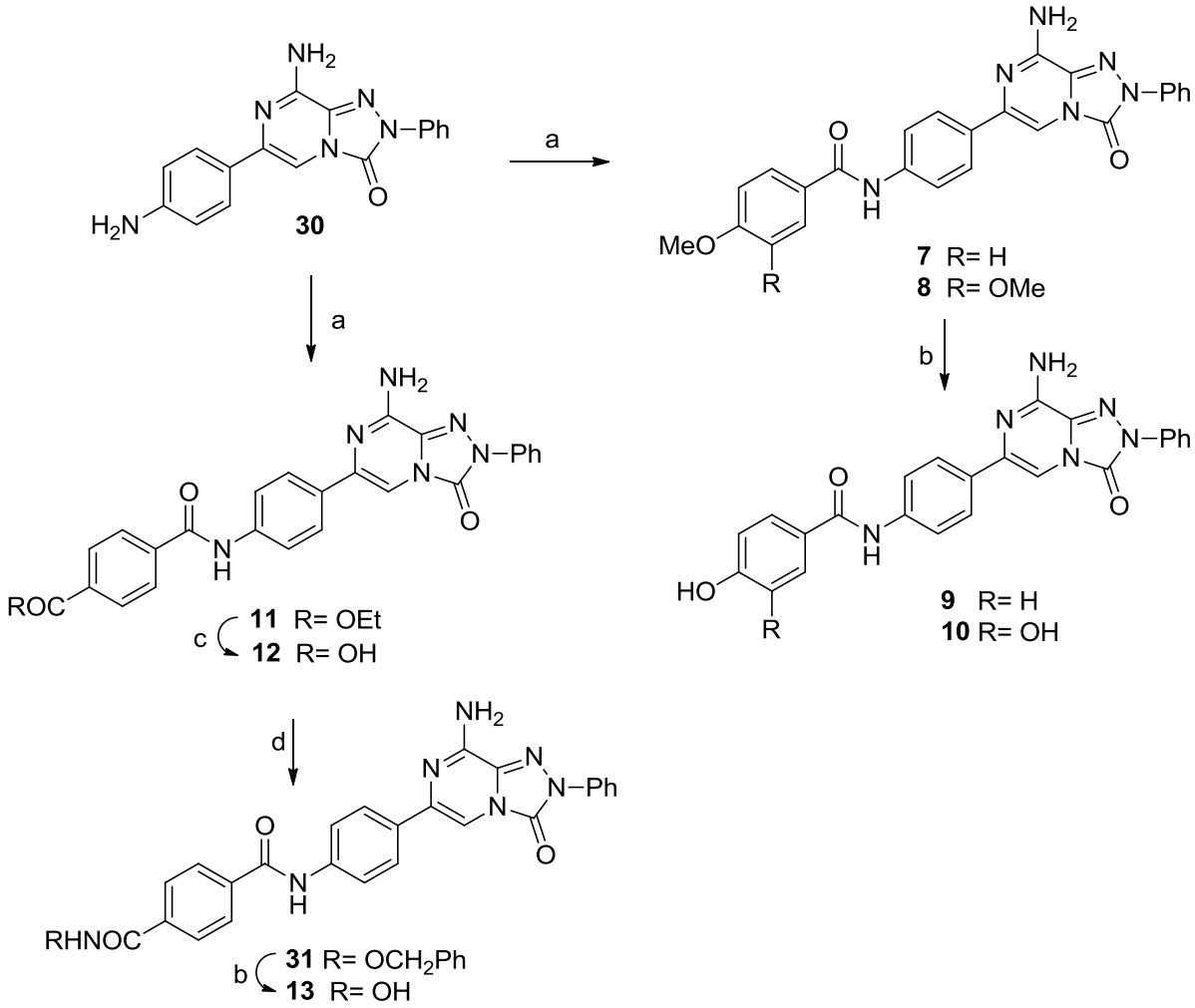

[a]Reagents and conditions: (a) suitable methoxy-substituted benzoic acid, NEt_3, 1-(3-(dimethylamino)-propyl))-3-ethylcarbodiimide hydrochloride, 1-hydroxybenzotriazole, anhydrous DMF, rt; (b) BBr_3, anhydrous CH_2Cl_2, 0 °C-rt; (c) 1M NaOH, EtOH, reflux; (d) O-benzylhydroxylamine HCl; Et_3N, 1-(3-(dimethylamino)-propyl))-3-ethylcarbodiimide, hydrochloride 1-hydroxybenzotriazole, anhydrous DMF, rt.

Scheme 4 displays the synthesis of the triazolopirazines **14-17**, featuring the benzensulfonamide group. The amides **14** and **15** were synthesized by treatment of **30** with the suitable sulfamoylbenzoic acids, in the presence of carboxylic group activators. Derivatives **16** and **17** were obtained by alkylation of the para-amino residue of **30** with 4-(bromomethyl)benzenesulfonamide [31] and 4-(2-bromoacetyl)benzenesulfonamide [29], respectively.

Scheme 4

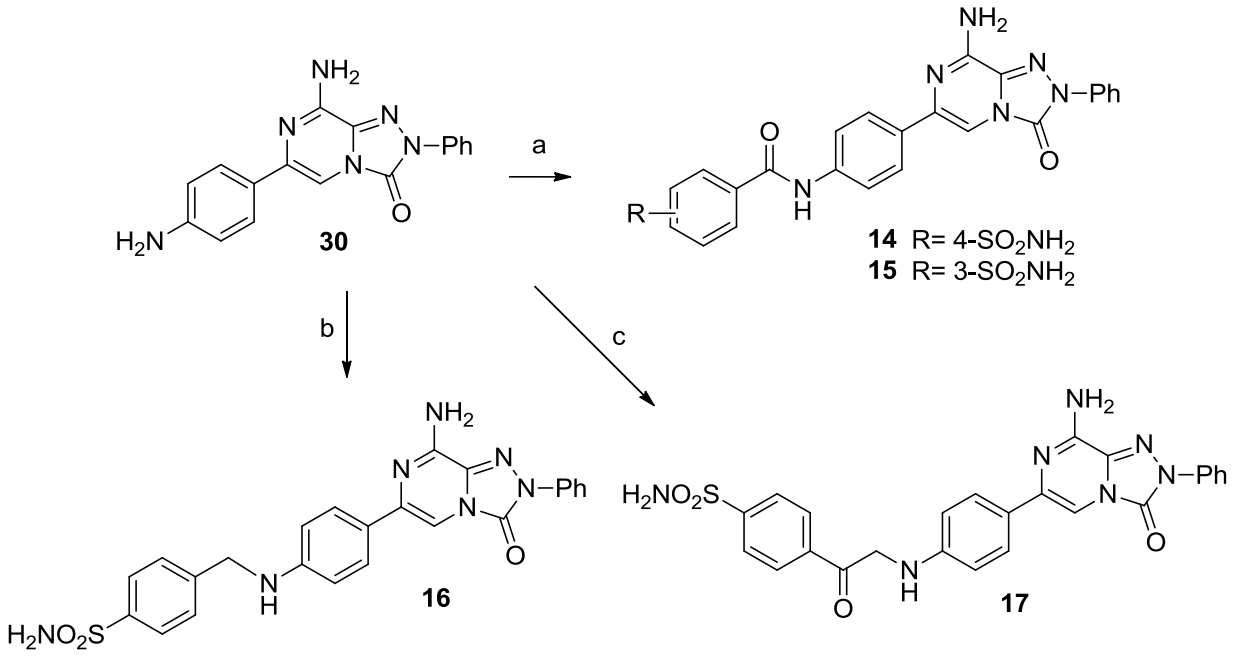

[a]Reagents and conditions: (a) suitable sulfamoylbenzoic acid, NEt_3, 1-(3-(dimethylamino)-propyl))-3-ethylcarbodiimide, hydrochloride 1-hydroxybenzotriazole, anhydrous DMF, rt; (b) 4-(bromomethyl)benzenesulfonamide, K_2CO_3, THF, reflux. (c) 4-(2-bromoacetyl)benzenesulfonamide, K_2CO_3, THF, reflux.

The synthesis of the triazolopirazine **18-21** (Scheme 5) started from the previously reported 6-(4-acrylammido-phenyl) substituted derivative **31** [24]. When the latter was reacted with the 4-(2-aminoethyl)benzenesulfonamide [32], compound **18** was obtained. Its lower homologue **19** was

synthesized allowing 4-(bromoethyl)benzenesulfonamide [31] to react with the triazolopyrazine **32** [24], that was in turn obtained by heating **31** in a saturated ethanol solution of ammonia. The sulfonamide derivatives **20** and **21** were prepared by treatment of compound **32** with the suitable sulfamoylbenzoic acids, in the same experimental conditions described above to obtain the triazolopyrazine derivatives **7-11** and **15-16**.

Scheme 5

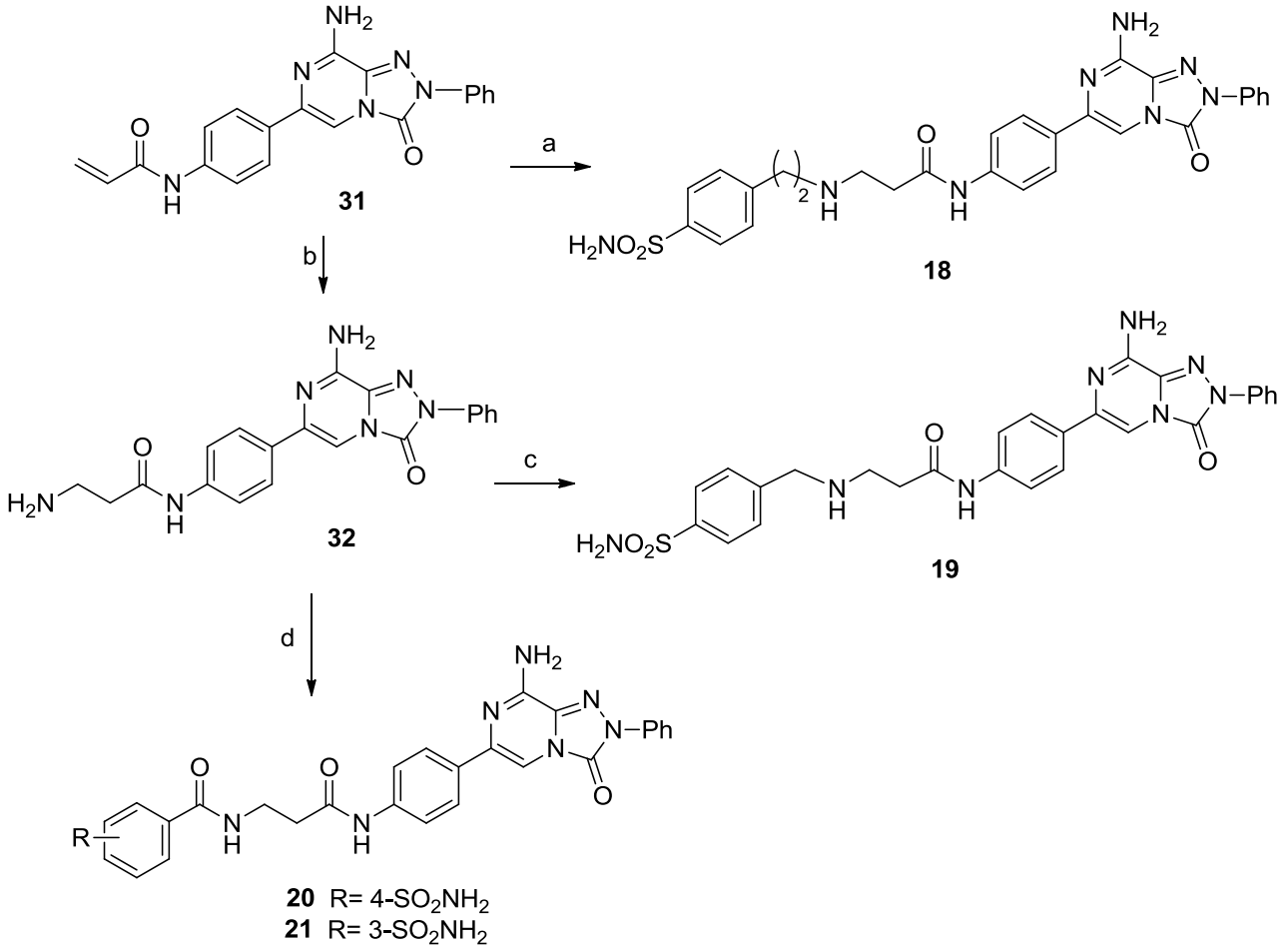

[a]Reagents and conditions: (a) 4-(2-aminoethyl)benzenesulfonamide, THF, reflux; (b) NH_3 gas/ absolute EtOH, sealed tube, 130 °C; (c) 4-(bromomethyl)benzenesulfonamide, K_2CO_3, THF, reflux; (d) suitable sulfamoylbenzoic acid, Et_3N, 1-(3-(dimethylamino)-propyl))-3-ethylcarbodiimide hydrochloride, 1-hydroxybenzotriazole, anhydrous DMF, rt.

Finally, Scheme 6 depicts the synthesis of compounds **22** and **23** that were obtained by treatment of the previously reported triazolopyrazine **33 [**24] with 4 (bromoethyl)benzenesulfonamide [32] and 4-sulfamoylbenzoic acid, respectively.

Scheme 6

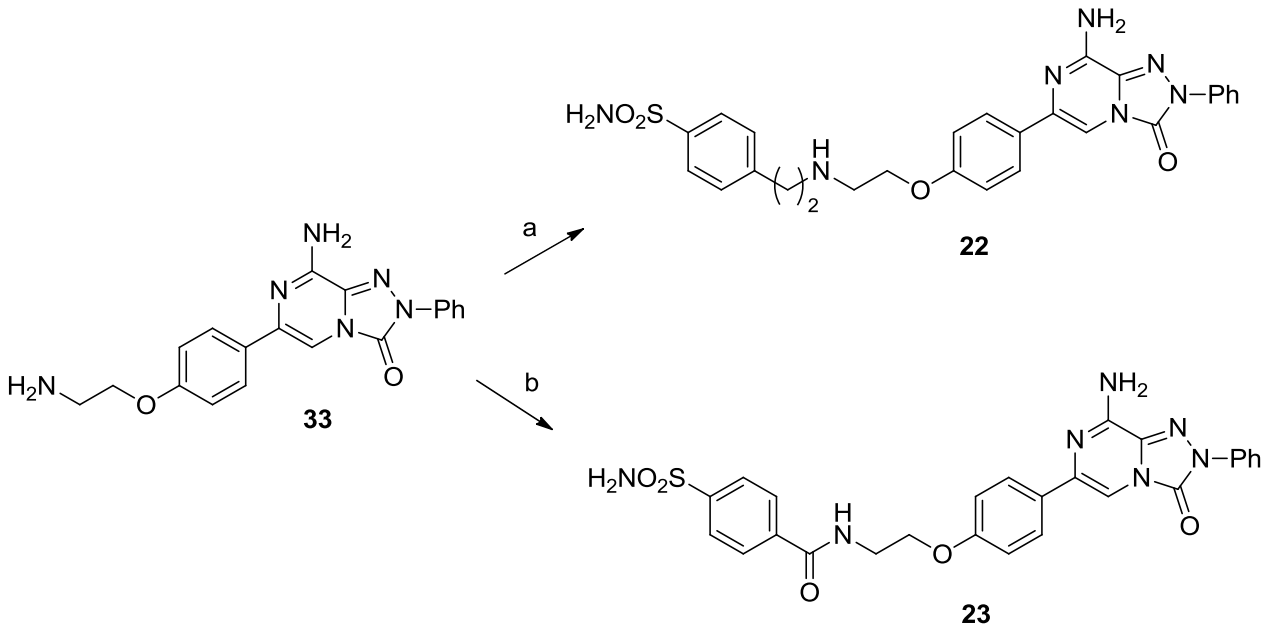

[a]Reagents and conditions: 4-(bromoethyl)benzenesulfonamide, THF, K_2CO_3, reflux; (b) 4-sulfamoylbenzoic acid, Et_3N, 1-(3-(dimethylamino)-propyl))-3-ethylcarbodiimide hydrochloride, 1-hydroxybenzotriazole, anhydrous DMF, rt.

2.2. Structure-activity relationship studies

The triazolopyrazines **1-23** were biologically tested to determine their hA_{2A} AR affinity, and selectivity versus the other hARs, and to assess their inhibitory activity against the tumor-associated hCA IX and XII isoforms. The compounds were also tested against the hCAI and II isoforms because these isozymes are abundantly expressed throughout the body, thus responsible for the side effects of non-selective inhibitors.

Derivatives **14** and **20**, showing the best combined activity at the desired targets, were selected to assess their hA_{2A} AR antagonistic profile, which was determined by evaluating their effect on cAMP production in CHO cells, stably expressing hA_{2A} ARs.

For sake of clarity, compounds have been subdivided into three sets and relative biological data are shown in Tables 1-3. This division also reflects the different steps of the work.

Table 1. Biological evaluation of compound **1-6** and **4a.**

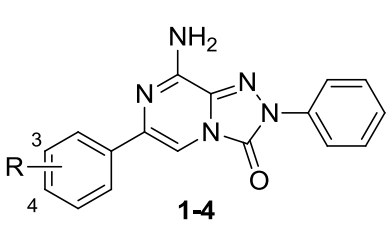

1-4

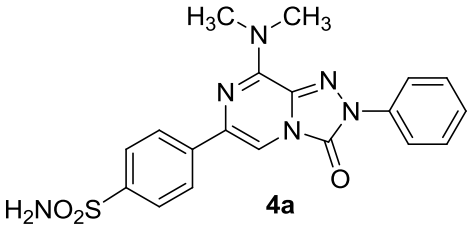

4a

Biological activity at human adenosine receptors[a]

		Binding experiments K_i (nM)			cAMP assays IC_{50} (nM)
	R	hA_1[b]	hA_{2A}[c]	hA_3[d]	hA_{2B}[e]
1[f]	2-OH	16.3 ± 0.3	2.4 ± 0.5	44.5±8.3	>30000
2[g]	3-OH	14 ± 2	3.5 ± 0.6	134 ± 13	>30000
3[g]	4-OH	45 ± 10	45 ± 12	53 ± 13	>30000
4	4-SO_2NH_2	205 ± 29	856.6 ± 188	14830 ± 320	>30000
4a	-	435.3 ± 61	3886.5 ± 833.5	19495 ± 1785	>30000
5	4-$NHCH_2COOEt$	771 ± 81	6296 ± 1140	>30000	>30000
6	4-$NHCO(CH_2)_2COOH$	2300 ± 431	573 ± 91	6957 ± 1223	>30000

Inhibition data against hCAI, II, IX and XII isoforms as determined by a stopped-flow CO_2 hydrase assay. Acetazolamide (AZA) is reported as reference compound

		K_i (μM)[h]			
	R	CAI	CAII	CAIX	CAXII
1	2-OH	>100	19.0	>100	>100
2	3-OH	>100	93.0	>100	>100

3	4-OH	>100	>100	>100	>100
4	4-SO_2NH_2	8.023	0.703	8.920	0.602
4a	-	2.093	0.464	6.729	0.358
5	4-$NHCH_2COOEt$	>100	>100	>100	>100
6	4-$NHCO(CH_2)_2COOH$	>100	>100	>100	>100
	AZA	0.250	0.0121	0.0254	0.0056

[a]Data (n= 3-5) are expressed as means ± standard errors. [b]Displacement of specific [^{3}H]-CCPA binding at hA_1 AR expressed in CHO cells. [c]Displacement of specific [^{3}H]-NECA binding at hA_{2A} AR expressed in CHO cells. [d]Displacement of specific [^{3}H]-HEMADO binding at hA_3 AR expressed in CHO cells. [e]IC_{50} values of the inhibition of NECA-stimulated adenylyl cyclase activity in CHO cells expressing hA_{2B} AR. [f]Ref. 22. [g]Ref 18. [h]Mean from three different assays, and errors were within 5-10% of the reported values.

Taking a look at the obtained results, it emerges that the aim of the work was achieved because some multi-target compounds, acting at the hA_{2A} AR and on the tumor-associated CA IX and/or XII isoforms, were obtained. The triazolopyrazines **14** and **20** are endowed with the best combined activities (Table 2), but also derivatives **17**-**19** are of interest (Table 3).

Analyzing the biological data in detail, and considering the first set of triazolopyrazines **1-6** (Table 1), we can observe that derivatives **1-3**, bearing a hydroxy group at the three positions of the 6-phenyl ring, displayed high hA_{2A} AR affinity but scarce ability to inhibit the tested hCAs. The sole results of interest are those of the 2-hydroxy- and 3-hydroxy- substituted derivatives **1** and **2** against the hCA II isozyme, that was blocked at micromolar concentration (K_i= 19 and 93 μM, respectively). As expected, the presence of the 4-sulfonamide residue on the 6-phenyl ring (derivatives **4** and **4a**) was more advantageous for hCA inhibitory activity. Compounds **4** and **4a** showed K_i values of micromolar order towards all the hCAs, the best being those relative to the hCA XII isoform (K_i= 0.602 and 0.358 μM, respectively) and the off-target CA II (K_i= 0.702 and 0.464 μM). hA_{2A} AR affinity of **4** and **4a** were quite scarce, particularly of the latter. The lower

affinity of **4a**, with respect to **4**, was probably due to the loss of hydrogen-bonding interaction that the 8-amino group typically engages with Asn254 residue [18,22,24] (see also molecular modeling studies section). The triazolopyrazines **5** and **6**, featuring, respectively, an ethyl glycine and a succinamide moiety at the para-position of the 6-phenyl ring, showed only some hA_{2A} AR affinity while they were not able to inhibit the hCAs.

In the second step of the work, the R substituents addressing activity toward hCAs were attached at the para position of a benzamide moiety that, in turn, was appended on the 6-phenyl ring (derivatives **7-15**, Table 2). This modification introduced on the molecule a long tail that was supposed to permit a better accommodation inside the enzymes. Moreover, a long pendant was also thought to maintain high hA_{2A} AR affinity and selectivity, as suggested by previous data obtained in this series of AR antagonists [26].

Table 2. Biological evaluation of compound **7-15**.

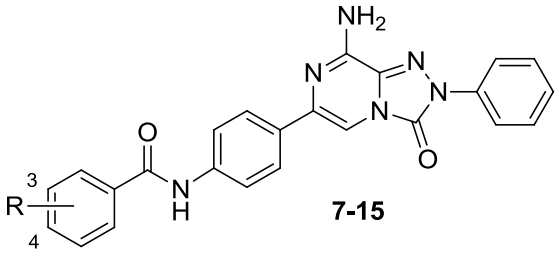

7-15

Biological activity at human adenosine receptors[a]					
		Binding Experiments K_i (nM)			cAMP assays IC_{50} (nM)
	R	hA_1[b]	hA_{2A}[c]	hA_3[d]	hA_{2B}[e]
7	4-OMe	417.7 ± 52.7	0.7 ± 0.03	279 ± 67.5	>30000
8	3,4-di OMe	98.8 ± 23.5	20.6 ± 3.7	>30000	>30000
9	4-OH	194 ± 29	41.2 ± 5	1072 ± 102	>30000
10	3,4-diOH	545.7 ± 1.5	9 ± 2.2	1248 ± 69	>30000
11	4-COOEt	7478.5 ± 748.5	1357 ± 82	>30000	>30000
12	4-COOH	2366 ± 377	81.2 ± 9.5	>30000	>30000
13	4-CONHOH	395 ± 1	36 ± 7.8	546.2 ± 68.2	>30000
14	4-SO_2NH_2	4189 ± 59.5	6.4 ± 1.5	>30000	>30000
15	3-SO_2NH_2	1211 ± 126.5	13.5 ± 0.02	>30000	>30000

Inhibition data against hCA I, II, IX and XII isoforms as determined by a stopped-flow CO_2 hydrase assay.

		K_i (μM)[f]			
	R	CAI	CAII	CAIX	CAXII
7	4-OMe	>100	>100	>100	>100
8	3,4-di OMe	>100	>100	>100	>100
9	4-OH	>100	47.3	>100	4.4
10	3,4-diOH	>100	31.7	44.3	>100
11	4-COOEt	>100	>100	>100	>100
12	4-COOH	>100	>100	>100	>100
13	4-CONHOH	>100	63.02	>100	>100
14	4-SO_2NH_2	8.351	0.046	0.466	0.006
15	3-SO_2NH_2	2.288	0.367	0.810	0.303

[a]Data (n= 3-5) are expressed as means ± standard errors. [b]Displacement of specific [^{3}H]-CCPA binding at hA_1 AR expressed in CHO cells. [c]Displacement of specific [^{3}H]-NECA binding at hA_{2A} AR expressed in CHO cells. [d]Displacement of specific [^{3}H]-HEMADO binding at hA_3 AR expressed in CHO cells. [e]IC_{50} values of the inhibition of NECA-stimulated adenylyl cyclase activity in CHO cells expressing hA_{2B} AR. [f] Mean from three different assays, and errors were within 5-10% of the reported values.

As expected, several triazolopyrazines of this set displayed nanomolar hA_{2A} affinity (compounds **7-10**, **12-15**) and some were also highly selective, the best being the 4-methoxy-derivative **7**, the 3,4-dihydroxy-substituted compound **10** and the sulfonamido derivatives **14** and **15**. Derivatives **14** and **15** also showed good activity as hCA inhibitors. In fact, their potency spans from the micromolar to the nanomolar range, the para-substituted compound **14** being the most potent against the targeted hCAs. The other triazolopyrazines of this set were less active or inactive as hCAs inhibitors, the only exception being the phenol- and cathecol-substituted derivatives **9** and **10** and the hydroxamic acid **13**. They all showed some inhibitory activity against the hCA II, while compound **9** and **10** were also active, respectively, against the hCA XII (K_i= 4.4 μM) and hCA IX (K_i= 44.3 μM).

The relevant activity of compounds **14** and **15** indicated that, among the probed substituents, benzensulfonamide was the best one to target both the hA_{2A} AR and the tumor-associated hCA

isozymes. Moreover, the significantly higher activity of compound **14,** with respect to **4**, clearly indicated that the greater distance between the benzensolfonamide moiety and the bicyclic core favored accommodation of the inhibitor inside the enzymes, as also emerged from the docking studies at the CAs (see molecular modeling section). Thus, in the subsequent derivatives (**16-23**, Table 3) only the benzesulfonamide pendant was inserted to address activity against hCAs. In particular, it was linked at the para position of the 6-phenyl ring through spacers of different length and flexibility. These modifications were more successful than the previous ones. In fact, all the new triazolopyrazines **16-23** showed nanomolar affinity for the hA_{2A} AR and were also able to inhibit the tested hCAs with different degrees of selectivity. One of the most relevant multi-target derivatives was **20**, that inhibited the hCAs IX and XII with K_i values of 5.0 and 27.0 nM, respectively, and showed relatively good hA_{2A} AR affinity (K_i= 108 nM). Derivatives **17** and **18** also showed an interesting profile, being active at low nanomolar concentrations both at the hA_{2A} AR and against the hCA XII isozyme. A similar potency at this CA isoform was found for compound **19**, the lower homologue of **18**.

It is not easy to rationalize the effect of the spacer on the target-ligand recognition process but, obviously, both the length and flexibility of the chain play a role. Considering the hA_{2A} AR binding, elongation of the CH_2NH spacer of derivative **16** with a CO function did not changed much the A_{2A} affinity (compound **17**, K_i= 26 nM) while its replacement with the more rigid CONH group enhanced about 4-fold the A_{2A} AR affinity (derivative **14**, K_i= 6.4 nM). Compound **18**, featuring the longest spacer, showed a higher hA_{2A} AR affinity (K_i= 10 nM) than those of compounds bearing shorter pendants (compounds **16** and **17**) and of its homologue **19**. Compound **21**, bearing the sulfonamide group at the meta position, is worth noting, being at least 10-fold more active than its regioisomer **20**. Considering activity against hCAs, it is evident that compounds **17-20** inhibited the hCA XII isoform with similar potency (K_i= 25.7-41.5 nM), although featuring much different spacers. Instead, against the hCA IX isozyme only compound **20** was active in the low nanomolar range.

Table 3. Biological evaluation of compound **16-23**.

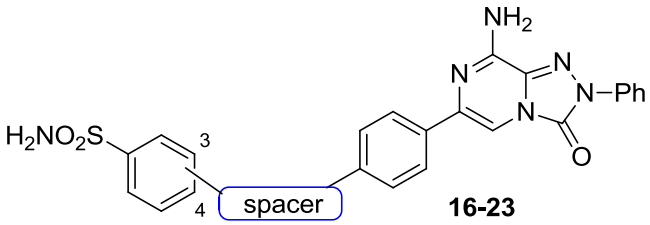

16-23

Biological activity at human adenosine receptors[a]					
		Binding Experiments K_i (nM)			cAMP Assays IC_{50} (nM)
	spacer	hA_1[c]	hA_{2A}[d]	hA_3[a,b]	hA_{2B}[e]
16	4-CH_2NH-	87.7 ± 9	27.9 ± 3	>30000	>30000
17	4-$COCH_2NH$-	131 ± 18.5	26 ± 6	6760 ± 387	>30000
18	4-$(CH_2)_2NH(CH_2)_2CONH$-	1031 ± 28	10.6 ± 2.2	5833 ± 905	>30000
19	4-$CH_2NH(CH_2)_2CONH$-	839 ± 18.9	96.3 ± 0.8	>30000	>30000
20	4-$CONH(CH_2)_2CONH$-	1074 ± 254.5	108 ± 25	>30000	>30000
21	3-$CONH(CH_2)_2CONH$-	418 ± 103.6	9.2 ± 2.4	>30000	>30000
22	4-$(CH_2)_2NH(CH_2)_2O$-	283.2 ± 46	87.9 ± 18	701.3 ± 142	>30000
23	4-$CONH(CH_2)_2O$-	420.4 ± 77.3	6.8 ± 0.18	6645 ± 517	>30000

Inhibition data against hCA I, II, IX and XII isoforms as determined by a stopped-flow CO_2 hydrase assay.

		Ki (nM)			
	spacer	CAI	CAII	CAIX	CAXII
16	4-CH_2NH-	570.3	896.8	5968	624.9
17	4-$COCH_2NH$-	588.7	246.3	9450	25.7
18	4-$(CH_2)_2NH(CH_2)_2CONH$-	8713	526.5	108.8	26.3
19	4-$CH_2NH(CH_2)_2CONH$-	9001	6763	318.7	41.5
20	4-$CONH(CH_2)_2CONH$-	51.5	8.6	5.0	27.0
21	3-$CONH(CH_2)_2CONH$-	7277	341.0	6925	830.0
22	4-$(CH_2)_2NH$-$(CH_2)_2O$-	973.1	933.8	9463	794.7
23	4-$CONH(CH_2)_2O$-	933.9	183.4	5951	528.3

[a]Data (n= 3-5) are expressed as means ± standard errors. [b]Displacement of specific [^{3}H]-CCPA binding at hA_1 AR expressed in CHO cells. [c]Displacement of specific [^{3}H]-NECA binding at hA_{2A} AR expressed

in CHO cells. [d]Displacement of specific [^{3}H]-HEMADO binding at hA_3 AR expressed in CHO cells. [e]IC_{50} values of the inhibition of NECA-stimulated adenylyl cyclase activity in CHO cells expressing hA_{2B} AR. [f] Mean from three different assays, and errors were within 5-10% of the reported values.

Compounds **22** and **23** were synthesized as analogues of derivatives **18** and **20**, respectively, in which the amide function linked at the para position of the 6-phenyl ring was replaced with an ethereal oxygen. This modification, which enhanced the lateral chain flexibility, was not profitable for the multi-target action because **22** and **23** were scarcely active against all the hCAs. Regarding hA_{2A} AR affinity, it produced opposite effects. Compound **22** was, in fact, about 8-fold less active than **18**, while derivative **23** was 15-fold-more active than compound **20**.

Compounds **14** and **20**, showing the best combined hA_{2A} AR affinity-hCA IX/XII inhibitory potency, behaved as hA_{2A} AR antagonists, being able to counteract NECA-stimulated cAMP production in CHO cells (IC_{50}= 90.8 ± 26 nM and 926 ± 111 nM, respectively).

2.3. Molecular modeling studies at hA_{2A} AR

Docking studies were carried out to simulate the binding mode of the synthesized compounds at the hA_{2A} AR cavity. For this analysis, as biomolecular target it was chosen the crystal structures of the hA_{2A} AR in complex with the antagonist/inverse agonist ZM241385 (http://www.rcsb.org; pdb code: 5NM4; 1.7-Å resolution [33]). MOE (Molecular Operating Environment 2014.09) software and the CCDC Gold docking tool [34,35] were used for docking analyses, with protocols set up and previously reported in other studies describing analogues of these molecules [18,24].

As expected, the docking conformations generally observed for the new derivatives are highly similar to the ones observed for the previously reported triazolopyrazines [18,24]. The bicyclic scaffold is located in the depth of the hA_{2A} AR binding cavity, making non-polar interaction with the side chains of Phe168 (EL2) and Leu249$^{6.51}$. Additional polar interaction is given by the

exocyclic amine function with the side-chains of Asn253$^{6.55}$ and Glu169 (EL2). Figure 2A shows the binding mode of compound **14** at the hA_{2A} AR binding cavity.

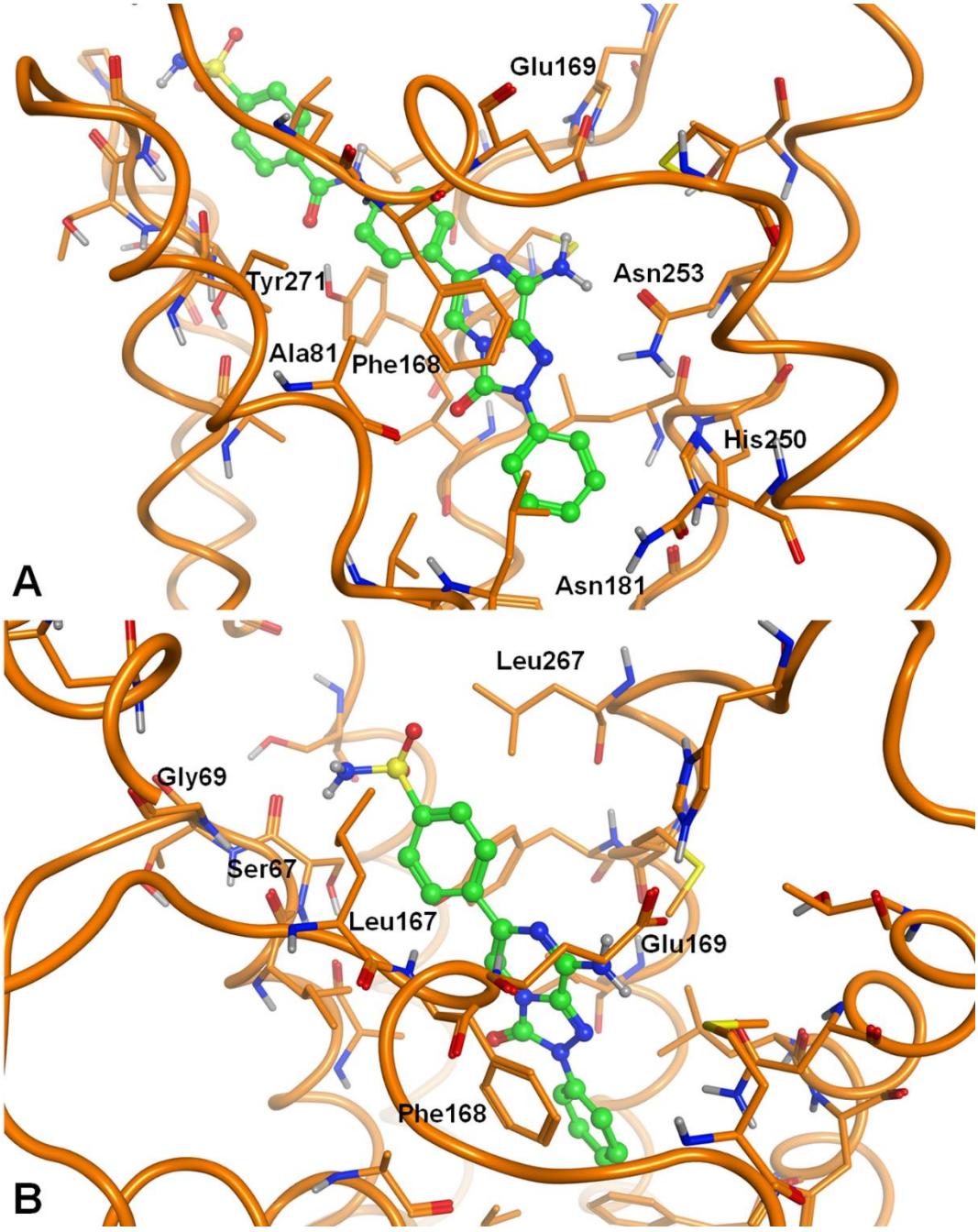

Fig. 2. (**A**) Binding mode of compound **14** at the hA_{2A} AR binding cavity, with indication of some key receptor residues. (**B**) Top-view of the binding mode of compound **4** within the hA_{2A} AR binding pocket. The view is focused on the 6-substituent and the receptor residues in its proximity.

The 6-phenyl ring is externally oriented and, as observed for previously reported analogues of this series [24], substituents on this ring modulate the hA_{2A} AR affinity through the interaction with receptor residues located at the entrance of the binding cavity. Introduction at the para-position of the 6-phenyl ring of a highly hydrophilic group, such as the sulfonamide, yielded a compound (**4**) endowed with a sub-micromolar affinity for the hA_{2A} AR. The sulfonamide group gets located between receptor residues with a non-polar or low polar profile, such as Ser67$^{2.65}$, Gly69$^{2.67}$, Leu167 (EL2) and Leu267 (EL3) (Fig. 2B), and this affords a non-favorable interaction between the ligand and the receptor, leading to a low affinity for the hA_{2A} AR. Introduction of two methyl groups on the 8-amine function of **4** leads to the loss of the above-described polar interaction between the amine and the sidechains of Asn253$^{6.55}$ and Glu169 (EL2), with a consequent decrease of the hA_{2A} AR affinity (compound **4a**, Table 1).

Introduction of larger substituents at the para-position of the 6-phenyl ring leads to various degrees of hA_{2A} AR affinity and selectivity. Compounds **7-17**, in which the groups targeting the hCAs were inserted on a phenyl group attached by small spacers (CONH, CH_2NH, $COCH_2NH$) to the 6-phenyl ring, showed hA_{2A} AR affinities in the low nanomolar range. Docking conformations for these compounds are highly similar (see compound **14**, Fig. 2A), with the external phenyl ring located at the entrance of the cavity but exposed to the solvent. These substituents make interactions with several receptor residues and docking scores present a similar trend with respect to the hA_{2A} AR affinities of these compounds. In particular, affinity data of **7-17** display a very similar trend with respect to the LogP values of the same molecules (calculated with MOE; LogP data are reported in the supporting material), with the lower LogP data associated to molecules with higher affinities (compound **7** being an outlier). The physicochemical profile of the substituent inserted at the para- and/or meta-position of the external phenyl ring appears critical to modulate the affinity at the hA_{2A} AR. Still considering this set of compounds, even the type of spacer linking the two phenyl rings is critical. In fact, compound **14**, bearing an amide spacer in this position, exhibits higher hA_{2A} AR affinity with respect to compound **16**, which presents a methylamine linker. Docking conformations

show that the carbonyl group of the amide spacer makes, as H-bond acceptor, a polar interaction with the side chain of Tyr271$^{7.36}$, which is not given by the methylamine linker.

Compounds **18**, **19**, **21**-**23**, featuring even larger 6-substituents, present a wide series of conformations due to the high flexibility of this group. Hence, while the bicyclic core of these molecules conserves the above-described position and orientation within the depth of the cavity, their 6-substituents have several possible arrangements and interactions with externally located receptor residues. Thus, a clear interpretation of the affinity data is not feasible. Almost all these compounds present the spacer starting with an amide group that provides analogue interaction with Tyr271$^{7.36}$, as described above. Similar to the amide function, even the ether oxygen atom at the beginning of the linker of compound **23** makes interaction with Tyr271$^{7.36}$, contributing to the high hA_{2A} AR affinity of this molecule.

2.4. Molecular modeling studies at hCAs

Docking studies were performed at crystal structures of hCAs II, IX and XII isoforms. Figure 3 depicts the interaction mode of a representative compound per subset (**4**, **14** and **20**) in the active site of the selected hCAs. As expected, the benzenesulfonamide moiety of all docked compounds coordinates the Zn(II) ion, and establishes two H-bonds with Thr199 from the three binding sites (Fig. 3).

The length of the spacers linking the 1,2,4-triazolo[4,3-a]pyrazin-3-one to the benzensulfonamide moiety influences the binding efficiency of the heterocycle nucleus to distinct pockets of hCAs II, IX and XII active site. The triazolopyrazine scaffold of compound **4** is located in the middle of the binding cavity of the three isoforms, mainly forming van der Waals contacts with different amino acids depending on the isozyme (Fig. 3A, D, G). π-π interactions with Phe131 from hCA II (Fig. 3A) are absent in the adduct with the hCA IX, where the residue is replaced by the smaller and not aromatic Val131 (Fig. 3D), thus resulting in a weaker inhibition profile. In contrast, the presence of Ser residues (132 and 135) in hCA XII drives the bicyclic core of compound **4** towards a new

positioning and interactions in the active site likely responsible for restoring a sub-micromolar inhibition (Fig. 3G).

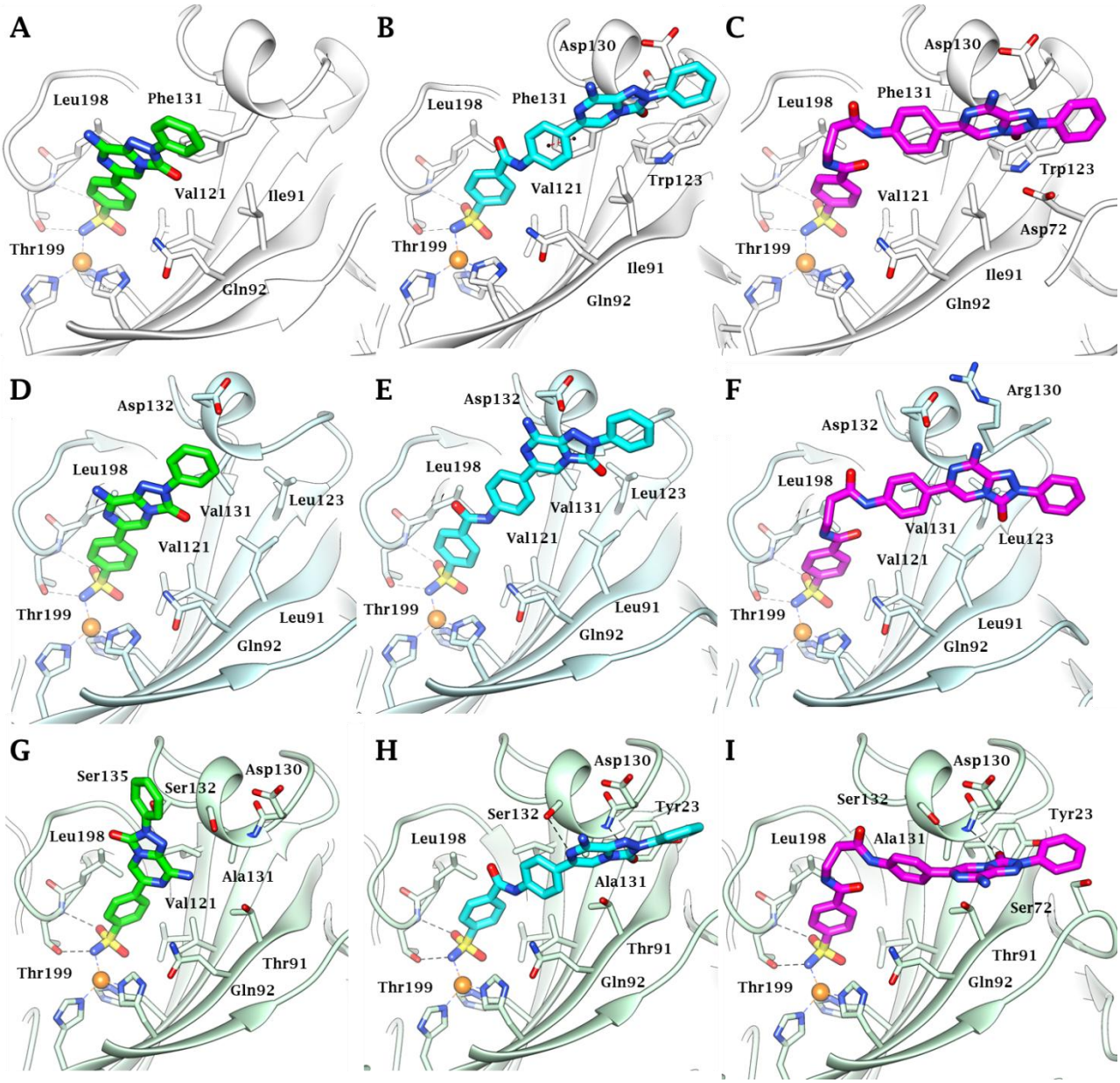

Fig. 3. *In silico* predicted binding mode of compounds **4** (green), **14** (cyan) and **20** (magenta) to hCA II (white), hCA IX (light cyan) and hCA XII (light green). Active site view of hCA II in adduct with A) **4**, B) **14** and C) **20**; active site view of hCA IX in adduct with D) **4**, E) **14** and G) **20**; active site view of hCA XII in adduct with G) **4**, H) **14** and I) **20**. Hydrogen bonds and π-π interactions are represented as black and red dashed lines, respectively.

The triazolopyrazin-3-one scaffold of compound **14** accommodates at the edge of the binding cavity of the three isozymes. In hCA II, the 6-phenyl moiety is in π-π stacking distance with Phe131 and, at the same time, the backbone NH of the residue acts as a H-bond donor towards the 3-oxo group of the heterocycle (Fig. 1B). In hCA XII, in addition to the already described NH···O=C interaction, a further H-bond is formed involving the Ser132-hydroxyl function and the pyrazine nitrogen at position 7 (Fig. 3H).

The absence of such interactions in the complex formed by **14** and hCA IX is most likely the cause of the reduced inhibition observed with this isozyme in comparison to hCAs II and XII.

The conformation assumed by the ethylene linker of **20** directs the triazolopyrazin-3-one core in pockets which, though featured by amino acids of different nature, all ensure an efficient binding, as indicated by the low nanomolar inhibition against both hCAs II, IX and XII. Indeed, the moiety lies in the cleft formed by Asp130, Phe131, Trp123 and Asp72 in hCA II, where a H-bond is established between the backbone NH of Phe131 and the 3-oxo group of the heterocycle (Fig. 3C). In hCA XII, an analogous NH···O=C interaction, involving Ala131, exists in the ligand/target adduct with the bicyclic scaffold accommodating in the cleft formed by Asp130, Ala131, Tyr123 and Ser72 (Fig. 3I). On the contrary, the most marked hydrophobic nature of the pocket lodging the triazolopyrazine core in hCA IX, where leucine and proline residues replace the Trp(II)/Tyr(XII)123 and Asp(II)/Ser(XII)72 respectively, favors the formation of π-alkyl contacts between the heterocycle and the pocket (Fig. 3F).

3. Conclusion

This work has led to the identification of the first-in-class multi-target hA_{2A} adenosine receptor antagonists-hCA IX and/or XII inhibitors. The new derivatives ensued from structural modifications of the 8-amino-2,6-diphenyl-1,2,4-triazolo[4,3-*a*]pyrazin-3-one, a potent previously reported hA_{2A} AR antagonist, that was decorated with substituents addressing activity against hCAs. Most of the new triazolopyrazines were endowed with nanomolar hA_{2A} AR affinity and high selectivity versus

the other ARs. The most active multi-target compounds bear a benzensulfonamide residue attached through different spacers to the 6-phenyl ring (compounds **14**, **16-20**). The best combined activity at the hA_{2A} AR and hCA IX and/or hCA XII isoforms was shown by derivatives **14** and **20**, which can be therefore considered as promising candidates for further pharmacological evaluation as anticancer agents.

4. Experimental section

4.1. Chemistry

The microwave-assisted syntheses were performed using an Initiator EXP Microwave Biotage instrument (frequency of irradiation: 2.45 GHz). Analytical silica gel plates (0.20 mm, F254, Merck, Germany) and silica gel 60 (Merck, 70-230 mesh) was used for analytical and column chromatography, respectively. All melting points were determined on a Gallenkamp melting point apparatus and are uncorrected. Elemental analyses were performed with a Flash E1112 Thermofinnigan elemental analyzer for C, H, N and the results were within 0.4% of the theoretical values. All final compounds revealed purity not less than 95%. The IR spectra were recorded with a Perkin-Elmer Spectrum RX I spectrometer in Nujol mulls and are expressed in cm^{-1}. NMR spectra were recorded on a Bruker Avance 400 spectrometer (400 MHz for ^{1}H- and 100 Mz for ^{13}C- NMR). The chemical shifts are reported in δ (ppm) and are relative to the central peak of the solvent which was $CDCl_3$ or $DMSOd_6$. The following abbreviations are used: s= singlet, d= doublet, t= triplet, q= quartet, m= multiplet, br= broad and ar= aromatic protons.

Compounds were named following IUPAC rules as applied by ChemDrawUtra 9.0.

*4.1.1. 4-(8-Amino-3-oxo-2-phenyl-2,3-dihydro-1,2,4-triazolo[4,3-a]pyrazin-6-yl)benzensolfonamides (**4**)* and *4-(8-dimethylamino-3-oxo-2-phenyl-2,3-dihydro-1,2,4-triazolo[4,3-a]pyrazin-6-yl)benzensulfonamide (**4a**).*

A suspension of N^1-((8-chloro-3-oxo-2-phenyl-2,3-dihydro-1,2,4-triazolo[4,3-a]pyrazin-6-yl)sulfonyl)-N,N-dimethylformimidamide **29**, in a saturated ethanolic solution of NH_3 (50 mL), was heated at 120 °C in a sealed tube for 14h. The mixture was cooled at rt, the suspended solid was collected by filtration and washed with water (about 5-10 mL). The crude product was constituted by the desired 8-amino-triazolopyrazine **4** and its 8-dimethylamino derivate **4a** (about ratio 1:1, from ^{1}H-NMR spectrum) which were separated by column chromatography (eluent $CHCl_3$ 9.3/ MeOH 0.7).

*4.1.1.1. Compound **4***. Yield 32%; mp >300 °C; ^{1}H NMR (DMSO-d_6) 8.19 (d, 2H, ar, J = 8.4 Hz), 8.08 (d, 2H, ar, J = 8.1 Hz), 7.96 (s, 1H, H-5), 7.87 (d, 2H, ar, J = 8.4 Hz), 7.67 (s, 2H, NH_2), 7.57 (t, 2H, ar, J = 7.9 Hz), 7.43-7.34 (m, 3H, 1 ar + NH_2 sulfonamide). Anal.$C_{17}H_{14}N_6O_3S$ (C, H, N).

*4.1.1.2. Compound **4a***. Yield 30%; mp 270-273 °C; ^{1}H NMR (DMSO-d_6) 8.24 (d, 2H, ar, J = 8.3 Hz), 8.08 (d, 2H, ar, J = 7.6 Hz), 7.95 (s, 1H, H-5), 7.86 (d, 2H, ar, J = 8.3 Hz), 7.57 (t, 2H, ar, J = 7.8 Hz), 7.43-7.32 (m, 3H, 1ar + SO_2NH_2), 3.55 (s, 6H, $2CH_3$). Anal.$C_{19}H_{18}N_6O_3S$ (C, H, N).

*4.1.2. Ethyl 2-((4-(8-amino-3-oxo-2-phenyl-2,3-dihydro-1,2,4-triazolo[4,3-a]pyrazin-6-yl)phenyl)amino)acetate (**5**).*

A mixture of the 6-(4-aminophenyl)-substituted triazolopyrazine **30** [22] (1.0 mmol), ethyl 2-bromoacetate (4.0 mmol) and Et_3N (2.0 mmol) in anhydrous THF (15 mL) was heated under microwave irradiation at 120 °C for 1h and 30 min. The solvent was eliminated at reduced pressure and the resulting solid was rinsed with water (5 mL), collected by filtration, washed with Et_2O (10 mL) and recrystallized from CH_3CN. Yield 72%; mp 237-239 °C; ^{1}H NMR (DMSO-d_6) 8.08 (d, 2H, ar, J = 8.0 Hz), 7.71 (d, 2H, ar, J = 8.6 Hz,), 7.56 (t, 2H, ar, J = 7.9 Hz), 7.51 (s, 1H, ar), 7.44 (br s, 2H, NH_2), 7.35 (t, 1H, ar, J = 7.4 Hz), 6.60 (d, 2H, ar, J = 8.6 Hz), 6.20 (t, 1H, NH, J = 6.3 Hz), 4.14 (q, 2H, CH_2, J = 7.1 Hz,), 3.94 (d, 2H, CH_2, J = 6.3 Hz), 1.21 (t, 3H, CH_3, J = 7.1 Hz).

^{13}C-NMR (DMSO-d_6) 171.64, 148.69, 147.59, 138.04, 136.72, 131.52, 129.62, 126.86, 126.68, 124.97, 119.86, 112.45, 99.06, 60.78, 45.15, 14.61. Anal.$C_{21}H_{20}N_6O_3$ (C, H, N).

*4.1.3. (4-(8-Amino-3-oxo-2-phenyl-2,3-dihydro-1,2,4-triazolo[4,3-a]pyrazin-6-yl)phenyl)glycine (**5a**).*

1N sodium hydroxide (0.75 mmol) was added to a suspension of the ethyl ester **5** (0.25 mmol) in EtOH (4 mL), and the mixture was heated at 30 °C for about 1h and 30 min. The solvent was concentrated at reduced pressure and the resulting mixture was diluted with water (10 mL) and acidified with 6N HCl to pH = 2. The resulting solid was collected by filtration, washed with Et_2O (20 ml) and dried. It was not possible to purify the obtained acid because it was unstable upon recrystallization (EtOH) and on silica gel. Yield 64% (crude compound); ^{1}H NMR (DMSO-d_6) 8.53 (br s, 1H, OH), 8.06 (d, 2H, ar, J = 7.8 Hz), 7.67 (d, 2H, ar, J = 8.3 Hz), 7.63-7.53 (m, 4H,2H ar + NH_2), 7.38 (t, 1H, ar, J = 7.2 Hz), 6.64 (d, 2H, ar, J = 8.4 Hz), 3.87 (s, 1H, CH_2).

*4.1.4. 4-((4-(8-Amino-3-oxo-2-phenyl-2,3-dihydro-1,2,4-triazolo[4,3-a]pyrazin-6-yl)phenyl)amino)-4-oxobutanoic acid (**6**).*

A mixture of the 6-(4-aminophenyl)-triazolopyrazine derivative **30** [22] (1.0 mmol) and succinic anhydride (1.0 mmol) in anhydrous THF (15 mL) was refluxed for about 8-10 h. The mixture was cooled at rt, the suspended solid was collected by filtration, washed with Et_2O (about 5-10 mL), dried and recrystallized from MeOH. Yield 77%; mp 260-263 °C; ^{1}H NMR (DMSO-d_6) 12.03 (br s, 1H, OH), 10.07 (s, 1H, NH), 8.08 (d, 2H, ar, J = 7.7 Hz), 7.91 (d, 2H, ar, J = 8.7 Hz), 7.70 (s, 1H, H-5), 7.64 (d, 2H, ar, J = 8.7 Hz), 7.62-7.52 (m, 4H, 2 ar + NH_2), 7.36 (t, 1H, ar, J = 7.4 Hz), 2.63-2.54 (m, 4H, 2 CH_2). ^{13}C-NMR (DMSO-d_6) 174.27, 170.60, 147.80, 147.62, 139.66, 137.98, 135.78, 131.57, 131.38, 129.65, 126.75, 126.34, 119.89, 119.23, 101.00, 31.58, 29.32. Anal.$C_{21}H_{18}N_6O_4$ (C, H, N).

*4.1.5. General procedure for the synthesis of methoxy-substituted N-(4-(8-amino-3-oxo-2-phenyl-2,3-dihydro-1,2,4-triazolo[4,3-a]pyrazin-6-yl)phenyl)-benzamides **7** and **8**.*

A mixture of the 6-(4-aminophenyl)-triazolopyrazine derivative **30** [22] (0.79 mmol), the suitably substituted benzoic acid (0.95 mmol), 1-(3-(dimethylamino)-propyl))-3-ethylcarbodiimide hydrochloride (1.57 mmol), Et_3N (1.98 mmol) and 1-hydroxybenzotriazole (1.57 mmol), in anhydrous DMF (3 mL) was stirred for about 24h at rt, under nitrogen atmosphere. The mixture was diluted with water (20 mL) and the solid was collected by filtration, rinsed with water (3 mL), Et_2O (10 mL) and dried. The crude compounds were purified by column chromatography.

*4.1.5.1. N-(4-(8-Amino-3-oxo-2-phenyl-2,3-dihydro-1,2,4-triazolo[4,3-a]pyrazin-6-yl)phenyl)-4-methoxybenzamide (**7**).*

Yield 40%; eluent $CHCl_3$ 9.7/MeOH 0.3; mp 286-288 °C; ^{1}H NMR (DMSO-d_6) 10.17 (s, 1H, NH), 8.08 (d, 2H, ar, J = 7.7 Hz), 8.04-7.91 (m, 4H, ar), 7.85 (d, 2H, ar, J = 8.8 Hz), 7.74 (s, 1H, H-5), 7.62.7.50 (m, 4H, 2ar + NH_2), 7.36 (t, 1H, ar, J = 7.4 Hz), 7.08 (d, 2H, ar, J = 8.8 Hz), 3.85 (s, 3H, CH_3). Anal.$C_{25}H_{20}N_6O_3$ (C, H, N).

*4.1.5.2. N-(4-(8-Amino-3-oxo-2-phenyl-2,3-dihydro-1,2,4-triazolo[4,3-a]pyrazin-6-yl)phenyl)-3,4-dimethoxybenzamide (**8**).*

Yield 45%; eluent $CHCl_3$ 9.7/MeOH 0.3; mp 256-259 °C; ^{1}H NMR (DMSO-d_6) 10.16 (s, 1H, NH), 8.08 (d, 2H, ar, J = 7.8 Hz), 7.98 (d, 2H, ar, J = 8.6 Hz), 7.84 (d, 2H, ar, J = 8.6 Hz), 7.75 (s, 1H, ar), 7.65 (d, 1H, ar, J = 8.4 Hz), 7.62-7.50 (m, 5H, 2ar + H-5 + NH_2), 7.36 (t, 1H, ar, J = 7.3 Hz), 7.10 (d, 1H, ar, J = 8.5 Hz), 3.86 (s, 3H, CH_3), 3.85 (s, 3H, CH_3). ^{13}C-NMR (DMSO-d_6) 165.34, 152.17, 148.81, 147.80, 147.62, 139.68, 137.96, 135.76, 131.87, 131.58, 129.64, 127.43, 126.74, 126.18, 121.56, 120.68, 119.88, 111.61, 111.46, 101.14, 56.16. Anal.$C_{26}H_{22}N_6O_4$ (C, H, N).

*4.1.6. General procedure for the synthesis of hydroxy-substituted N-(4-(8-amino-3-oxo-2-phenyl-2,3-dihydro-1,2,4-triazolo[4,3-a]pyrazin-6-yl)phenyl)-benzamides **9** and **10**.*

1M BBr_3 solution in CH_2Cl_2 (2 mL) was slowly added at 0 °C, under nitrogen atmosphere, to a suspension of the methoxy-substituted derivatives **7** or **8** (0.37 mmol) in anhydrous CH_2Cl_2 (20 mL). The mixture was stirred at rt until the disappearance of the starting material (TLC monitoring, 16-48 h). Then the suspension was diluted with water (10 mL) and neutralized with a $NaHCO_3$ saturated solution. Most of the organic solvent was removed by evaporation at reduced pressure and the obtained solid was collected by filtration. The crude derivatives were dried and purified by column chromatography (**9**) or by recrystallization (**10**).

*4.1.6.1. N-(4-(8-Ammino-3-oxo-2-phenyl-2,3-dihydro-1,2,4-triazolo[4,3-a]pyrazin-6-yl)phenyl)-4-hydroxybenzamide (**9**).*

Yield 65%; eluent $CHCl_3$ 9.5/MeOH 0.5; mp >300 °C; ^{1}H NMR (DMSO-d_6) 10.10 (s, 1H, NH), 10.07 (s, 1H, OH), 8.08 (d, 2H, ar, J = 7.9 Hz), 7.95 (d, 2H, ar, J = 8.4 Hz), 7.91-7.79 (m, 4H, ar), 7.73 (s, 1H, H-5), 7.64-7.51 (m, 4H, 2ar + NH_2), 7.40-7.32 (m,1H, ar), 6.87 (d, 2H, J = 8.3 Hz). Anal.$C_{24}H_{18}N_6O_3$ (C, H, N).

*4.1.6.2. N-(4-(8-Ammino-3-oxo-2-phenyl-2,3-dihydro-1,2,4-triazolo[4,3-a]pyrazin-6-yl)phenyl)-3,4-dihydroxybenzamide (**10**).*

Yield 42%; mp 300 °C dec (MeOH); ^{1}H NMR (DMSO-d_6) 10.01 (s, 1H, NH), 9.60 (s, 1H, OH), 9.22 (s, 1H, OH), 8.09 (d, 2H, ar, J = 7.9 Hz), 7.94 (d, 2H, ar, J = 8.5 Hz), 7.83 (d, 2H, ar, J = 8.6 Hz), 7.72 (s, 1H, H-5), 7.63-7.50 (m, 4H, 2ar + NH_2), 7.47–7.31 (m, 3H, 2ar + H-5), 6.84 (d, 1H, ar, J = 8.2 Hz). ^{13}C-NMR (DMSO-d_6) 165.72, 149.39, 148.63, 147.81, 147.64, 145.44, 139.94, 137.98, 135.83, 131.59, 129.65, 126.74, 126.36, 126.14, 120.42, 120.13, 119.89, 115.93, 115.38, 101.04. Anal.$C_{24}H_{18}N_6O_4$ (C, H, N).

*4.1.7. Ethyl 4-((4-(8-amino-3-oxo-2-phenyl-2,3-dihydro-1,2,4-triazolo[4,3-a]pyrazin-6-yl)phenyl)carbamoyl)benzoate (**11**).*

A mixture of the 6-(4-aminophenyl)-substituted triazolopyrazine derivative **30** [22] (0.62 mmol), 4-(ethoxycarbonyl)benzoic acid [30] (1.57 mmol), 1-(3-(dimethylamino)-propyl))-3-

ethylcarbodiimide hydrochloride (2.37 mmol), Et_3N (2.77 mmol) and 1-hydroxybenzotriazole (2.37 mmol), in anhydrous DMF (3 mL), was stirred for about 6h, at rt and under nitrogen atmosphere. The mixture was diluted with water (20 mL) and the obtained solid was collected by filtration, washed with water (3 mL), Et_2O (10 mL), dried and recrystallized from a mixture of nitromethane/MeOH. Yield 30%; mp 296-298 °C; ^{1}H NMR (DMSO-d_6) 10.52 (s, 1H, NH), 8.21-8.06 (m, 6H, ar), 7.99 (d, 1H, J = 8.7 Hz), 7.86 (d, 2H, ar, J = 8.7 Hz), 7.75 (s, 1H, H-5), 7.64-7.51 (m, 4H, 2ar + NH_2), 7.36 (t, 1H, ar, J = 7.4 Hz), 4.37 (q, 3H, CH_3, J = 7.0 Hz), 1.36 (t, 3H, CH_3, J = 7.1 Hz). ^{13}C-NMR (DMSO-d_6) 65.65, 165.10, 147.82, 147.62, 139.39, 139.26, 137.98, 135.68, 132.80, 132.37, 131.57, 129.62, 129.57, 128.51, 126.73, 126.25, 120.69, 119.86, 101.30, 61.56, 14.59. Anal.$C_{27}H_{22}N_6O_4$ (C, H, N).

*4.1.8. 4-((4-(8-Amino-2-phenyl-2,3-dihydro-1,2,4-triazolo[4,3-a]pyrazin-6-yl)phenyl)carbamoyl)benzoic acid (**12**).*

1N Sodium hydroxide (1.86 mmol) was added to a suspension of the ethyl ester **11** (0.62 mmol) in EtOH (30 mL) and the mixture was refluxed for about 1.5 h. The solvent was eliminated at reduced pressure and the resulting solid was rinsed with water (20 ml), collected by filtration, washed and recrystallized from MeOH/EtOH/$CHCl_3$. Yield 62%; mp >300 °C; ^{1}H NMR (DMSO-d_6) 13.25 (br s, 1H, COOH), 10.50 (s, 1H, NH), 8.13-8.00 (d, 6H, ar, J = 5.9 Hz), 7.99 (d, 2H, ar, J = 8.5 Hz), 7.86 (d, 2H, ar, J = 8.5 Hz), 7.75 (s, 1H, H-5), 7.63-7.51 (m, 4H, 2ar + NH_2), 7.36 (t, 1H, ar, J = 7.3 Hz). Anal.$C_{25}H_{18}N_6O_4$ (C, H, N).

*4.1.9. N^1-(4-(8-Amino-3-oxo-2-phenyl-2,3-dihydro-1,2,4-triazolo[4,3-a]pyrazin-6-yl)phenyl)-N^4-hydroxytereftalamide (**13**).*

1M BBr_3 solution in CH_2Cl_2 (0.87 mL) was slowly added at 0 °C, under nitrogen atmosphere, to a suspension of derivative **31** (0.17 mmol) in anhydrous CH_2Cl_2 (15 mL). The mixture was stirred at rt for 2h and the excess of BBr_3 was neutralized with methanol (10 ml). The solvent was removed at

reduced pressure and the resulting solid was collected by filtration, rinsed with water (20 ml) and purified by recrystallization from 2-methoxyethanol. Yield 62%; mp 275 °C dec ; ^{1}H NMR (DMSO-d_6) 11.40 (br s, 1H), 10.44 (br s, 1H, NH), 9.17 (br s, 1H, OH), 8.14-7.93 (m, 7H, ar), 7.94-7.82 (m, 3H, ar), 7.75 (s, 1H, H-5), 7.63-7.50 (m, 4H, 2ar + NH_2), 7.36 (t, 1H, J = 7.3 Hz). Anal.$C_{25}H_{19}N_7O_4$ (C, H, N).

*4.1.10. General procedure for the synthesis of N-(4-(8-amino-3-oxo-2-phenyl-2,3-dihydro-1,2,4-triazolo[4,3-a]pyrazin-6-yl)phenyl)-sulfamoylbenzamides **14** and **15**.*

A mixture of the 6-(4-aminophenyl)-substituted triazolopyrazine **30** [22] (1.0 mmol), the suitable sulfamoylbenzoic acid (2.4 mmol), 1-(3-(dimethylamino)-propyl))-3-ethylcarbodiimide hydrochloride (2.4 mmol), Et_3N (2.9 mmol) and 1-hydroxybenzotriazole (2.4 mmol), in anhydrous DMF (3 mL), was stirred for about 48h, at rt and under nitrogen atmosphere. The mixture was diluted with water (20 mL) and the obtained solid was collected by filtration, rinsed with water (10 mL), Et_2O (10 mL), dried and purified by column chromatography (**14**) or by recrystallization (**15**).

*4.1.10.1. N-(4-(8-Amino-3-oxo-2-phenyl-2,3-dihydro-1,2,4-triazolo[4,3-a]pyrazin-6-yl)phenyl)-4-sulfamoylbenzamide (**14**).*

Yield 20%; mp >300 °C (acetone); ^{1}H NMR (DMSO-d_6) 10.52 (br s, 1H, NH), 8.14-8.08 (m, 4H, ar), 7.99 (t, 4H, ar, J = 9.9 Hz), 7.86 (d, 2H, ar, J = 8.4 Hz), 7.76 (s, 1H, ar), 7.57-7.54 (m, 4H, ar), 7.54 (br s, 2H, NH_2), 7.36 (t, 1H, ar, J = 7.2 Hz). ^{13}C-NMR (DMSO-d_6) 164.95, 147.83, 147.63, 147.01, 139.23, 138.27, 137.97, 135.62, 132.38, 131.57, 129.65, 128.85, 126.75, 126.28, 126.15, 120.62, 119.85, 101.33. IR 1717, 1684, 1647, 1558, 1541. Anal.$C_{24}H_{19}N_7O_4S$ (C, H, N).

*4.1.10.2. N-(4-(8-Amino-3-oxo-2-phenyl-2,3-dihydro-1,2,4-triazolo[4,3-a]pyrazin-6-yl)phenyl)-3-sulfamoylbenzamide (**15**).* Yield 18%; eluent $CHCl_3$ 9.5/MeOH 0.1; mp >300 °C; ^{1}H NMR (DMSO-d_6) 10.59 (br s, 1H, NH), 8.41 (s, 1H, ar), 8.21 (d, 1H, ar, J = 7.7 Hz), 8.10-7.94 (m, 5H,

ar), 7.86 (d, 2H, ar, J = 8.6 Hz), 7.83-7.72 (m, 2H, ar), 7.62-7.52 (m, 4H, 2ar + NH_2), 7.50 (br s, 2H, SO_2NH_2), 7.36 (t, 1H, ar, J = 7.3 Hz). Anal.$C_{24}H_{19}N_7O_4S$ (C, H, N).

*4.4.11. 4-(((4-(8-Amino-3-oxo-2-phenyl-2,3-dihydro-1,2,4-triazolo[4,3-a]pyrazin-6-yl)phenyl)amino)methyl)benzenesulfonamide (**16**).*

4-(Bromomethyl)benzenesulfonamide [31] (2.0 mmol) was added to a suspension of the 6-(4-aminophenyl)-substituted triazolopyrazine **30 [**22] (1.6 mmol) and K_2CO_3 (3.0 mmol) in anhydrous THF (15 mL) and the mixture was heated at reflux. After 5h and 24h, other two portions of 4-(bromomethyl)benzenesulfonamide were added (2.0 mmol and 1.0 mmol, respectively). The heating was maintained for further 24h, then the solvent was evaporated at reduced pressure. The resulting solid was treated with water (20 ml), collected by filtration, washed with Et_2O (10 mL) and recrystallized from nitromethane. Yield 93%; mp > 300 °C; ^{1}H NMR (DMSO-d_6) 8.07 (d, 2H, ar, J = 7.7 Hz), 7.78 (d, 2H, ar, J = 8.3 Hz), 7.67 (d, 2H, ar, J = 8.6 Hz), 7.55 (m, 4H, ar), 7.47 (s, 1H, ar), 7.42 (br s, 2H, NH_2), 7.34 (t, 1H, ar, J = 7.4 Hz), 7.27 (br s, 2H, NH_2), 6.67-6.60 (m, 3H, 1ar + NH_2), 4.42-4.40 (m, 2H, CH_2). ^{13}C-NMR (DMSO-d_6) 148.89, 147.55, 144.98, 142.98, 138.02, 136.73, 135.15, 131.49, 129.63, 127.88, 126.92, 126.69, 126.20, 124.62, 119.85, 112.62, 98.94, 46.36. IR 3368, 1695, 1647, 1541, 1520, 1457. Anal.$C_{24}H_{21}N_7O_3S$ (C, H, N).

*4.1.12. 4-((4-(8-Amino-3-oxo-2-phenyl-2,3-dihydro-1,2,4-triazolo[4,3-a]pyrazin-6-il)phenyl)glicyl)benzensulfonamide (**17**).*

A mixture of 6-(4-aminophenyl)-substituted triazolopyrazine **30** [22] (0.31 mmol), 4-(2-bromoacetyl)benzenesulfonamide [29] (0.62 mmol) and K_2CO_3 (0.62 mmol) in anhydrous THF (15 mL) was refluxed for about 28h. The solvent was evaporated at reduced pressure and the resulting solid was suspended in water (10 mL). The suspension was acidified with 1N HCl until pH= 4 and the obtained solid was collected by filtration, washed with water (20 ml) and Et_2O and

recrystallized from acetone. Yield 23%; mp 235-237 °C dec; ^{1}H NMR (DMSO-d_6) 8.25 (d, 2H, ar, J = 8.2 Hz), 8.08 (d, 2H, ar, J = 8.0 Hz), 7.99 (d, 2H, ar, J = 8.3 Hz), 7.72 (d, 2H, ar, J = 8.4 Hz), 7.60–7.50 (m, 5H, 3ar + SO_2NH_2), 7.44 (br s, 2H, NH_2), 7.35 (t, 1H, ar, J = 7.3 Hz), 6.75 (d, 2H, ar, J = 8.5 Hz), 6.16-6.10 (m, 1H, NH), 4.79 (d, 2H, CH_2, J = 5.2 Hz). Anal.$C_{25}H_{21}N_7O_4S$ (C, H, N).

*4.1.13. N-(4-(8-Amino-3-oxo-2-phenyl-2,3-dihydro-1,2,4-triazolo[4,3-a]pyrazin-6-yl)phenyl)-3-((4-sulfamoylphenethyl)amino)propanamide (**18**).* A mixture the 6-(4-acrylamidophenyl)-substituted derivative **31** [24] (6.0 mmol) and 4-(2-aminoethyl)benzensulfonamide [32] (36.0 mmol) in anhydrous THF (15 mL) was refluxed for about 24h. The solvent was eliminated at reduced pressure and the resulting solid was rinsed with EtOH (5-10 mL), collected by filtration, and recrystallized from nitromethane. Yield 69%; mp 228-230 °C; ^{1}H NMR (DMSO-d_6) 10.15 (br s, 1H, NH), 8.08 (d, 2H, ar, J = 7.7 Hz), 7.90 (d, 2H, ar, J = 8.7 Hz), 7.73 (d, 2H, ar, J = 8.2 Hz), 7.69 (s, 1H, H-5), 7.62-7.54 (m, 6H, 4ar + NH_2), 7.42 (d, 2H, ar, J = 8.3 Hz), 7.36 (t, 1H, ar, J = 7.4 Hz), 7.28 (s, 2H, SO_2NH_2), 2.85 (t, 2H, CH_2, J = 6.6 Hz), 2.80 (br s, 4H, $2CH_2$), 2.46 (t, 2H, CH_2, J = 6.5 Hz). ^{13}C-NMR (DMSO-d_6) 170.95, 147.80, 147.62, 145.24, 142.29, 139.58, 137.98, 135.78, 131.56, 131.44, 129.65, 129.52, 126.75, 126.34, 126.09, 119.87, 119.32, 101.01, 50.76, 45.69, 37.36, 35.96. IR 3327, 3310, 1699, 1539, 1506, 1456. Anal.$C_{28}H_{28}N_8O_4S$ (C, H, N).

*4.1.14. N-(4-(8-Amino-3-oxo-2-phenyl-2,3-dihydro-1,2,4-triazolo[4,3-a]pyrazin-6-yl)phenyl)-3-((4-sulfamoylbenzyl)amino)propanamide (**19**).* A mixture of the 6-(4-(3-aminopropanamido)phenyl derivative **32** (1.00 mmol), prepared from derivative **31** as previously reported [24], 4-(bromomethyl)benzenesulfonamide [31] (0.5 mmol) and K_2CO_3 (2.00 mmol) in anhydrous THF (15 mL) was refluxed. After 5h and 11h, other two portions of 4-(bromomethyl)benzenesulfonamide were added (0.5 mmol and 0.2 mmol, respectively). The heating was maintained for further 13h. The solvent was eliminated at reduced pressure and the resulting solid suspended in water (10 mL). The suspension was acidified with HCl 1N until pH= 4 and the obtained solid was collected by

filtration, washed with water (20 ml) and Et_2O (10 mL) and purified by column chromatography. Yield 20%; eluent $CHCl_3$ 9.0/MeOH 1.0; mp 256-258 °C; ^{1}H NMR (DMSO-d_6) 10.14 (br s, 1H, NH), 8.08 (d, 2H, ar, J = 7.7 Hz), 7.91 (d, 2H, ar, J = 8.7 Hz), 7.78 (d, 2H, ar, J = 8.3 Hz), 7.70 (s, 1H, H-5), 7.64 (m, 2H, ar), 7.58-7.52 (m, 6H, ar + NH_2), 7.35 (t, 1H, ar, J = 7.4 Hz), 7.30 (br s, 2H, SO_2NH_2), 3.82 (s, 2H, CH_2), 2.81 (t, 2H, CH_2, J = 6.7 Hz), 2.53-2.51 (m, 2H, CH_2). ^{13}C-NMR (DMSO-d_6) 170.84, 147.79, 147.62, 145.24, 142.94, 139.59, 137.97, 135.74, 131.56, 131.45, 129.65, 128.73, 126.74, 126.33, 126.02, 119.85, 119.35, 101.01, 52.50, 45.14, 37.26. IR 3352, 3335, 3308, 3296, 1682, 1506. Anal.$C_{27}H_{26}N_8O_4S$ (C, H, N).

4.1.15. General procedure for the synthesis of sulfamoyl-substituted N-(3-((4-(8-amino-3-oxo-2-phenyl-2,3-dihydro-1,2,4-triazolo[4,3-a]pyrazin-6-yl)phenyl)amino)-3-oxopropyl)-benzamides ***20*** *and* ***21****.*

A mixture of the 6-(4-(3-aminopropanamido)-phenyl derivative **32** [24] (1.0 mmol), the suitable sulfamoylbenzoic acid (1.1 mmol), 1-(3-(dimethylamino)-propyl))-3-ethylcarbodiimide hydrochloride (1.1 mmol), triethylamine (1.1 mmol) and 1-hydroxybenzotriazole (1.1 mmol), in anhydrous DMF (3 mL), was stirred for about 2h, at rt and under nitrogen atmosphere. The mixture was diluted with water (20 mL) and the obtained solid was collected by filtration, rinsed with water (10 mL), Et_2O (10 mL), dried and purified by recrystallization (**20**) or by column chromatography (**21**).

*4.1.15.1. N-(3-((4-(8-Amino-3-oxo-2-phenyl-2,3-dihydro-1,2,4-triazolo[4,3-a]pyrazin-6-yl)phenyl)amino)-3-oxopropyl)-4-sulfamoylbenzamide (****20****).*

Yield 75%; mp 298-300 °C (nitromethane); ^{1}H NMR (DMSO-d_6) 10.09 (br s, 1H, NH), 8.81 (br s, 1H, NH), 8.08 (d, 2H, ar, J = 8.1 Hz), 8.00 (d, 2H, ar, J = 8.4 Hz), 7.93-7.89 (m, 4H, ar), 7.70-7.66 (m, 3H, ar), 7.58-7.55 (m, 2H, ar), 7.56 (br s, 2H, NH_2), 7.55 (br s, 2H, NH_2), 7.36 (t, 1H, ar, J = 7.1 Hz), 3.59 (t, 2H, CH_2, J = 6.9 Hz), 2.67 (t, 2H, CH_2, J = 6.8 Hz). IR 3365.78, 3282.84, 1683.86, 1647.21, 1558.48, 1521.84. Anal.$C_{27}H_{24}N_8O_5S$ (C, H, N).

*4.1.15.2. N-(3-((4-(8-Amino-3-oxo-2-phenyl-2,3-dihydro-1,2,4-triazolo[4,3-a]pyrazin-6-yl)phenyl)amino)-3-oxopropyl)-3-sulfamoylbenzamide (**21**).* Yield 24%; eluent $CHCl_3$ 9/MeOH 1; mp 272-274 °C. ^{1}H NMR (DMSO-d_6) 10.09 (br s, 1H, NH), 8.87 (br t, 1H, NH, J = 5.43 Hz), 8.32 (s, 1H, ar), 8.08-8.04 (m, 3H, ar), 7.96 (d, 1H, ar, J = 7.9 Hz), 7.91 (d, 2H, ar, J = 8.7 Hz), 7.69-7.65 (m, 4H, ar), 7.58-7.54 (m, 4H, 2ar + NH_2), 7.44 (s, 2H, SO_2NH_2), 7.35 (t, 1H, ar, J= 7.4 Hz), 3.62-3.57 (m, 2H, CH_2), 2.67 (t, 2H, CH_2, J = 6.8 Hz). ^{13}C-NMR (DMSO-d_6) 169.92, 165.63, 148.00, 147.61, 144.87, 139.55, 131.97, 135.73, 135.60, 131.56, 130.61, 129.66, 129.59, 128.57, 126.75, 126.32, 125.19, 119.86, 119.41, 101.03, 36.71, 36.54. Anal.$C_{27}H_{24}N_8O_5S$ (C, H, N).

*4.1.16. 4-(2-((2-(4-(8-Amino-3-oxo-2-phenyl-2,3-dihydro-1,2,4-triazolo[4,3-a]pyrazin-6-yl)phenoxy)ethyl)amino)ethyl)benzensulfonamide (**22**).*

A mixture of the 6-(4-(2-aminoethoxy)phenyl)triazolopyrazine **33** [24] (1 mmol), 4-(2-bromomethyl)benzenesulfonamide [31] (4 mmol) and K_2CO_3 (4 mmol) in anhydrous THF (15 mL) was refluxed for about 48h. The solvent was evaporated at reduced pressure and the obtained solid was collected by filtration, washed with water (20 mL) and Et_2O (10 mL) and purified by column chromatography. Yield 26%; eluent (CH_2Cl_2 9.5/MeOH 0.5); mp 239-241 °C; ^{1}H NMR (DMSO-d_6) 8.08 (d, 2H, ar, J = 7.7 Hz), 7.90 (d, 2H, ar, J = 8.8 Hz), 7.74 (d, 2H, ar, J = 8.3 Hz), 7.65 (s, 1H, H-5), 7.58-7.53 (m, 4H, ar + NH_2), 7.43 (d, 2H, ar, J = 8.3 Hz), 7.36 (t, 1H, ar, J = 7.4 Hz), 7.27 (br s, 2H, NH_2), 6.98 (d, 2H, ar, J = 8.9 Hz), 4.06 (t, 2H, CH_2, J = 5.6 Hz), 2.93 (t, 2H, CH_2, J = 5.6 Hz), 2.86-2.82 (m, 4H). ^{13}C-NMR (DMSO-d_6) 158.06, 147.77, 147.65, 145.71, 142.48, 137.99, 135.83, 131.82, 129.66, 129.57, 129.46, 127.31, 126.75, 126.15, 119.87, 114.93, 100,61, 50.47, 48.05, 35.18, 30,37. IR 3325, 1715, 1700, 1541, 1506, 1457. Anal.$C_{27}H_{27}N_7O_4S$ (C, H, N).

*4.1.17. N-(2-(4-(8-Amino-3-oxo-2-phenyl-2,3-dihydro-1,2,4-triazolo[4,3-a]pyrazin-6-yl)phenoxy)ethyl)-4-sulfamoylbenzamide (**23**).*

A mixture of the 6-(4-(2-aminoethoxy)phenyl)triazolopyrazine **33** [24] (0.55 mmol), 4-sulfamoylbenzoic acid (0.61 mmol), 1-(3-(dimethylamino)-propyl))-3-ethylcarbodiimide hydrochloride (0.63 mmol), triethylamine (0.93 mmol) and 1-hydroxybenzotriazole (0.63 mmol), in anhydrous DMF (3 mL), was stirred for about 2h, at rt and under nitrogen atmosphere. The mixture was diluted with water (20 mL) and the obtained solid was collected by filtration, rinsed with water (10 mL), Et_2O (10 mL), dried and purified by column chromatography. Yield 30%; eluent CH_2Cl_2 9.5/MeOH 0.5; mp 178-182 °C; ^{1}H NMR (DMSO-d_6) 8.93 (m, 1H, NH), 8.07 (d, 2H, ar, J = 7.8 Hz), 8.03 (d, 2H, ar, J = 8.4 Hz), 7.95-7.87 (m, 4H, ar), 7.67 (s, 1H, H-5), 7.72-7.55 (m, 4H, 2ar + NH_2), 7.50 (s, 2H, $SONH_2$), 7.35 (t, 1H, ar, J = 7.4 Hz), 7.02 (d, 2H, ar, J = 8.8 Hz), 4.19 (t, 2H, CH_2, J = 5.5 Hz), 3.72-3.64 (m, 2H, CH_2). ^{13}C-NMR (DMSO-d_6) 166.01, 158.92, 147.77, 147.61, 146.77, 137.98, 137.60, 135.78, 131.53, 129.66, 129.46, 128.38, 127.32, 126.75, 126.11, 119.85, 114.92, 100.61, 66.45, 65.38. Anal.$C_{26}H_{23}N_7O_5S$ (C, H, N).

*4.1.18. Ethyl 5-oxo-4-(2-oxo-2-(4-sulfamoylphenyl)ethyl)-1-phenyl-4,5-dihydro-1H-1,2,4-triazolo-3-carboxylate (**26**).*

4-(2-Bromoacetyl)benzenesulfonamide **25** [29] (1.2 mmol) was added dropwise to a mixture of ethyl 1,2,4-triazole-3-carboxylate derivative **24** [28] (1.0 mmol) and potassium carbonate (2.0 mmol) in DMF/CH_3CN (1:9, 10 mL). The suspension was stirred at rt for 4h. The solvent removed at reduced pressure and the residue was treated with water (20 mL). The resulting precipitate was collected by filtration, washed with water (30 mL) and Et_2O (20 mL). This intermediate was pure enough (NMR, TLC) to be used for the next step without further purification. Yield 91%; ^{1}H NMR (DMSO-d_6) 8.29 (d, 2H, ar, J = 8.3 Hz), 8.03 (d, 2H, ar, J = 8.4 Hz), 7.94 (d, 2H, ar, J = 8.1 Hz), 7.63 (br s, 2H, $SONH_2$), 7.56 (t, 1H, ar, J = 7.9 Hz), 7.37 (t, 1H, ar, J = 7.4 Hz), 5.63 (s, 2H, CH_2), 4.29 (q, 2H, CH_2, J = 7.1 Hz), 1.20 (t, 3H, CH_3, J = 7.1 Hz).

*4.1.19. 3,8-Dioxo-2-phenyl-2,3,7,8-tetrahydro-1,2,4-triazolo[4,3-a]pyrazine-6-sulfonamide (**27**).* A mixture of the ethyl 1,2,4-triazole-3-carboxylate derivative **26** (1 mmol) and anhydrous ammonium acetate (7 mmol) was heated in a sealed tube at 140 °C for 4h. The residue was taken up with EtOH (1 mL) and Et_2O (5 mL), collected by filtration, washed with water (20 mL) and recrystallized from 2-methoxyethanol. Yield 60%; ^{1}H NMR (DMSO-d_6) 11.74 (s, 1H, NH), 8.02 (d, 2H, ar, J = 7.9 Hz), 7.95-7.85 (m, 4H, ar), 7.57 (t, 2H, ar, J = 7.9 Hz), 7.52-7.43 (m, 3H, H-5 + $SONH_2$), 7.37 (t, 1H, ar, J = 7.4 Hz). ^{13}C-NMR (DMSO-d_6) 153.49, 147.77, 144.83, 137.65, 135.98, 134.54, 129.81, 127.38, 127.13, 126.99, 126.43, 119.58, 101.81. Anal. Calcd. for $C_{17}H_{13}N_5O_4S$ (C, H, N).

*4.1.20. N^1-((3,8-Dioxo-2-phenyl-2,3,7,8-tetrahydro-1,2,4-triazolo[4,3-a]pyrazin-6-yl)sulfonyl)-N,N-dimethylformimidamide (**28**).* N,N-dimethylformamide dimethylacetal (2 mmol) was added dropwise to a mixture of the benzensulfonamide derivative **27** (1 mmol) in DMF (2 mL) at 0 °C. The mixture was stirred at rt for 20 min, then treated with water (15 mL) and extracted with CH_2Cl_2 (15 mL x 3). The organic phase was washed with water (20 mL x 3) and anhydrified (Na_2SO_4). The solvent was eliminated at reduced pressure and the resulting solid was collected by filtration and dried. This intermediate was pure enough (NMR, TLC) to be used for the next step without further purification. Yield 70%; ^{1}H NMR (DMSO-d_6) 11.71 (s, 1H, NH), 8.27 (s, 1H, CH), 8.01 (d, 2H, J = 7.7 Hz), 7.85 (q, 4H, ar, J = 8.7 Hz), 7.57 (t, 2H, ar, J = 8.0 Hz), 7.44 (s, 1H, H-5), 7.37 (t, 1H, ar, J = 7.4 Hz), 3.17 (s, 3H, CH_3), 2.93 (s, 3H, CH_3). ^{13}C-NMR (DMSO-d_6) 160.42, 153.45, 147.75, 143.79, 137.64, 135.96, 134.46, 129.81, 127.48, 127.10, 126.99, 126.76, 119.57, 101.84, 41.43, 40.60, 40.40, 40.19, 39.98, 39.77, 39.56, 39.35, 35.59.

*4.1.21. N^1-((8-Chloro-3-oxo-2-phenyl-2,3-dihydro-1,2,4-triazolo[4,3-a]pyrazin-6-yl)sulfonyl)-N,N-dimethylformimidamide (**29**).*

A suspension of the 3,8-dioxo-triazolopyrazine derivative **28** (1 mmol) in phosphorus oxychloride (2 mL) was heated in a sealed tube at 160 °C for 1h. The excess of phosphorus oxychloride was

distilled off and the residue was treated with cyclohexane. The obtained solid was collected by filtration, washed with abundant water and dried. This intermediate was pure enough (NMR, TLC) to be used for the next step without further purification. Yield 85%; ^{1}H NMR (DMSO-d_6) 8.78 (s, 1H, CH), 8.26 (s, 1H, H_5), 8.20 (d, 2H, ar, J = 8.4 Hz), 8.06 (d, 2H, ar, J = 7.9 Hz), 7.86 (d, 2H, ar, J = 8.4 Hz), 7.60 (t, 2H, ar, J = 7.8 Hz), 7.41 (t, 1H, ar, J = 7.4 Hz), 3.17 (s, 3H, CH_3), 2.93 (s, 3H, CH_3).

*4.1.22. N^1-(4-(8-Amino-3-oxo-2-phenyl-2,3-dihydro-1,2,4-triazolo[4,3-a]pyrazin-6-yl)phenyl)-N^4-(benzyloxy)tereftalamide (**31**).* Et_3N (0,21 mmol) was added to a solution of O-benzylhydroxylamine HCl (0.21 mmol) in anhydrous DMF (3 mL) and the mixture was stirred at rt. After 15 min, the carboxylic acid **12** (0.21 mmol), 1-(3-(dimethylamino)-propyl))-3-ethylcarbodiimide hydrochloride (0.42 mmol), Et_3N (0.52 mmol) and 1-hydroxybenzotriazole (0.42 mmol) were added and the suspension was stirred at rt for 3h. The mixture was diluted with water (20 mL) and the obtained solid was collected by filtration, rinsed with water (3 mL), Et_2O (10 mL), dried and used for the next step without further purification. Yield 62%; ^{1}H NMR (DMSO-d_6) 11.85 (br s, 1H, NH), 10.45 (br s, 1H, NH), 8.17-7.9 (m, 5H, ar), 7.92-7.82 (m, 4H, ar), 7.75 (s, 1H, H-5), 7.65-7.50 (m, 5H, ar), 7.49-7.44 (m, 2H, ar), 7.43-7.31 (m, 4H, ar), 4.97 (s, 2H, CH_2).

4.2. Molecular Modeling at ARs.

4.2.1. Refinement of the hA_{2A} AR Structures. The crystal structure of the hA_{2A} AR in complex with ZM241385 was retrieved from the Protein Data Bank (http://www.rcsb.org; pdb code: 5NM4; 1.7-Å resolution [33]) and added of all hydrogen atoms within MOE (Molecular Operating Environment 2014.09) [34].

4.5.2. Molecular docking analysis. All compound structures were docked into the binding site of the AR structures using the Induced Fit docking protocol of MOE and the genetic algorithm docking

tool of CCDC Gold [33,34]. The Induced Fit docking protocol of MOE is divided into a number of stages: *Conformational Analysis of ligands*. The algorithm generated conformations from a single 3D conformation by conducting a systematic search. In this way, all combinations of angles were created for each ligand. *Placement*. A collection of poses was generated from the pool of ligand conformations using Alpha Triangle placement method. Poses were generated by superposition of ligand atom triplets and triplet points in the receptor binding site. The receptor site points are alpha sphere centers which represent locations of tight packing. At each iteration, a random conformation was selected, a random triplet of ligand atoms and a random triplet of alpha sphere centers were used to determine the pose. *Scoring*. Poses generated by the placement methodology were scored using the *Alpha HB* scoring function, which combines a term measuring the geometric fit of the ligand to the binding site and a term measuring hydrogen bonding effect. *Induced Fit*. The generated docking conformations were subjected to energy minimization within the binding site and the protein sidechains are included in the refinement stage. In detail, the protein backbone is set as rigid while the side chains are not set to "free to move" but are set to "tethered", where an atom tether is a distance restraint that restrains the distance not between two atoms but between an atom and a fixed point in space. *Rescoring*. Complexes generated by the Induced Fit methodology stage were scored using the *Alpha HB* scoring function. Gold tool was used with default efficiency settings through MOE interface, by selecting ChemScore as scoring function.

4.3. Molecular Modeling at CAs.

The crystal structure of hCA II (PDB 5LJT) [36], hCA IX (PDB 5FL4) [37] and XII (pdb JLD0) [38] were prepared using the Protein Preparation Wizard tool implemented in Maestro - Schrödinger suite, assigning bond orders, adding hydrogens, deleting water molecules, and optimizing H-bonding networks [39]. Energy minimization protocol with a root mean square deviation (RMSD) value of 0.30 was applied using an Optimized Potentials for Liquid Simulation (OPLS3e) force field. 3D ligand structures were prepared by Maestro [39a] and evaluated for their

ionization states at pH 7.4 with Epik [39b]. OPLS3e force field in Macromodel [39e] was used for energy minimization for a maximum number of 2500 conjugate gradient iteration and setting a convergence criterion of 0.05 kcal $mol^{-1}Å^{-1}$. The docking grid was centered on the center of mass of the co-crystallized ligands and Glide used with default settings. Ligands were docked with the standard precision mode (SP) of Glide [39f] and the best 5 poses of each molecule retained as output. The best pose for each compound, evaluated in terms of coordination, hydrogen bond interactions and hydrophobic contacts, was refined with Prime [39d] with a VSGB solvation model considering the target flexible within 3Å around the ligand [40-42].

4.4. Pharmacology

4.4.1. Binding Assay at ARs.

4.4.1.1 Membrane preparation.

Membranes for radioligand binding were prepared as described earlier [24]. In brief, after homogenization of CHO (Chinese Hamster Ovary) cells, stably transfected with hARs, membranes were prepared in a two-step procedure. A first low-speed step (1000 g), where cell fragments and nuclei were removed, was followed by a high-speed centrifugation (100 000g) to sediment the crude membrane fraction. The resulting membrane pellets were resuspended in the buffer used for the respective binding experiments (hA_1 ARs: 50 mM Tris/HCl buffer pH 7.4; hA_{2A} ARs: 50 mM Tris/HCl, 50 mM $MgCl_2$ pH 7.4; hA_3 ARs: 50 mM Tris/HCl, 10 mM $MgCl_2$, 1 mM EDTA, pH 8.25), frozen in liquid nitrogen, and stored in aliquots at −80 °C.

4.4.1.2. Radioligand binding.

The affinity of compounds **1**–**23** for the hAR subtypes, hA_1, hA_{2A}, hA_3, was determined with radioligand competition experiments in CHO cells that were stably transfected with the individual receptor subtypes. The radioligands used were 1.0 nM [^{3}H]CCPA) for hA_1, 10 nM [^{3}H]NECA for hA_{2A} and 1.0 nM [^{3}H]HEMADO for hA_3 receptors. Results were expressed as K_i values

(dissociation constants), which were calculated with the program GraphPad (GraphPAD Software, San Diego, CA, USA). Each concentration was tested three-five times in triplicate and the values are given as the mean ± standard error (S.E.).

The potency of antagonists at the hA_{2B} receptor (expressed on CHO cells) was determined by inhibition of NECA- stimulated adenylyl cyclase activity.

4.4.2. GloSensor cAMP Assay.

Functional A_{2A} and A_{2B} activity was determined as described earlier [43,44]. Briefly, cells stably expressing the hA_{2A} or hA_{2B} AR and transiently the biosensor, were harvested and incubated in equilibration medium containing a 3% v/v GloSensor cAMP reagent stock solution, 10% FBS, and 87% CO_2 independent medium. After 2h of incubation at rt, cells were dispensed in the wells of a 384-well plate and NECA reference agonist or the understudy compounds, at different concentrations, were added. When compounds were unable to stimulate the cAMP production they were studied as antagonists. In particular, the antagonist profile was evaluated by assessing the ability of these compounds to counteract NECA-induced increase of cAMP accumulation.

Responses were expressed as percentage of the maximal relative luminescence units (RLU). Concentration–response curves were fitted by a nonlinear regression with the Prism programme. The antagonist profile of the compounds was expressed as IC_{50}, which is the concentration of antagonists that produces 50% inhibition of the agonist effect. Each concentration was tested three-five times in triplicate and the values are given as the mean ± S.E. [45].

4.5. CA inhibition Assay

An applied photophysics stopped-flow instrument has been used for assaying the hCA catalyzed CO_2 hydration activity [46]. Phenol red (at a concentration of 0.2 mM) has been used as indicator, working at the absorbance maximum of 557 nm, with 20 mM Hepes (pH 7.4) as buffer, and 20 mM Na_2SO_4

for maintaining constant the ionic strength (this anion is not inhibitory and has a K_i> 200mM against these enzymes), following the initial rates of the CA-catalyzed CO_2 hydration reaction for a period of 10–100 s. The CO_2 concentrations ranged from 1.7 to 17 mM for the determination of the kinetic parameters and inhibition constants. For each measurement three traces of the initial 5–10% of the reaction have been used for determining the initial velocity (which was the mean of the three traces), working with 10-fold decreasing inhibitor concentrations ranging between 0.1nM and 10–100 mM (depending on the inhibitor potency, but at least five points at different inhibitor concentrations were employed for determining the inhibition constants). The uncatalyzed rates were determined in the same manner and subtracted from the total observed rates. Stock solutions of inhibitor (0.1 mM) were prepared in distilled-deionized water with 10% DMSO and dilutions up to 0.1 nM were done thereafter with the assay buffer. Inhibitor and enzyme solutions were preincubated together for 15 min at room temperature prior to assay, in order to allow for the formation of the E-I complex. The inhibition constants were obtained by non-linear least-squares methods using the Cheng–Prusoff equation, and represent the mean from three independent experiments. All human isoforms were recombinant enzymes produced as described earlier in our laboratory [47-49].

Funding. The work was financially supported by the University of Florence (Fondi Ateneo Ricerca 2018).

Declaration of interests

The authors declare that they have no known competing financial interests or personal relationships that could have appeared to influence the work reported in this paper.

References

1. V. Ivasiv, C. Albertini, A.E. Goncalves, M. Rossi, M.L. Bolognesi, Molecular Hybridization as a Tool for Designing Multitarget Drug Candidates for Complex Diseases, Curr. Top. Med. Chem. 19 (2019) 1694-1711.
2. L. Antonioli, C. Blandizzi, P. Pacher, G. Haskò, Immunity, inflammation and cancer: a leading role for adenosine, Nature 13 (2013) 842-865.
3. P.A. Borea, S. Gessi, S. Merighi, F. Vincenzi, K. Varani, Pathological Overproduction: the Bad Side of Adenosine, Br. J. Pharmacol. 174 (2017) 1945−1960.
4. B. Allard, P.A Beavis, P.K. Darcy, J. Stagg. Immunosuppressive activities of adenosine in cancer, Curr. Opin. Pharmacol. 29 (2016) 7-16.
5. R.D. Leone, A.E. Leisha, Targeting adenosine for cancer immunotherapy, J. Immunother. Cancer 6 (2018) 6, 57.
6. D. Neri, C.T. Supuran, Interfering with pH regulation in tumors as a therapeutic strategy, Nat Rev. Drug Discovery 2011, 10, 767-777.
7. C.T. Supuran, Carbonic anhydrases: Novel therapeutic applications for inhibitors and activators. Nat. Rev. Drug Discovery 7 (2008) 168−181.
8. C.T. Supuran, Carbonic Anhydrase Inhibition and the Management of Hypoxic Tumors, Metabolites 7 (2017) 48.
9. C.T. Supuran, Carbonic anhydrase inhibitors as emerging agents for the treatment and imaging hypoxic tumors, Exp. Opin. Invest. Drugs 27 (2018) 963–970.
10. J. Stagg, M.J. Smyth, Extracellular adenosine triphosphate and adenosine in cancer, Oncogene 29 (2010) 5346-5358.
11. S. Merighi, E. Battistello, L. Giacomelli, K. Varani, F. Vincenzi, P.A. Borea, S. Gessi, Targeting A_3 and A_{2A} adenosine receptors in the fight against cancer, Exp. Opin. Ther. Targets, 23 (2019) 669-678.

12. S. Gessi, S. Bencivenni, E. Battistello, F. Vincenzi, V. Colotta, D. Catarzi, F. Varano, S. Merighi, P.A. Borea, K. Varani, Inhibition of A_{2A} Adenosine Receptor Signaling in Cancer Cells Proliferation by the Novel Antagonist TP455. Front. Pharmacol. 8 (2017) 888.
13. L. Fong, A. Hotson, J.D. Powderly, M. Sznol, R S. Heist, T.K. Choueiri, S. George, B.G.M. Hughes, M.D. Hellmann, D.R. Shepard, B.I. Rini, S. Kummar, A.M. Weise, M.J. Riese, B. Markman, L.A. Emens, D. Mahadevan, J.J. Luke, G. Laport, J.D. Brody, L. Hernandez-Aya, P. Bonomi, J.W. Goldman, L. Berim, D.J. Renouf, R.A. Goodwin, B. Munneke, P.Y. Ho, J. Hsieh, I. McCaffery, L. Kwei, S.B. Willingham, R.A. Miller, Adenosine A_{2A} Receptor Blockade as an Immunotherapy for Treatment-Refractory Renal Cell Cancer, Cancer Discov. 2019. doi: 10.1158/2159-8290.
14. C.T. Supuran, Advances in structure-based drug discovery of carbonic anhydrase inhibitors, Exp. Opin. Drug Discovery, 12 (2017) 61-88.
15. F. Varano, D. Catarzi, F. Vincenzi, M. Betti, M. Falsini, A. Ravani, P.A. Borea, V. Colotta, K. Varani, Design, Synthesis, and Pharmacological Characterization of 2‑(2-Furanyl)thiazolo[5,4-*d*]pyrimidine-5,7-diamine derivatives: new highly potent A_{2A} adenosine receptor inverse agonists with antinociceptive activity, J. Med. Chem. 59 (2016) 10564-10576.
16. D. Poli, M. Falsini, F. Varano, M. Betti, K. Varani, F. Vincenzi, A.M. Pugliese, F. Pedata, D. Dal Ben, A. Thomas, I. Palchetti, F. Bettazzi, D. Catarzi, V. Colotta. Imidazo[1,2-a]pyrazin-8-amine core for the design of new adenosine receptor antagonists: Structural exploration to target the A_3 and A_{2A} subtypes, Eur. J. Med. Chem, 125 (2017) 611-628.
17. L. Squarcialupi, M. Betti, D. Catarzi, F. Varano, M. Falsini, A. Ravani, S. Pasquini, F. Vincenzi, V. Salmaso, M. Sturlese, K. Varani, S. Moro, V Colotta. The role of 5-arylalkylamino- and 5-piperazino- moieties on the 7-aminopyrazolo[4,3-*d*]pyrimidine core in affecting adenosine A_1 and A_{2A} receptor affinity and selectivity Profiles, J. Enz. Inhib. Med. Chem. 32 (2017) 248-263.

18. M. Falsini, L. Squarcialupi, D. Catarzi, F. Varano, M. Betti, D. Dal Ben, G. Marucci, M. Buccioni, R. Volpini, T. De Vita, A. Cavalli, V. Colotta, The 1,2,4-triazolo[4,3-a]pyrazin-3-one as a versatile scaffold for the design of potent adenosine human receptor antagonists. Structural investigations to target the A_{2A} Receptor, J. Med. Chem. 60 (2017) 5772-5790.
19. F. Varano, D. Catarzi, M. Falsini, F. Vincenzi, S. Pasquini, K. Varani, V. Colotta, Identification of novel thiazolo[5,4-d]pyrimidine derivatives as human A_1 and A_{2A} adenosine receptor antagonists/inverse agonists, Bioorg. Med. Chem. 26 (2018) 3688-3695.
20. F. Varano, D. Catarzi, F. Vincenzi, M. Falsini, S. Pasquini, P.A. Borea, V. Colotta, K. Varani, Structure-activity relationship studies and pharmacological characterization of N5-heteroarylalkyl-substituted-2-(2-furanyl)thiazolo[5,4-d]pyrimidine-5,7-diamine-based derivatives as inverse agonists at human A_{2A} adenosine receptor, Eur. J. Med. Chem. 155 (2018) 552-561.
21. F. Varano, D. Catarzi, M. Falsini, D. Dal Ben, M. Buccioni, G. Marucci, R. Volpini, V. Colotta, Novel human adenosine receptor antagonists based on the 7-amino-thiazolo[5,4-d]pyrimidine scaffold. Structural investigations at the 2-, 5- and 7-positions to enhance affinity and tune selectivity, Bioorg. Med. Chem. Lett. 29 (2019) 563-569.
22. M. Falsini, D. Catarzi, F. Varano, D. Dal Ben, G. Marucci, M. Buccioni, R. Volpini, L. Di Cesare Mannelli, C. Ghelardini, V. Colotta, Novel 8-amino-1,2,4-triazolo[4,3-a]pyrazin-3-one derivatives as potent human adenosine A_1 and A_{2A} receptor antagonists. Evaluation of their protective effect against □-amyloid-induced neurotoxicity in SH-SY5Y cells, Bioorg. Chem. 87 (2019) 380-394.
23. M. Betti, D. Catarzi, F. Varano, M. Falsini, K. Varani, F. Vincenzi, S. Pasquini, L. Di Cesare Mannelli, C. Ghelardini, E. Lucarini, D. Dal Ben, A. Spinaci, G. Bartolucci, M. Menicatti, V. Colotta, Modifications on the amino-3,5-dicyanopyridine core to obtain multifaceted adenosine receptor ligands with antineuropathic activity, J. Med. Chem. 62 (2019) 6894-6912.

24. M. Falsini, D. Catarzi, F. Varano, C. Ceni, D. Dal Ben, G. Marucci, M. Buccioni, R. Volpini, L. Di Cesare Mannelli, E. Lucarini, C. Ghelardini, G. Bartolucci, M. Menicatti, V. Colotta, Antioxidant-conjugated 1,2,4-triazolo[4,3-a]pyrazin-3-one derivatives: highly potent and selective human A_{2A} adenosine receptor antagonists possessing protective efficacy in neuropathic pain, J. Med. Chem. 62 (2019) 8511-8531.
25. A. Bonardi, M. Falsini, D. Catarzi, F. Varano, L. Di Cesare Mannelli, B. Tenci, C. Ghelardini, A. Angeli C.T. Supuran, V. Colotta, Structural investigations on coumarins leading to chromeno[4,3-c]pyrazol-4-ones and pyrano[4,3-c]pyrazol-4-ones: new scaffolds for the design of the tumor-associated carbonic anhydrase isoforms IX and XII, Eur. J. Med. Chem. 146 (2018) 47-59.
26. M. Falsini, L. Squarcialupi, D. Catarzi, F. Varano, M. Betti, L. Di Cesare Mannelli, B. Tenci, C. Ghelardini, M. Tanc, A. Angeli, C.T. Supuran, V. Colotta, 3-Hydroxy-1H-quinazoline-2,4-dione as a new scaffold to develop potent and selective inhibitors of the tumor-associated carbonic anhydrases IX and XII, J. Med. Chem. 60 (2017) 6428-6439.
27. A. Karioti, F. Carta, C.T. Supuran, Phenol and poliphenols as carbonic anhydrases inhibitors, Molecules, 21 (2016) 1649.
28. V.S. Matiychuk, M.A. Potopnyk, R. Luboradzki, M.D. Obushak, A New method for the synthesis of 1-aryl-1,2,4-triazole derivatives, Synthesis 11 (2011) 1799–1803.
29. M. Scobie, O. Wallner, T. Koolmeister, K.S.A. Vallin, C.M. Henriksson, S. Jacques, E. Homan, T. Helleday, Diaminopyrimidines as MTH-1 inhibitors for treatment of cancer and their preparation, WO 2015187088, A1 20151210
30. E.-D. Chenot, D. Bernardi, A. Comel, G. Kirsch, Preparation of monoalkyl terephthalates: an overview, Synth. Comm. 37 (2007) 483-490.
31. R. Guillon, F. Pagniez, F. Giraud, D. Crepin, C. Picot, M. LeBorgne, F. Morio, M. Duflos, C. Loge, P. LePape, Design, synthesis, and in vitro antifungal activity of 1-[(4-Substituted-

benzyl)methylamino]-2-(2,4-difluorophenyl)-3-(1H-1,2,4-triazol-1-yl)propan-2-ols, Chem.Med.Chem, 6 (2011) 816-825.

32. G.W. Hardy, L.A. Lowe, G. Mills, P.Y. Sang, D.S.A. Simpkin, R.L. Follenfant, C. Shankley, T.W. Smith, Peripherally acting enkephalin analogues. 2. Polar tri- and tetrapeptides, J. Med. Chem. 32 (1989) 1108-1118.
33. T. Weinert, N. Olieric, R. Cheng, S. Brunle, D. James, D. Ozerov, D. Gashi, L. Vera, M. Marsh, K. Jaeger, F. Dworkowski, E. Panepucci, S. Basu, P. Skopintsev, A.S. Dore, T. Geng, R.M. Cooke, M. Liang, A.E. Prota, V. Panneels, P. Nogly, U. Ermler, G. Schertler, M. Hennig, M.O. Steinmetz, M. Wang, J. Standfuss, Serial millisecond crystallography for routine room-temperature structure determination at synchrotrons, Nat. Commun. 8 (2017) 542.
34. Molecular Operating Environment, C.C.G., Inc., 1255 University St., Suite 1600, Montreal, Quebec, Canada, H3B 3X3.
35. G. Jones, P. Willett, R.C. Glen, A.R. Leach, R. Taylor, Development and validation of a genetic algorithm for flexible docking, J. Mol. Biol. 267 (1997) 727-748.
36. A. Nocentini, M. Ferraroni, F. Carta, M. Ceruso, P. Gratteri, C. Lanzi, E. Masini, C.T. Supuran, Benzenesulfonamides incorporating flexible triazole moieties are highly effective carbonic anhydrase inhibitors: synthesis and kinetic, crystallographic, computational, and intraocular pressure lowering investigations, J. Med. Chem. 59 (2016) 10692e10704.
37. J. Leitans, A. Kazaks, A. Balode, J. Ivanova, R. Zalubovskis, C.T. Supuran, K. Tars, Efficient expression and crystallization system of cancer-associated carbonic anhydrase isoform IX, J. Med. Chem. 58 (2015) 9004e9009.
38. D.A. Whittington, A. Waheed, B. Ulmasov, G.N. Shah, J.H. Grubb, W.S. Sly, D.W. Christianson. Crystal structure of the dimeric extracellular domain of human carbonic anhydrase XII, a bitopic membrane protein overexpressed in certain cancer tumor cells. Proc. Natl. Acad. Sci. U S A. 2001; 98:9545-50.

39. Schrödinger Suite Release 2019-1, Schrödinger, LLC, New York, NY, 2018: (a) Maestro v.11.9; (b) Epik, v.4.7; (c) Impact, v.8.2; (d) Prime, v.5.5; (e) Macromodel v.12.3. (f) Glide, v.8.2.

40. A. Nocentini, P. Gratteri. C.T. Supuran, Phosphorus versus Sulfur: Discovery of Benzenephosphonamidates as Versatile Sulfonamide-Mimic Chemotypes Acting as Carbonic Anhydrase Inhibitors, Chemistry 25 (2019) 1188-1192.

41. S. Bua, L. Lucarini, L. Micheli, M. Menicatti, G. Bartolucci, S. Selleri, L. Di Cesare Mannelli, C. Ghelardini, E. Masini, F. Carta, P. Gratteri, A. Nocentini, C.T. Supuran, Bioisosteric Development of Multi-target Nonsteroidal Anti-inflammatory Drug - Carbonic Anhydrases Inhibitor Hybrids for the Management of Rheumatoid Arthritis, J. Med. Chem. 2019, doi: 10.1021/acs.jmedchem.9b01130.

42. A. Nocentini, F. Carta, M. Tanc, S. Selleri, C.T. Supuran. C. Bazzicalupi, P. Gratteri, Deciphering the Mechanism of Human Carbonic Anhydrases Inhibition with Sulfocoumarins: Computational and Experimental Studies, Chemistry 24 (2018) 7840-7844.

43. A. Thomas, M. Buccioni, D. Dal Ben, C. Lambertucci, G. Marucci, C. Santinelli, A. Spinaci, S. Kachler, K.-N. Klotz, R. Volpini, The length and flexibility of the 2-substituent of 9-ethyladenine derivatives modulate affinity and selectivity for the human A_{2A} adenosine receptor, Chem. Med. Chem. 11 (2016) 1829-1839.

44. M. Buccioni, C. Santinelli, P. Angeli, D. Dal Ben, C. Lambertucci, A. Thomas, R. Volpini, G. Marucci, Overview on Radiolabel-Free in vitro Assays for GPCRs. Mini Rev. Med. Chem. 17 (2017) 3-14.

45. M. Buccioni, G. Marucci, D. Dal Ben, D. Giacobbe, C. Lambertucci, L. Soverchia, A. Thomas, R. Volpini, G. Cristalli, Innovative functional cAMP assay for studying G protein-coupled receptors: application to the pharmacological characterization of GPR17, Purinerg. Signal. 7 (2011) 463-468.

46. R.G. Khalifah, The carbon dioxide hydration activity of carbonic anhydrase. I. Stop-flow kinetic studies on the native human isoenzymes B and C, J. Biol. Chem. 246 (1971) 2561-2567.
47. M. Ferraroni, F. Carta, A. Scozzafava, C.T. Supuran, Thioxocoumarins show an alternative carbonic anhydrase inhibition mechanism compared to coumarins, J. Med. Chem. 59 (2016) 462-473.
48. A. Scozzafava, F. Briganti, G. Mincione, L. Menabuoni, F. Mincione, C. T. Supuran, Carbonic anhydrase inhibitors: synthesis of water-soluble, aminoacyl/dipeptidyl sulfonamides possessing long-lasting intraocular pressure-lowering properties via the topical route, J. Med. Chem. 42 (1999) 3690-3700.
49. F. Carta, L. Di Cesare Mannelli, M. Pinard, C. Ghelardini, A. Scozzafava, R. McKenna, C. T. Supuran, A class of sulfonamide carbonic anhydrase inhibitors with neuropathic pain modulating effects, Bioorg. Med. Chem. 23 (2015) 1828-1840.

*Revised Manuscript
Click here to view linked References

Discovery of first-in-class multi-target adenosine A_{2A} receptor antagonists-carbonic anhydrase IX and XII inhibitors. 8-Amino-6-aryl-2-phenyl-1,2,4-triazolo[4,3-a]pyrazin-3-one derivatives as new potential antitumor agents

Costanza Ceni,[a] Daniela Catarzi,[a] Flavia Varano,[a] Diego Dal Ben,[b] Gabriella Marucci,[b] Michela Buccioni,[b] Rosaria Volpini,[b] Andrea Angeli,[a] Alessio Nocentini,[a,c] Paola Gratteri,[a] Claudiu T. Supuran,[a] Vittoria Colotta[a*]

[a]*Dipartimento di Neuroscienze, Psicologia, Area del Farmaco e Salute del Bambino, Sezione di Farmaceutica e Nutraceutica, Università degli Studi di Firenze, Via Ugo Schiff, 6, 50019 Sesto Fiorentino, Italy.*

[b]*Scuola di Scienze del Farmaco e dei Prodotti della Salute, Università degli Studi di Camerino, Via S. Agostino 1, 62032 Camerino (MC), Italy.*

[c]*Dipartimento di Neuroscienze, Psicologia, Area del Farmaco e Salute del Bambino, Sezione di Farmaceutica e Nutraceutica, Laboratorio di Molecular Modeling, Cheminformatics & QSAR, Università degli Studi di Firenze, Via Ugo Schiff, 6, 50019 Sesto Fiorentino, Italy.*

Key words: multi-target agents, 1,2,4-triazolo[4,3-*a*]pyrazin-3-one, adenosine A_{2A} receptor antagonists, carbonic anhydrase inhibitors, anticancer agents

Abstract

This paper describes identification of the first-in-class multi-target adenosine A_{2A} receptor antagonists-carbonic anhydrase (CA) IX and XII inhibitors, as new potential antitumor agents. To obtain the multi-acting ligands, the 8-amino-2,6-diphenyltriazolo[4,3-a]pyrazin-3-one, a potent adenosine hA_{2A} receptor (AR) antagonist, was taken as lead compound. To address activity against the tumor-associated CA isoforms, it was modified by introduction of different substituents (OH, COOH, CONHOH,SO_2NH_2) on the 6-phenyl ring or on a phenyl pendant connected to the former through different spacers. Among the new triazolopyrazines **1-23**, the most active were those featuring the sulfonamide residue. Derivative **20**, featuring a 4-sulfonamidophenyl residue attached through a $CONH(CH_2)_2CONH$ spacer at the para-position of the 6-phenyl ring, showed the best combination of activity at the three targets. In fact, it inhibited both the tumor-associated hCA IX and XII isozymes at nanomolar concentration (K_i= 5.0 and 27.0 nM), and also displayed a quite good affinity for the hA_{2A} AR (K_i= 108 nM). Compound **14**, bearing the 4-sulfonamidophenyl residue linked at the para-position of the 6-phenyl ring by a CONH spacer, was remarkable because both its hA_{2A} AR affinity and hCA XII inhibitory potency were in the low nanomolar range (K_i= 6.4 and 6.2 nM, respectively). Molecular docking studies highlighted the interaction mode of selected triazolopyrazines in the hA_{2A} AR recognition pocket and in the active site of hCA II, IX and XII isoforms.

1. Introduction

The multi-target approach has become an increasingly pursued strategy for the cure of different pathologies. In fact, a single-target therapy can be inadequate to obtain a satisfying therapeutic effect in complex diseases linked to the dysfunction of several biological targets [1]. The multi-target approach can be achieved either through combination of several drugs, administered in association or present in the same formulation, or by combining in the same molecule the capability to interact with the targets of interest. This latter strategy makes it possible to overcome various drawbacks, such as possible differences regarding pharmacokinetics of each component and the drug-drug interactions.

The design of multi-targeted drugs as anticancer agents has attracted much attention since several aberrant endogenous molecules and pathways can concur in the development and progression of cancer. Thus, simultaneous intervention on two or more targets can be useful for solving limited efficiencies, poor safety and, importantly, resistance profiles of a single-targeted drug [1].

In the last two decades, several studies have pointed out that the adenosine A_{2A} receptor and the carbonic anhydrase (CA) IX and XII isoforms can be useful targets for antineoplastic drugs [2-9].

Under physiological conditions, extracellular adenosine concentration is in the nanomolar order but it rises to the micromolar range when inflammation and hypoxia occur [2,3]. Hypoxic conditions are typical of many types of solid tumors and lead to the production of ATP, a danger signal released from surrounding cells, both cancer and healthy, following metabolic stress [10]. ATP is rapidly dephosphorylated by the ecto-nucleotidases CD39 and CD73, which are upregulated by hypoxia. CD73 transforms AMP into adenosine that elicits its effects through activation of four G-protein-coupled receptors, classified as A_1, A_{2A}, A_{2B} and A_3 subtypes [3]. A_1 and A_3 adenosine receptor (AR) are coupled with Gi, Gq and Go proteins, while A_{2A} and A_{2B} subtypes with Gs or Golf. AR activation increases (A_1, A_3) or decreases (A_{2A} and A_{2B}) cAMP intracellular levels but it also modulates other intracellular pathways implicated in cell growth and proliferation. All AR

subtypes have been shown to modulate adenosine actions in cancer, with A_1, A_{2A}, A_{2B} ARs being promoters of cell growth while the A_3 AR is an inhibitor [3,10,11]. In this context, the role of the A_{2A} AR subtype is notable. This receptor is expressed both in the central nervous systems and peripheral organs, and it is also present in blood vessel, platelets and in immune system cells. It has been demonstrated that A_{2A} AR is upregulated [10] in some tumors and its activation directly increases growth and proliferation of the cells [2,12]. However, the most relevant A_{2A} AR-mediated effect of adenosine is inhibition of the immune system [2,4]. The prolonged and sustained A_{2A} AR activation on immune and inflammatory cells, such as T and natural killer lymphocytes, dendritic cells, monocytes and macrophages, switches the role of the nucleoside from protective to deleterious. Adenosine, in fact, inhibits the response of the immune cells, thus depressing their defensive roles and promoting the tumor's escape. A_{2A} AR activation also potentiate the function of other cells in the tumor microenvironment, such as the endothelial cells which, through stimulation of angiogenesis, sustain tumor growth and metastasis [2].

On this basis, much research has been carried out in animal models to assess the therapeutic potential of human (h) A_{2A} AR antagonists, which have shown a remarkable activity in restoring antitumor immunity. Thus, some entered clinical trials [4,5,13] to be evaluated as single drugs or in combination with immunological anticancer drugs.

Hypoxia in the tumor microenvironment, besides being one of the leading causes triggering adenosine A_{2A} AR-mediated immunoescaping, also makes the role of the hCA IX and XII isoforms relevant in the progression of tumors and metastases [6-9]. hCAs are ubiquitous metalloenzymes differing in tissue distribution, subcellular localization and catalytic activity. Almost 15 hCA isoforms are known, and 12 isoforms are catalytically active. They contain the zinc ion in the catalytic site and are involved in the regulation of physiological functions connected to carbon dioxide hydration and its equilibrium with bicarbonate. hCA activity affects pH regulation, ion transport, secretion of electrolytes and many metabolic processes, such as lipogenesis and gluconeogenesis. hCA IX and XII isoforms are membrane-bound enzymes whose

expression is significantly increased in hypoxic tumors [6-9]. Hypoxia switches metabolism toward glycolysis, producing high levels of acidic species, such as lactic acid, carbon dioxide and protons. The consequent intracellular acidification is not compatible with metabolic processes of normal cells but tumor cells activate pumps and ion-exchangers to extrude the acidic species and maintain a slightly alkaline intracellular pH. Overexpression of the CAIX and XII isoforms significantly contribute to this process: the bicarbonate ion, deriving from carbon dioxide hydration, enters the cell through an active transport, thus alkalizing the inner pH, while the proton increases acidosis of the extracellular medium. These conditions are known to favor the onset and development of solid tumors. Thus, selective inhibition of the tumor-associated hCAs IX and XII proved to be a promising strategy to counteract cancer [6,9,14].

On this basis, and due to our involvement in the research field of AR ligands[12,15-24] and hCA inhibitors [25,26], we thought it interesting to focus on the development of new compounds able to behave as combined hA_{2A} AR antagonists and hCAs IX/XII inhibitors because the blockade of both the hA_{2A} AR- and hCA-activated pathways could lead to a synergistic effect. To design the new compounds, we exploited our experience which has lead us to identify many potent antagonists of the hA_{2A} AR [12,15,17-24] belonging to different classes. Among them, the triazolo[4,3-*a*]pyrazine series was selected [18,22,24] and the 8-amino-2,6-diphenyl-1,2,4-triazolo[4,3-a]pyrazin-3-one **A** [18], a potent hA_{2A} AR antagonist, was taken as lead compound. To obtain the new hybrid ligands (**1-23**, Fig. 1), in the first phase of the work simple substituents, such as OH, COOH, CONHOH and SO_2NH_2, were inserted directly or by small chains on the 6-phenyl ring (**1-6**) of **A**. Then, the above cited groups were introduced on a lateral phenyl pendant, linked to the 6-phenyl ring through an amide chain (**7-15**) or through other spacers of different length and flexibility (**16-23**). These small substituents used to decorate the new compounds were chosen because they usually confer good hCA inhibitory activities [14,27] as they are able to interact with the zinc ion in the catalytic site, either directly or through a water molecule.

Fig. 1. From the hA_{2A} AR antagonist **A** to the new multi-target 8-amino-6-aryl-2-phenyl-1,2,4-triazolo[4,3-*a*]pyrazin-3-ones **1-23**.

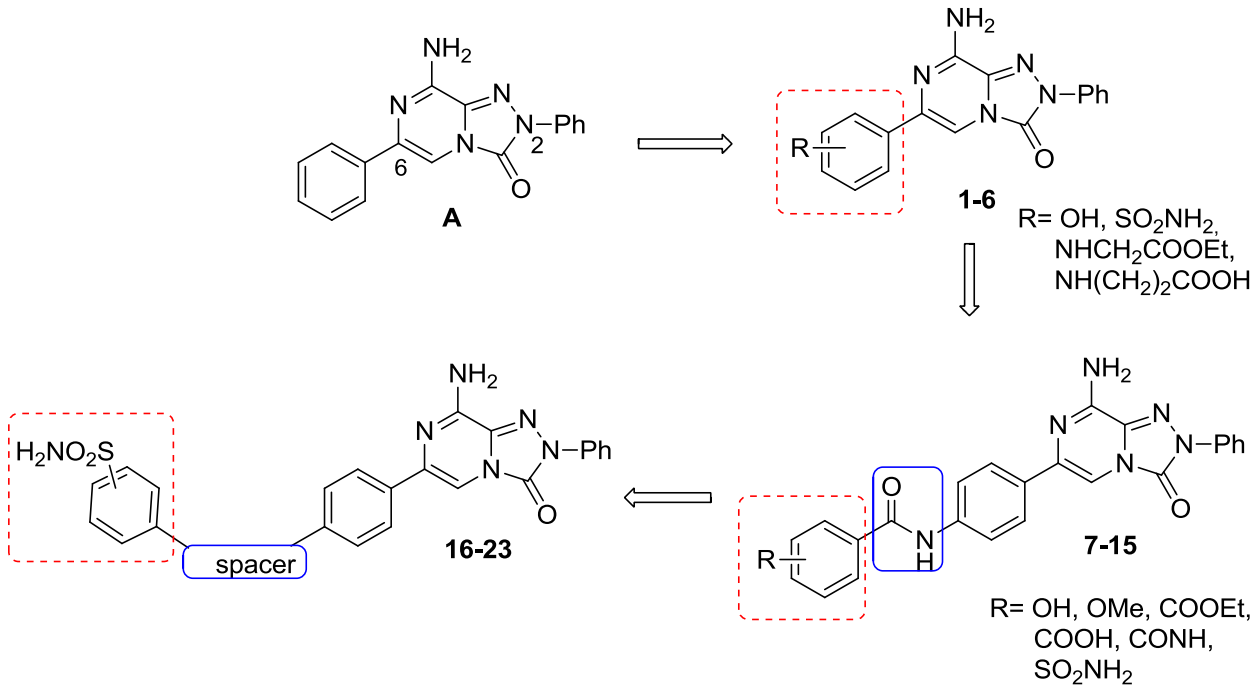

2. Results and Discussion

2.1. Chemistry

The target derivatives were synthesized as shown in Schemes 1-5. The 8-amino-2-phenyl-1,2,4-triazolopyrazin-3-one derivatives **1-3**, featuring a hydroxy group, respectively, at the 2-, 3- and 4-position of the 6-phenyl ring, were prepared as previously described by us [18,22], following the procedure employed for **4** (Scheme 1). Briefly, the ethyl 1-phenyl-5-oxo-1,2,4-triazole-3-carboxylate **24** [28] was reacted with 4-(2-bromoacetyl)benzenesulfonamide **25 [**29] to give the N^4-alkylated triazole derivative **26**. The latter was cyclized by heating with ammonium acetate to provide the 1,2,4-triazolo[4,3-a]pyrazine-3,8-dione derivative **27**. Then, to protect its sulfonamide residue, **27** was reacted with dimethylformamide dimethylacetal and the resulting derivative **28** was heated in a sealed tube with phosphorus oxychloride to afford the corresponding 8-chloro derivative **29**. When this compound was heated in a saturated ethanolic solution of ammonia, the desired 8-

amino-triazolopyrazine **4** was obtained, together with the unexpected 8-dimethylamino derivative **4a**.

Scheme 1[a]

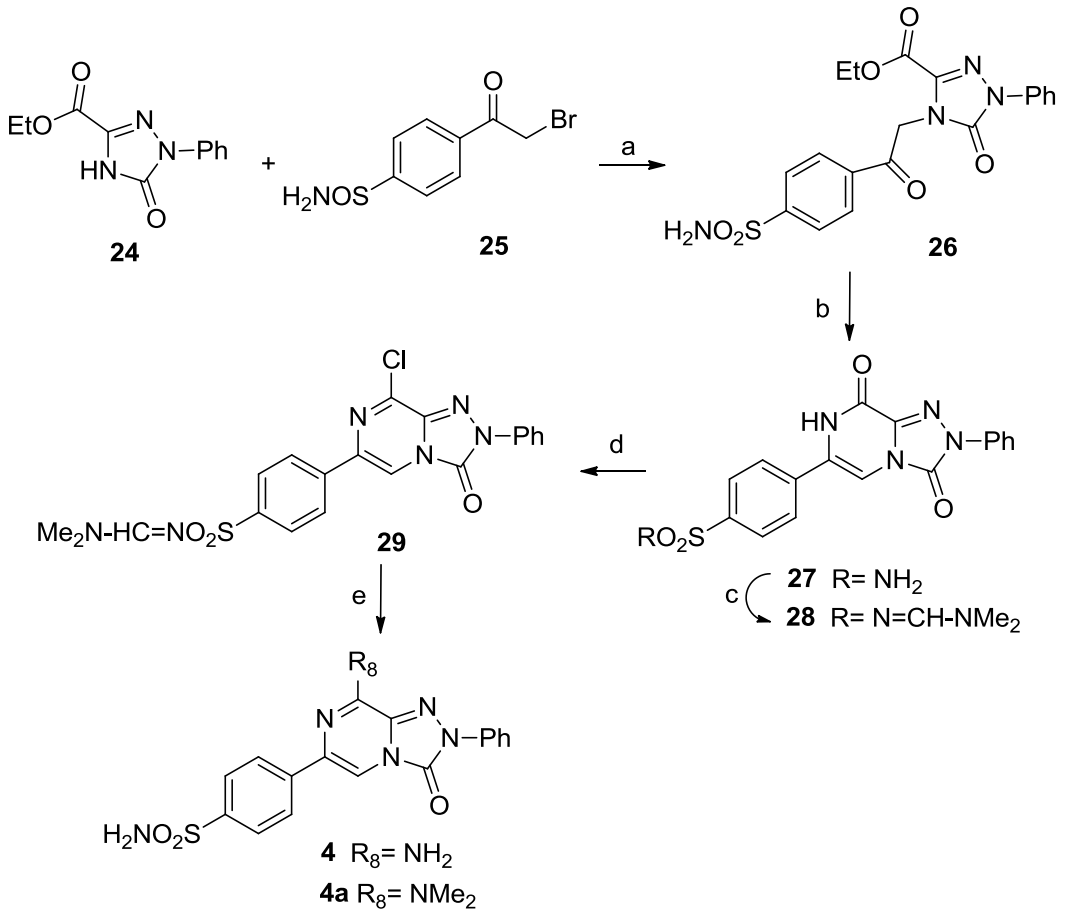

[a]Reagents and conditions: (a) K_2CO_3, DMF/MeCN, rt; (b) NH_4OAc, 140 °C sealed tube; (c) $N(Me)_2C(OMe)_2$, DMF, 0 °C-rt; (d) $POCl_3$, sealed tube, 160 °C; (e) NH_3 gas/absolute EtOH, sealed tube, 120 °C.

The triazolopyrazines **5-21**, featuring substituents connected by different linkers to the para position of 6-phenyl ring, were synthesized as depicted in Schemes 2-4. Scheme 2 describes the synthesis of derivatives **5-13**. Compounds **5** and **6**, bearing small carboxylic chains, were prepared by reacting

the 6-(4-aminophenyl)-2-phenyltriazolopyrazine **30 [**22] with ethyl 2-bromoacetate and succinic anhydride, respectively. Hydrolysis of the ester **5** afforded the relative carboxylic acid **5a** which proved to be unstable when purified by recrystallization or by silica gel column. Indeed, compound **5a** was not biologically tested because its low level of purity.

Schema 2[a]

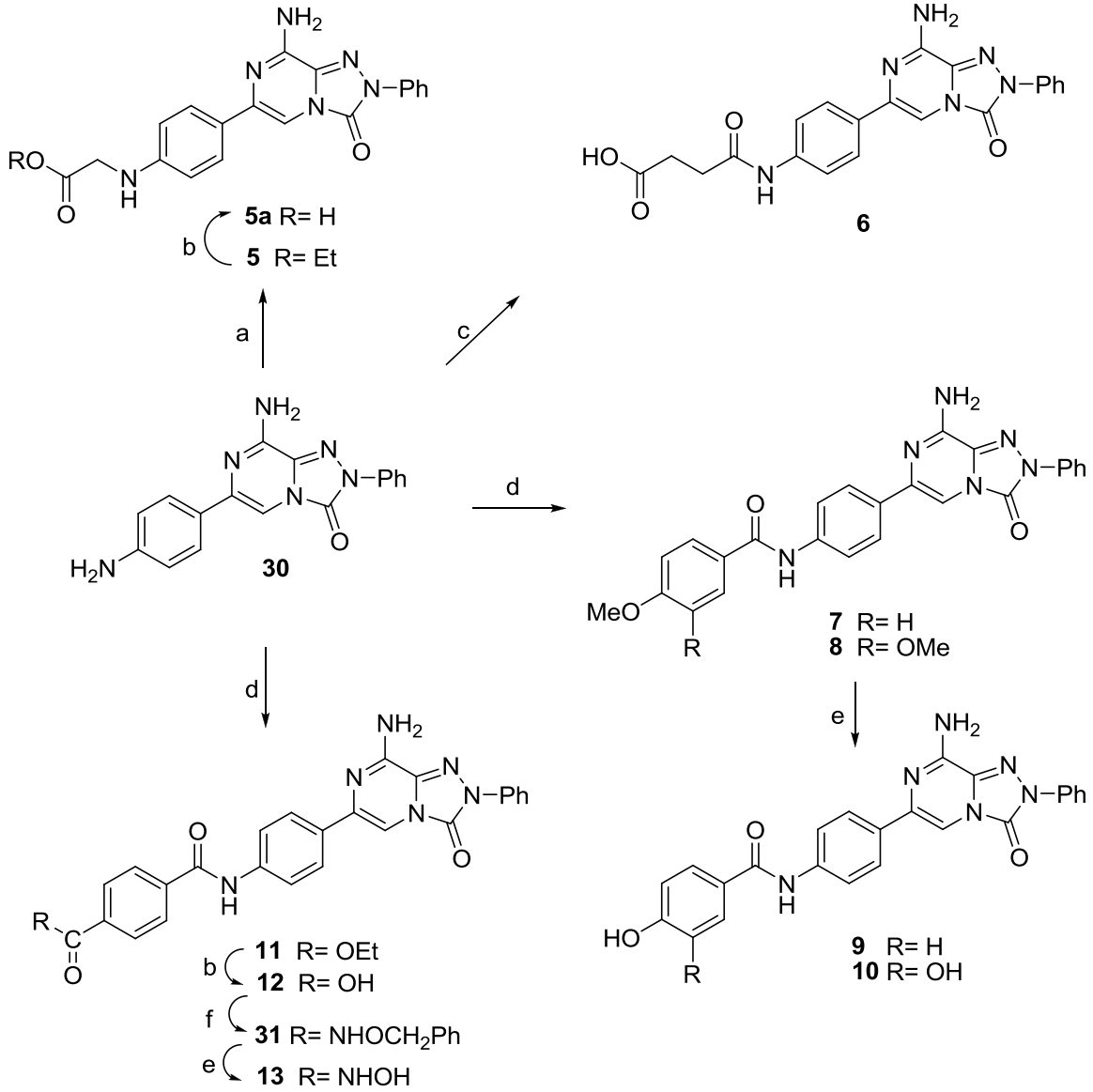

[a]Reagents and conditions: (a) ethyl 2-bromoacetate, Et_3N, THF, mw, 120 °C; (b) 1M NaOH, EtOH, reflux; (c) succinic anhydride, THF, reflux; (d) suitable benzoic acid, NEt_3, 1-(3-(dimethylamino)-

propyl))-3-ethylcarbodiimide hydrochloride, 1-hydroxybenzotriazole, anhydrous DMF, rt; (e) BBr_3, anhydrous CH_2Cl_2, 0 °C-rt; (f) O-benzylhydroxylamine HCl; Et_3N, 1-(3-(dimethylamino)-propyl))-3-ethylcarbodiimide, hydrochloride 1-hydroxybenzotriazole, anhydrous DMF, rt.

Compounds **7-13** were prepared starting from the para-amino substituted compound **30 [**22] which was reacted with suitable benzoic acids, in the presence of carboxylic group activators. When the methoxy-substituted benzoic acids were employed, the triazolopyrazines **7** and **8** were obtained, which were demethylated with a BBr_3 solution, thus providing the desired phenols **9** and **10**. Reaction of **30** with 4-(ethoxycarbonyl)benzoic acid [30] yielded derivative **11** which was hydrolyzed to give the relative acid **12**. Treatment of this latter with O-benzylhydroxylamine produced the corresponding N-hydroxybenzylcarboxamido derivative **31** whose debenzylation with a BBr_3 solution afforded compound **13**.

Scheme 3 displays the synthesis of the triazolopirazines **14-17**, featuring the benzensulfonamide group. The amides **14** and **15** were synthesized by treatment of **30** with the suitable sulfamoylbenzoic acids while derivatives **16** and **17** were obtained by alkylation of **30** with 4-(bromomethyl)benzenesulfonamide [31] and 4-(2-bromoacetyl)benzenesulfonamide [29], respectively.

Scheme 3

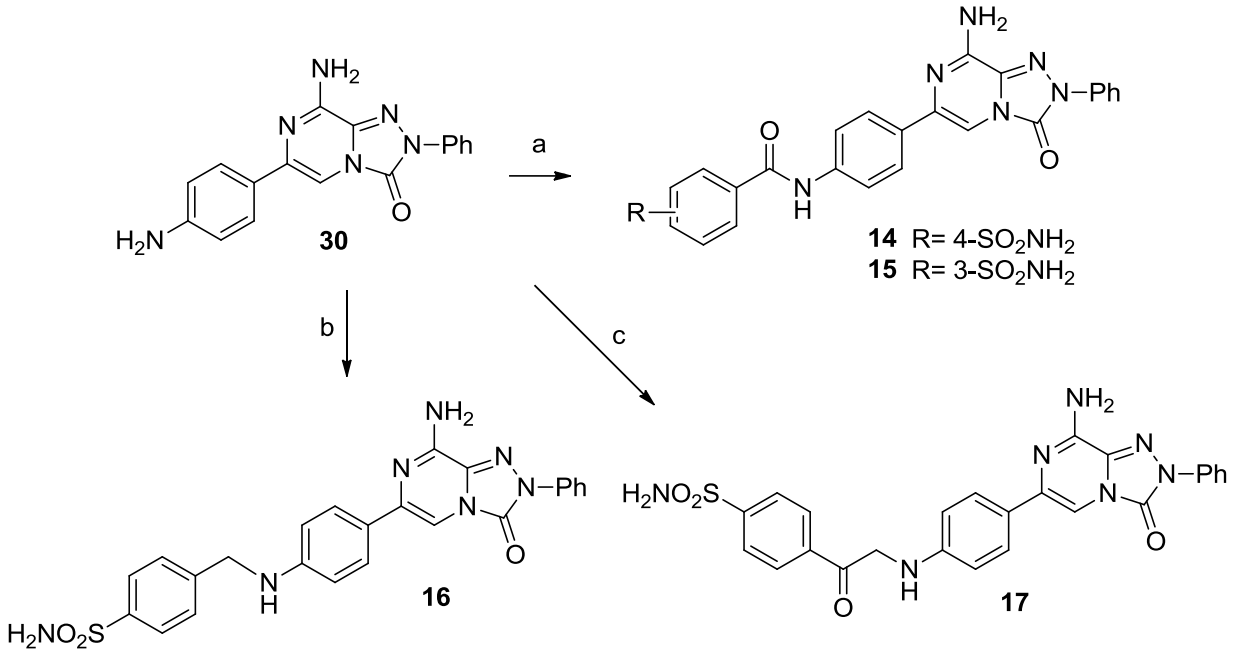

[a]Reagents and conditions: (a) suitable sulfamoylbenzoic acid, NEt_3, 1-(3-(dimethylamino)-propyl))-3-ethylcarbodiimide, hydrochloride 1-hydroxybenzotriazole, anhydrous DMF, rt; (b) 4-(bromomethyl)benzenesulfonamide, K_2CO_3, THF, reflux. (c) 4-(2-bromoacetyl)benzenesulfonamide, K_2CO_3, THF, reflux.

The synthesis of the triazolopirazine **18-21** (Scheme 4) started from the previously reported 6-(4-acrylammidophenyl) substituted derivative **31** [24]. When the latter was reacted with the 4-(2-aminoethyl)benzenesulfonamide [32], compound **18** was obtained. Its lower homologue **19** was synthesized allowing 4-(bromoethyl)benzenesulfonamide [31] to react with the triazolopyrazine **32** [24], that was in turn obtained by heating **31** in a saturated ethanol solution of ammonia. The sulfonamide derivatives **20** and **21** were prepared by treatment of **32** with the suitable sulfamoylbenzoic acids, in the same experimental conditions described above to obtain the triazolopyrazine derivatives **7**, **8**, **10**, **11** and **15, 16**.

Scheme 4

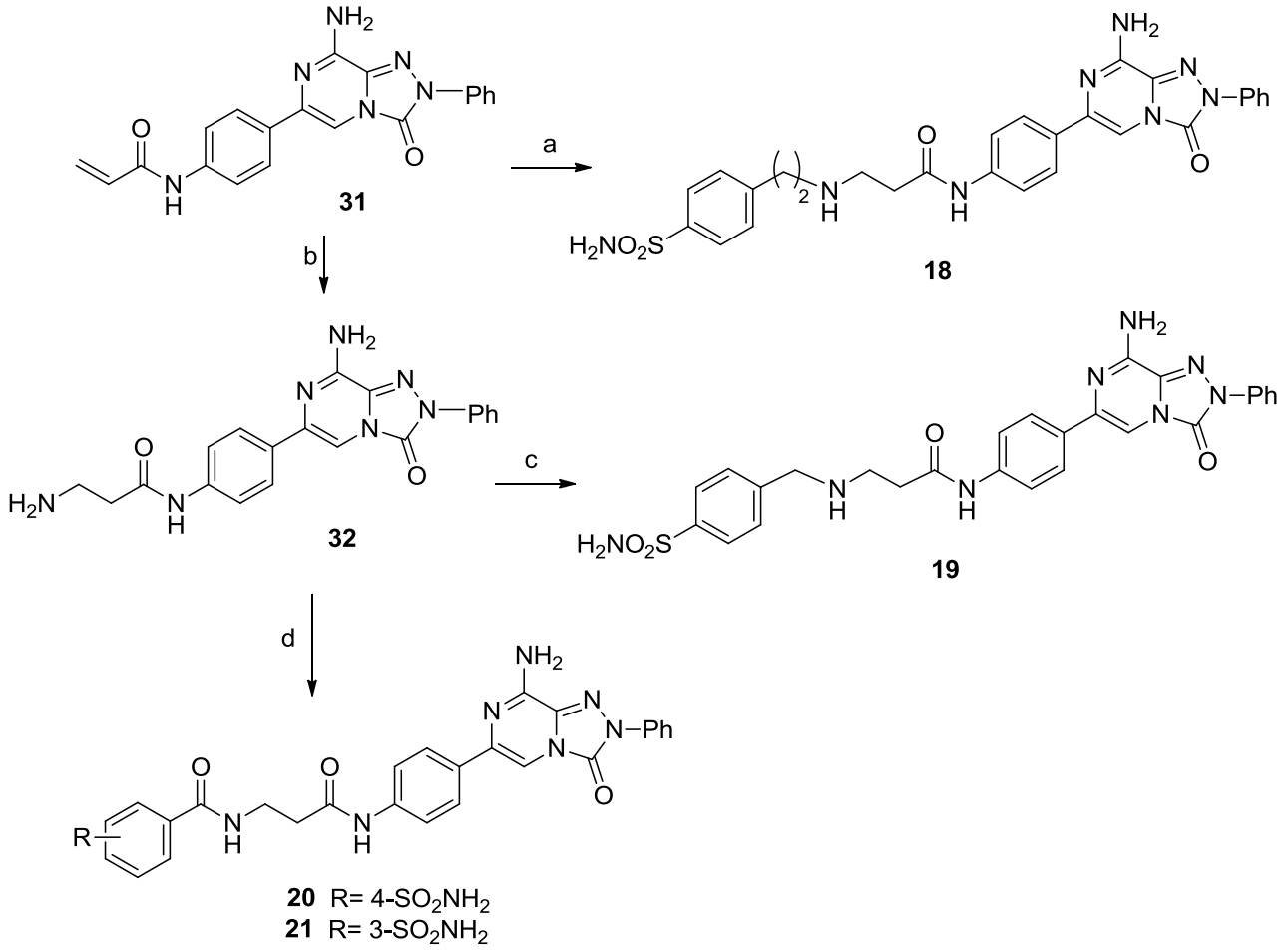

[a]Reagents and conditions: (a) 4-(2-aminoethyl)benzenesulfonamide, THF, reflux; (b) NH_3 gas/ absolute EtOH, sealed tube, 130 °C; (c) 4-(bromomethyl)benzenesulfonamide, K_2CO_3, THF, reflux; (d) suitable sulfamoylbenzoic acid, Et_3N, 1-(3-(dimethylamino)-propyl))-3-ethylcarbodiimide hydrochloride, 1-hydroxybenzotriazole, anhydrous DMF, rt.

Finally, Scheme 5 depicts the synthesis of compounds **22** and **23** that were obtained by treatment of the previously reported triazolopyrazine **33 [**24] with 4 (bromoethyl)benzenesulfonamide [32] and 4-sulfamoylbenzoic acid, respectively.

Scheme 5

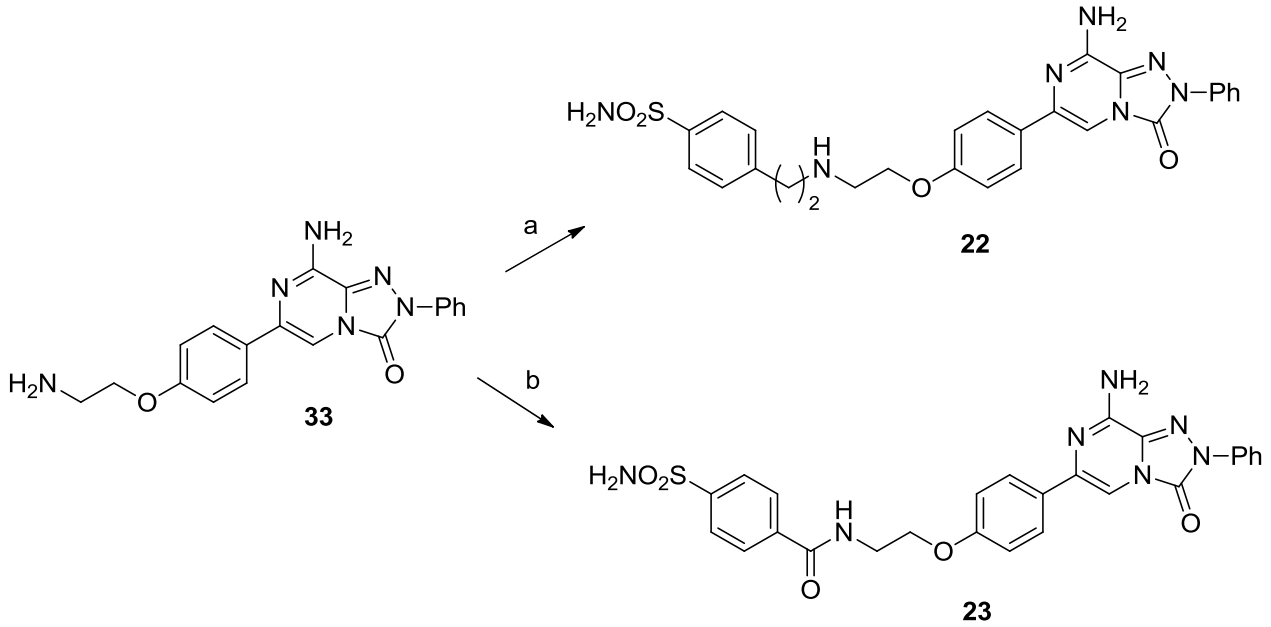

[a]Reagents and conditions: 4-(bromoethyl)benzenesulfonamide, THF, K_2CO_3, reflux; (b) 4-sulfamoylbenzoic acid, Et_3N, 1-(3-(dimethylamino)-propyl))-3-ethylcarbodiimide hydrochloride, 1-hydroxybenzotriazole, anhydrous DMF, rt.

2.2. Structure-activity relationship studies

The triazolopyrazines **1-23** were biologically tested to determine their hA_{2A} AR affinity, and selectivity versus the other hARs, and to assess their inhibitory activity against the tumor-associated hCA IX and XII isoforms. The compounds were also tested against the hCAI and II isoforms because these isozymes are abundantly expressed throughout the body, thus responsible for the side effects of non-selective inhibitors.

Derivatives **14** and **20**, showing the best combined activity at the desired targets, were selected to assess their hA_{2A} AR antagonistic profile, which was determined by evaluating their effect on cAMP production in CHO cells, stably expressing hA_{2A} ARs.

For sake of clarity, compounds have been subdivided into three sets and relative biological data are shown in Tables 1-3. This division also reflects the different steps of the work.

Biological data of 5-(N-ethyl-carboxamido)adenosine (NECA) and 2-chloro-N6-cyclopentyladenosine (CCPA), as AR reference ligands, and of acetazolamide (AZA), as standard CA inhibitor, are reported in Tables 1-3 for comparison.

Table 1. Biological evaluation of compounds **1-6** and **4a.**

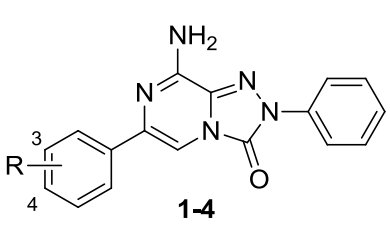

1-4

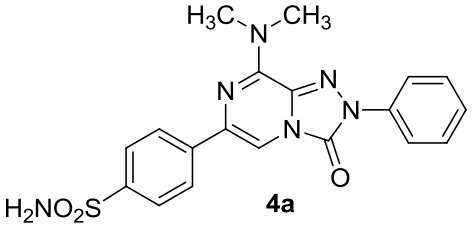

4a

Biological activity at human adenosine receptors[a]

		Binding experiments K_i (nM)		
	R	hA_1[b]	hA_{2A}[c]	hA_3[d]
1[e]	2-OH	16.3 ± 0.3	2.4 ± 0.5	44.5±8.3
2[f]	3-OH	14 ± 2	3.5 ± 0.6	134 ± 13
3[f]	4-OH	45 ± 10	45 ± 12	53 ± 13
4	4-SO_2NH_2	205 ± 29	856.6 ± 188	14830 ± 320
4a	-	435.3 ± 61	3886.5 ± 833.5	19495 ± 1785
5	4-$NHCH_2COOEt$	771 ± 81	6296 ± 1140	>30000
6	4-$NHCO(CH_2)_2COOH$	2300 ± 431	573 ± 91	6957 ± 1223
	NECA	4.6 ± 0.8	16 ± 3	12.8 ± 2.5
	CCPA	1.2 ± 0.2	2050 ± 400	26 ± 5

Inhibition data against hCAI, II, IX and XII isoforms as determined by a stopped-flow CO_2 hydrase assay. Acetazolamide (AZA) is reported as reference compound

		K_i (μM)[g]			
	R	CAI	CAII	CAIX	CAXII
1	2-OH	>100	19.0	>100	>100
2	3-OH	>100	93.0	>100	>100
3	4-OH	>100	>100	>100	>100

4	4-SO_2NH_2	8.023	0.703	8.920	0.602
4a	-	2.093	0.464	6.729	0.358
5	4-$NHCH_2COOEt$	>100	>100	>100	>100
6	4-$NHCO(CH_2)_2COOH$	>100	>100	>100	>100
	AZA	0.250	0.0121	0.0254	0.0056

[a]Data (n= 3-5) are expressed as means ± standard errors. [b]Displacement of specific [^{3}H]-CCPA binding at hA_1 AR expressed in CHO cells. [c]Displacement of specific [^{3}H]-NECA binding at hA_{2A} AR expressed in CHO cells. [d]Displacement of specific [^{3}H]-HEMADO binding at hA_3 AR expressed in CHO cells.. [e]Ref. 22. [f]Ref 18. [g]Mean from three different assays, and errors were within 5-10% of the reported values.

Taking a look at the obtained results, it emerges that the aim of the work was achieved because some multi-target compounds, acting at the hA_{2A} AR and on the tumor-associated CA IX and/or XII isoforms, were obtained. The triazolopyrazines **14** and **20** are endowed with the best combined activities (Table 2), but also derivatives **17-19** are of interest (Table 3). In general, compounds **1-23** possess hA_1, hA_{2A} and hA_3 AR affinities spanning from the micromolar to the nanomolar range while they are inactive in inhibiting the NECA-stimulated cAMP levels in hA_{2B} CHO cells (IC_{50} > 30,000 nM).

Analyzing the biological data in detail, and considering the first set of triazolopyrazines **1-6** (Table 1), we can observe that derivatives **1-3**, bearing a hydroxy group at the three positions of the 6-phenyl ring, displayed high hA_{2A} AR affinity but scarce ability to inhibit the tested hCAs. The sole results of interest are those of the 2-hydroxy- and 3-hydroxy- substituted derivatives **1** and **2** against the hCA II isozyme, that was blocked at micromolar concentration (K_i= 19 and 93 μM, respectively). As expected, the presence of the 4-sulfonamide residue on the 6-phenyl ring (derivatives **4** and **4a**) was more advantageous for hCA inhibitory activity. Compounds **4** and **4a** showed K_i values of micromolar order towards all the hCAs, the best being those relative to the

hCA XII isoform (K_i= 0.602 and 0.358 μM, respectively) and the off-target CA II (K_i= 0.702 and 0.464 μM). hA_{2A} AR affinity of **4** and **4a** were quite scarce, particularly of the latter. The lower affinity of **4a**, with respect to **4**, was probably due to the loss of hydrogen-bonding interaction that the 8-amino group typically engages with Asn254 residue [18,22,24] (see also molecular modeling studies section). The triazolopyrazines **5** and **6**, featuring, respectively, an ethyl glycine and a succinamide moiety at the para-position of the 6-phenyl ring, showed only some hA_{2A} AR affinity while they were not able to inhibit the hCAs.

In the second step of the work, the R substituents addressing activity toward hCAs were attached at the para position of a benzamide moiety that, in turn, was appended on the 6-phenyl ring (derivatives **7-15**, Table 2). This modification introduced on the molecule a long tail that was supposed to permit a better accommodation inside the enzymes. Moreover, a long pendant was also thought to maintain high hA_{2A} AR affinity and selectivity, as suggested by previous data obtained in this series of AR antagonists [26].

Table 2. Biological evaluation of compounds **7-15**

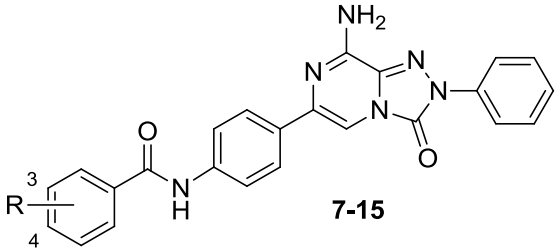

7-15

Biological activity at human adenosine receptors[a]				
		Binding Experiments K_i (nM)		
	R	hA_1[b]	hA_{2A}[c]	hA_3[d]
7	4-OMe	417.7 ± 52.7	0.7 ± 0.03	279 ± 67.5
8	3,4-di OMe	98.8 ± 23.5	20.6 ± 3.7	>30000
9	4-OH	194 ± 29	41.2 ± 5	1072 ± 102
10	3,4-diOH	545.7 ± 1.5	9 ± 2.2	1248 ± 69
11	4-COOEt	7478.5 ± 748.5	1357 ± 82	>30000
12	4-COOH	2366 ± 377	81.2 ± 9.5	>30000

13	4-CONHOH	395 ± 1	36 ± 7.8	546.2 ± 68.2
14	4-SO_2NH_2	4189 ± 59.5	6.4 ± 1.5	>30000
15	3-SO_2NH_2	1211 ± 126.5	13.5 ± 0.02	>30000
	NECA	4.6 ± 0.8	16 ± 3	12.8 ± 2.5
	CCPA	1.2 ± 0.2	2050 ± 400	26 ± 5

Inhibition data against hCA I, II, IX and XII isoforms as determined by a stopped-flow CO_2 hydrase assay. Acetazolamide (AZA) is reported as reference compound

		K_i (μM)[e]			
	R	CAI	CAII	CAIX	CAXII
7	4-OMe	>100	>100	>100	>100
8	3,4-di OMe	>100	>100	>100	>100
9	4-OH	>100	47.3	>100	4.4
10	3,4-diOH	>100	31.7	44.3	>100
11	4-COOEt	>100	>100	>100	>100
12	4-COOH	>100	>100	>100	>100
13	4-CONHOH	>100	63.02	>100	>100
14	4-SO_2NH_2	8.351	0.046	0.466	0.006
15	3-SO_2NH_2	2.288	0.367	0.810	0.303
	AZA	0.250	0.0121	0.0254	0.0056

[a]Data (n= 3-5) are expressed as means ± standard errors. [b]Displacement of specific [^{3}H]-CCPA binding at hA_1 AR expressed in CHO cells. [c]Displacement of specific [^{3}H]-NECA binding at hA_{2A} AR expressed in CHO cells. [d]Displacement of specific [^{3}H]-HEMADO binding at hA_3 AR expressed in CHO cells. [e]Mean from three different assays, and errors were within 5-10% of the reported values.

As expected, several triazolopyrazines of this set displayed nanomolar hA_{2A} affinity (compounds **7-10**, **12-15**) and some were also highly selective, the best being the 4-methoxy-derivative **7**, the 3,4-dihydroxy-substituted compound **10** and the sulfonamido derivatives **14** and **15**. Derivatives **14** and **15** also showed good activity as hCA inhibitors. In fact, their potency spans from the micromolar to the nanomolar range, the para-substituted compound **14** being the most potent against the targeted hCAs. The other triazolopyrazines of this set were less active or inactive as hCAs inhibitors, the only exception being the phenol- and cathecol-substituted derivatives **9** and **10** and the hydroxamic

acid **13**. They all showed some inhibitory activity against the hCA II, while compounds **9** and **10** were also active, respectively, against the hCA XII (K_i= 4.4 μM) and hCA IX (K_i= 44.3 μM).

The relevant activity of compounds **14** and **15** indicated that, among the probed substituents, benzensulfonamide was the best one to target both the hA_{2A} AR and the tumor-associated hCA isozymes. Moreover, the significantly higher activity of compound **14,** with respect to **4**, clearly indicated that the greater distance between the benzensolfonamide moiety and the bicyclic core favored accommodation of the inhibitor inside the enzymes, as also emerged from the docking studies at the CAs (see molecular modeling section). Thus, in the subsequent derivatives (**16-23**, Table 3) only the benzesulfonamide pendant was inserted to address activity against hCAs. In particular, it was linked at the para position of the 6-phenyl ring through spacers of different length and flexibility. These modifications were more successful than the previous ones. In fact, all the new triazolopyrazines **16-23** showed nanomolar affinity for the hA_{2A} AR and were also able to inhibit the tested hCAs with different degrees of selectivity. One of the most relevant multi-target derivatives was **20**, that inhibited the hCAs IX and XII with K_i values of 5.0 and 27.0 nM, respectively, and showed relatively good hA_{2A} AR affinity (K_i= 108 nM). Derivatives **17** and **18** also showed an interesting profile, being active at low nanomolar concentrations both at the hA_{2A} AR and against the hCA XII isozyme. A similar potency at this CA isoform was found for compound **19**, the lower homologue of **18**.

It is not easy to rationalize the effect of the spacer on the target-ligand recognition process but, obviously, both the length and flexibility of the chain play a role. Considering the hA_{2A} AR binding, elongation of the CH_2NH spacer of derivative **16** with a CO function did not changed much the A_{2A} affinity (compound **17**, K_i= 26 nM) while its replacement with the more rigid CONH group enhanced about 4-fold the A_{2A} AR affinity (derivative **14**, K_i= 6.4 nM). Compound **18**, featuring the longest spacer, showed a higher hA_{2A} AR affinity (K_i= 10 nM) than those of compounds bearing shorter pendants (compounds **16** and **17**) and of its homologue **19**. Compound **21**, bearing the sulfonamide group at the meta position, is worth noting, being at least 10-fold more active than its

regioisomer **20**. Considering activity against hCAs, it is evident that compounds **17**-**20** inhibited the hCA XII isoform with similar potency (K_i= 25.7-41.5 nM), although featuring much different spacers. Instead, against the hCA IX isozyme only compound **20** was active in the low nanomolar range.

Table 3. Biological evaluation of compounds **16-23**.

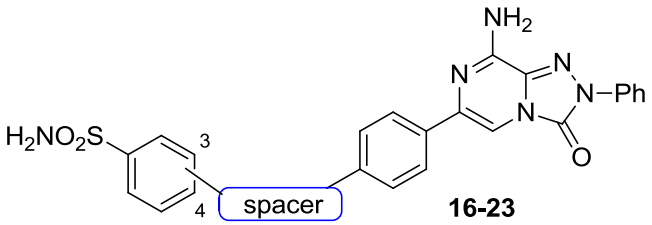

16-23

Biological activity at human adenosine receptors[a]				
		Binding Experiments K_i (nM)		
	spacer	hA_1[b]	hA_{2A}[c]	hA_3[d]
16	4-CH_2NH-	87.7 ± 9	27.9 ± 3	>30000
17	4-$COCH_2NH$-	131 ± 18.5	26 ± 6	6760 ± 387
18	4-$(CH_2)_2NH(CH_2)_2CONH$-	1031 ± 28	10.6 ± 2.2	5833 ± 905
19	4-$CH_2NH(CH_2)_2CONH$-	839 ± 18.9	96.3 ± 0.8	>30000
20	4-$CONH(CH_2)_2CONH$-	1074 ± 254.5	108 ± 25	>30000
21	3-$CONH(CH_2)_2CONH$-	418 ± 103.6	9.2 ± 2.4	>30000
22	4-$(CH_2)_2NH(CH_2)_2O$-	283.2 ± 46	87.9 ± 18	701.3 ± 142
23	4-$CONH(CH_2)_2O$-	420.4 ± 77.3	6.8 ± 0.18	6645 ± 517
	NECA	4.6 ± 0.8	16 ± 3	12.8 ± 2.5
	CCPA	1.2 ± 0.2	2050 ± 400	26 ± 5

Inhibition data against hCA I, II, IX and XII isoforms as determined by a stopped-flow CO_2 hydrase assay. Acetazolamide (AZA) is reported as reference compound

		Ki (nM)[e]			
	spacer	CAI	CAII	CAIX	CAXII
16	4-CH_2NH-	570.3	896.8	5968	624.9
17	4-$COCH_2NH$-	588.7	246.3	9450	25.7
18	4-$(CH_2)_2NH(CH_2)_2CONH$-	8713	526.5	108.8	26.3

19	4-$CH_2NH(CH_2)_2CONH$-	9001	6763	318.7	41.5
20	4-$CONH(CH_2)_2CONH$-	51.5	8.6	5.0	27.0
21	3-$CONH(CH_2)_2CONH$-	7277	341.0	6925	830.0
22	4-$(CH_2)_2NH$-$(CH_2)_2O$-	973.1	933.8	9463	794.7
23	4-$CONH(CH_2)_2O$-	933.9	183.4	5951	528.3
	AZA	0.250	0.0121	0.0254	0.0056

[a]Data (n= 3-5) are expressed as means ± standard errors. [b]Displacement of specific [^{3}H]-CCPA binding at hA_1 AR expressed in CHO cells. [c]Displacement of specific [^{3}H]-NECA binding at hA_{2A} AR expressed in CHO cells. [d]Displacement of specific [^{3}H]-HEMADO binding at hA_3 AR expressed in CHO cells. [e] Mean from three different assays, and errors were within 5-10% of the reported values.

Compounds **22** and **23** were synthesized as analogues of derivatives **18** and **20**, respectively, in which the amide function linked at the para position of the 6-phenyl ring was replaced with an ethereal oxygen. This modification, which enhanced the lateral chain flexibility, was not profitable for the multi-target action because **22** and **23** were scarcely active against all the hCAs. Regarding hA_{2A} AR affinity, it produced opposite effects. Compound **22** was, in fact, about 8-fold less active than **18**, while derivative **23** was 15-fold-more active than compound **20**.

Compounds **14** and **20**, showing the best combined hA_{2A} AR affinity-hCA IX/XII inhibitory potency, behaved as hA_{2A} AR antagonists, being able to counteract NECA-stimulated cAMP production in CHO cells (IC_{50}= 90.8 ± 26 nM and 926 ± 111 nM, respectively).

2.3. Molecular modeling studies at hA_{2A} AR

Docking studies were carried out to simulate the binding mode of the synthesized compounds at the hA_{2A} AR cavity. For this analysis, as biomolecular target it was chosen the crystal structures of the hA_{2A} AR in complex with the antagonist/inverse agonist ZM241385 (http://www.rcsb.org; pdb code: 5NM4; 1.7-Å resolution [33]). MOE (Molecular Operating Environment 2014.09) software

and the CCDC Gold docking tool [34,35] were used for docking analyses, with protocols set up and previously reported in other studies describing analogues of these molecules [18,24].

As expected, the docking conformations generally observed for the new derivatives are highly similar to the ones observed for the previously reported triazolopyrazines [18,24]. The bicyclic scaffold is located in the depth of the hA_{2A} AR binding cavity, making non-polar interaction with the side chains of Phe168 (EL2) and Leu249$^{6.51}$. Additional polar interaction is given by the exocyclic amine function with the side-chains of Asn253$^{6.55}$ and Glu169 (EL2). Figure 2A shows the binding mode of compound **14** at the hA_{2A} AR binding cavity.

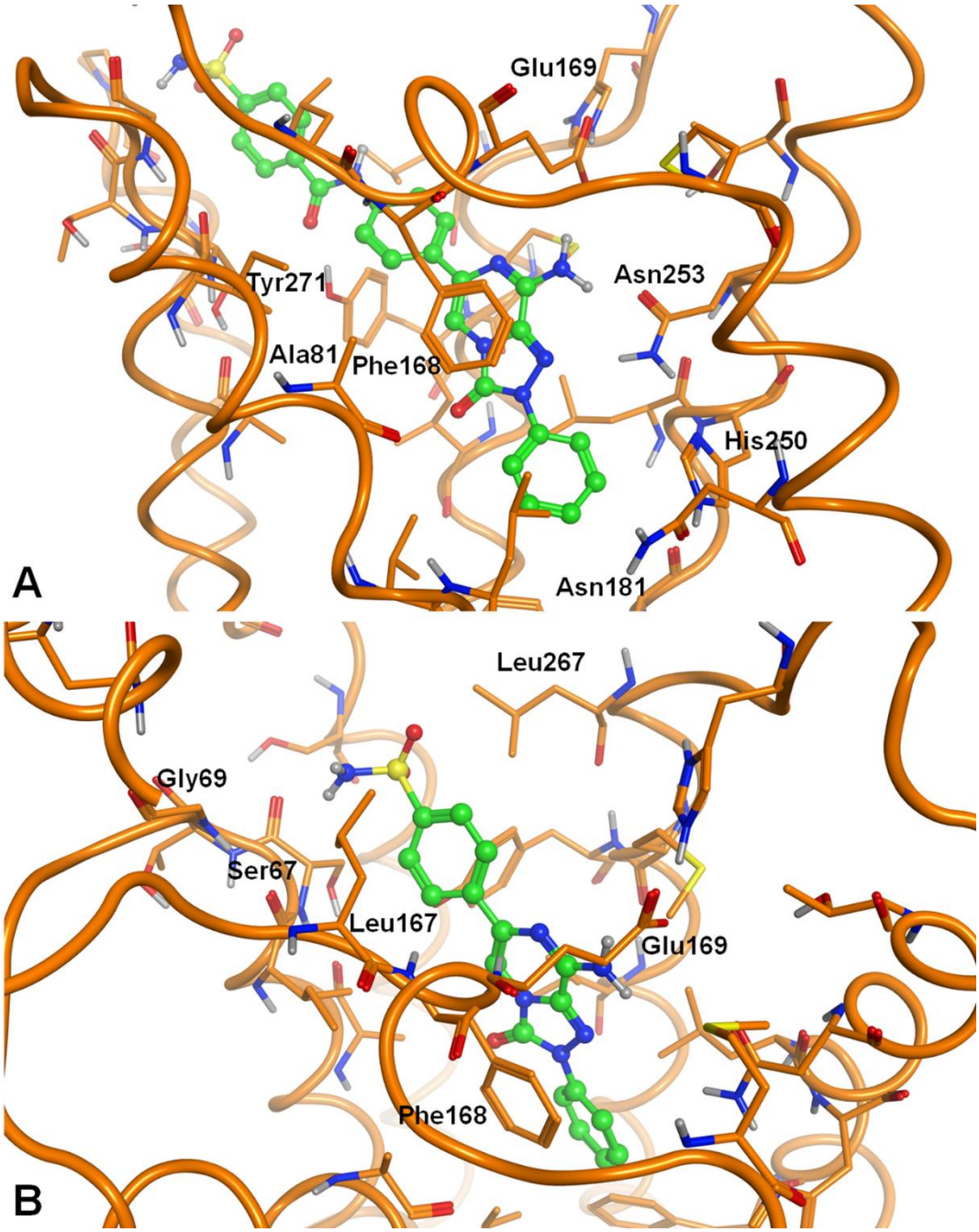

Fig. 2. (**A**) Binding mode of compound **14** at the hA_{2A} AR binding cavity, with indication of some key receptor residues. (**B**) Top-view of the binding mode of compound **4** within the hA_{2A} AR binding pocket. The view is focused on the 6-substituent and the receptor residues in its proximity.

The 6-phenyl ring is externally oriented and, as observed for previously reported analogues of this series [24], substituents on this ring modulate the hA_{2A} AR affinity through the interaction with receptor residues located at the entrance of the binding cavity. Introduction at the para-position of

the 6-phenyl ring of a highly hydrophilic group, such as the sulfonamide, yielded a compound (**4**) endowed with a sub-micromolar affinity for the hA_{2A} AR. The sulfonamide group gets located between receptor residues with a non-polar or low polar profile, such as Ser67$^{2.65}$, Gly69$^{2.67}$, Leu167 (EL2) and Leu267 (EL3) (Fig. 2B), and this affords a non-favorable interaction between the ligand and the receptor, leading to a low affinity for the hA_{2A} AR. Introduction of two methyl groups on the 8-amine function of **4** leads to the loss of the above-described polar interaction between the amine and the sidechains of Asn253$^{6.55}$ and Glu169 (EL2), with a consequent decrease of the hA_{2A} AR affinity (compound **4a**, Table 1).

Introduction of larger substituents at the para-position of the 6-phenyl ring leads to various degrees of hA_{2A} AR affinity and selectivity. Compounds **7-17**, in which the groups targeting the hCAs were inserted on a phenyl group attached by small spacers (CONH, CH_2NH, $COCH_2NH$) to the 6-phenyl ring, showed hA_{2A} AR affinities in the low nanomolar range. Docking conformations for these compounds are highly similar (see compound **14**, Fig. 2A), with the external phenyl ring located at the entrance of the cavity but exposed to the solvent. These substituents make interactions with several receptor residues and docking scores present a similar trend with respect to the hA_{2A} AR affinities of these compounds. In particular, affinity data of **7-17** display a very similar trend with respect to the LogP values of the same molecules (calculated with MOE; LogP data are reported in the supporting material), with the lower LogP data associated to molecules with higher affinities (compound **7** being an outlier). The physicochemical profile of the substituent inserted at the para- and/or meta-position of the external phenyl ring appears critical to modulate the affinity at the hA_{2A} AR. Still considering this set of compounds, even the type of spacer linking the two phenyl rings is critical. In fact, compound **14**, bearing an amide spacer in this position, exhibits higher hA_{2A} AR affinity with respect to compound **16**, which presents a methylamine linker. Docking conformations show that the carbonyl group of the amide spacer makes, as H-bond acceptor, a polar interaction with the side chain of Tyr271$^{7.36}$, which is not given by the methylamine linker.

Compounds **18**, **19**, **21**-**23**, featuring even larger 6-substituents, present a wide series of conformations due to the high flexibility of this group. Hence, while the bicyclic core of these molecules conserves the above-described position and orientation within the depth of the cavity, their 6-substituents have several possible arrangements and interactions with externally located receptor residues. Thus, a clear interpretation of the affinity data is not feasible. Almost all these compounds present the spacer starting with an amide group that provides analogue interaction with Tyr271$^{7.36}$, as described above. Similar to the amide function, even the ether oxygen atom at the beginning of the linker of compound **23** makes interaction with Tyr271$^{7.36}$, contributing to the high hA_{2A} AR affinity of this molecule.

2.4. Molecular modeling studies at hCAs

Docking studies were performed at crystal structures of hCAs II, IX and XII isoforms. Figure 3 depicts the interaction mode of a representative compound per subset (**4**, **14** and **20**) in the active site of the selected hCAs. As expected, the benzenesulfonamide moiety of all docked compounds coordinates the Zn(II) ion, and establishes two H-bonds with Thr199 from the three binding sites (Fig. 3).

The length of the spacers linking the 1,2,4-triazolo[4,3-a]pyrazin-3-one to the benzensulfonamide moiety influences the binding efficiency of the heterocycle nucleus to distinct pockets of hCAs II, IX and XII active site. The triazolopyrazine scaffold of compound **4** is located in the middle of the binding cavity of the three isoforms, mainly forming van der Waals contacts with different amino acids depending on the isozyme (Fig. 3A, D, G). π-π interactions with Phe131 from hCA II (Fig. 3A) are absent in the adduct with the hCA IX, where the residue is replaced by the smaller and not aromatic Val131 (Fig. 3D), thus resulting in a weaker inhibition profile. In contrast, the presence of Ser residues (132 and 135) in hCA XII drives the bicyclic core of compound **4** towards a new positioning and interactions in the active site likely responsible for restoring a sub-micromolar inhibition (Fig. 3G).

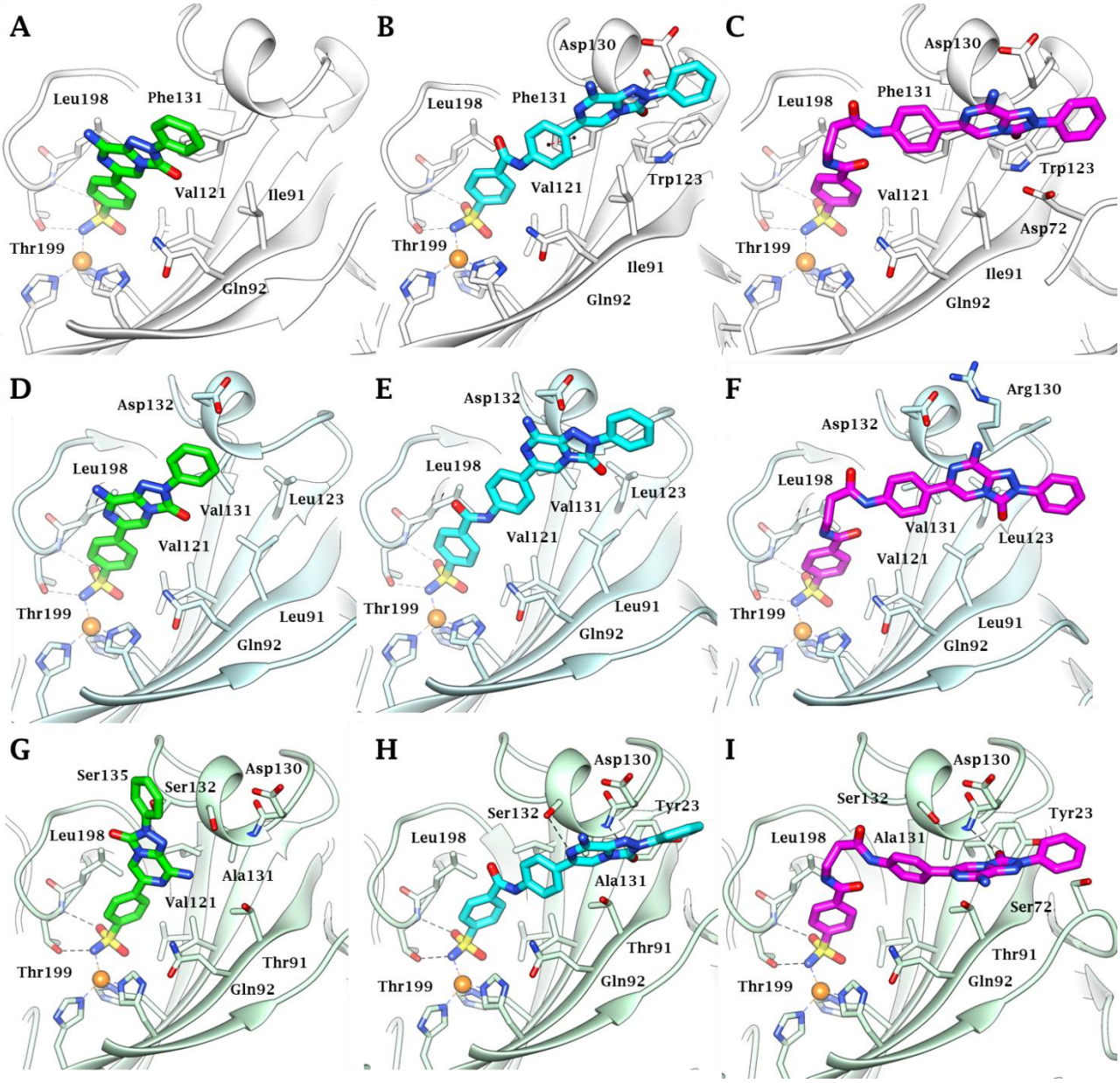

Fig. 3. *In silico* predicted binding mode of compounds **4** (green), **14** (cyan) and **20** (magenta) to hCA II (white), hCA IX (light cyan) and hCA XII (light green). Active site view of hCA II in adduct with A) **4**, B) **14** and C) **20**; active site view of hCA IX in adduct with D) **4**, E) **14** and G) **20**; active site view of hCA XII in adduct with G) **4**, H) **14** and I) **20**. Hydrogen bonds and π-π interactions are represented as black and red dashed lines, respectively.

The triazolopyrazin-3-one scaffold of compound **14** accommodates at the edge of the binding cavity of the three isozymes. In hCA II, the 6-phenyl moiety is in π-π stacking distance with Phe131 and,

at the same time, the backbone NH of the residue acts as a H-bond donor towards the 3-oxo group of the heterocycle (Fig. 1B). In hCA XII, in addition to the already described NH···O=C interaction, a further H-bond is formed involving the Ser132-hydroxyl function and the pyrazine nitrogen at position 7 (Fig. 3H).

The absence of such interactions in the complex formed by **14** and hCA IX is most likely the cause of the reduced inhibition observed with this isozyme in comparison to hCAs II and XII.

The conformation assumed by the ethylene linker of **20** directs the triazolopyrazin-3-one core in pockets which, though featured by amino acids of different nature, all ensure an efficient binding, as indicated by the low nanomolar inhibition against both hCAs II, IX and XII. Indeed, the moiety lies in the cleft formed by Asp130, Phe131, Trp123 and Asp72 in hCA II, where a H-bond is established between the backbone NH of Phe131 and the 3-oxo group of the heterocycle (Fig. 3C).

In hCA XII, an analogous NH···O=C interaction, involving Ala131, exists in the ligand/target adduct with the bicyclic scaffold accommodating in the cleft formed by Asp130, Ala131, Tyr123 and Ser72 (Fig. 3I). On the contrary, the most marked hydrophobic nature of the pocket lodging the triazolopyrazine core in hCA IX, where leucine and proline residues replace the Trp(II)/Tyr(XII)123 and Asp(II)/Ser(XII)72 respectively, favors the formation of π-alkyl contacts between the heterocycle and the pocket (Fig. 3F).

3. Conclusion

This work has led to the identification of the first-in-class multi-target hA_{2A} adenosine receptor antagonists-hCA IX and/or XII inhibitors. The new derivatives ensued from structural modifications of the 8-amino-2,6-diphenyl-1,2,4-triazolo[4,3-*a*]pyrazin-3-one, a potent previously reported hA_{2A} AR antagonist, that was decorated with substituents addressing activity against hCAs. Most of the new triazolopyrazines were endowed with nanomolar hA_{2A} AR affinity and high selectivity versus the other ARs. The most active multi-target compounds bear a benzensulfonamide residue attached through different spacers to the 6-phenyl ring (compounds **14**, **16**-**20**). The best combined activity at

the hA_{2A} AR and hCA IX and/or hCA XII isoforms was shown by derivatives **14** and **20**, which can be therefore considered as promising candidates for further pharmacological evaluation as anticancer agents.

4. Experimental section

4.1. Chemistry

The microwave-assisted syntheses were performed using an Initiator EXP Microwave Biotage instrument (frequency of irradiation: 2.45 GHz). Analytical silica gel plates (0.20 mm, F254, Merck, Germany) and silica gel 60 (Merck, 70-230 mesh) was used for analytical and column chromatography, respectively. All melting points were determined on a Gallenkamp melting point apparatus and are uncorrected. Elemental analyses were performed with a Flash E1112 Thermofinnigan elemental analyzer for C, H, N and the results were within 0.4% of the theoretical values. All final compounds revealed purity not less than 95%. The IR spectra were recorded with a Perkin-Elmer Spectrum RX I spectrometer in Nujol mulls and are expressed in cm^{-1}. NMR spectra were recorded on a Bruker Avance 400 spectrometer (400 MHz for ^{1}H- and 100 Mz for ^{13}C- NMR). The chemical shifts are reported in δ (ppm) and are relative to the central peak of the solvent which was $CDCl_3$ or $DMSOd_6$. The following abbreviations are used: s= singlet, d= doublet, t= triplet, q= quartet, m= multiplet, br= broad and ar= aromatic protons.

Compounds were named following IUPAC rules as applied by ChemDrawUtra 9.0.

*4.1.1. 4-(8-Amino-3-oxo-2-phenyl-2,3-dihydro-1,2,4-triazolo[4,3-a]pyrazin-6-yl)benzensolfonamides (**4**)* and *4-(8-dimethylamino-3-oxo-2-phenyl-2,3-dihydro-1,2,4-triazolo[4,3-a]pyrazin-6-yl)benzensulfonamide (**4a**).*

A suspension of N^1-((8-chloro-3-oxo-2-phenyl-2,3-dihydro-1,2,4-triazolo[4,3-a]pyrazin-6-yl)sulfonyl)-N,N-dimethylformimidamide **29**, in a saturated ethanolic solution of NH_3 (50 mL), was

heated at 120 °C in a sealed tube for 14h. The mixture was cooled at rt, the suspended solid was collected by filtration and washed with water (about 5-10 mL). The crude product was constituted by the desired 8-amino-triazolopyrazine **4** and its 8-dimethylamino derivate **4a** (about ratio 1:1, from ^{1}H-NMR spectrum) which were separated by column chromatography (eluent $CHCl_3$ 9.3/ MeOH 0.7).

*4.1.1.1. Compound **4***. Yield 32%; mp >300 °C; ^{1}H NMR (DMSO-d_6) 8.19 (d, 2H, ar, J = 8.4 Hz), 8.08 (d, 2H, ar, J = 8.1 Hz), 7.96 (s, 1H, H-5), 7.87 (d, 2H, ar, J = 8.4 Hz), 7.67 (s, 2H, NH_2), 7.57 (t, 2H, ar, J = 7.9 Hz), 7.43-7.34 (m, 3H, 1 ar + NH_2 sulfonamide). Anal.$C_{17}H_{14}N_6O_3S$ (C, H, N).

*4.1.1.2. Compound **4a***. Yield 30%; mp 270-273 °C; ^{1}H NMR (DMSO-d_6) 8.24 (d, 2H, ar, J = 8.3 Hz), 8.08 (d, 2H, ar, J = 7.6 Hz), 7.95 (s, 1H, H-5), 7.86 (d, 2H, ar, J = 8.3 Hz), 7.57 (t, 2H, ar, J = 7.8 Hz), 7.43-7.32 (m, 3H, 1ar + SO_2NH_2), 3.55 (s, 6H, $2CH_3$). Anal.$C_{19}H_{18}N_6O_3S$ (C, H, N).

*4.1.2. Ethyl 2-((4-(8-amino-3-oxo-2-phenyl-2,3-dihydro-1,2,4-triazolo[4,3-a]pyrazin-6-yl)phenyl)amino)acetate (**5**).*

A mixture of the 6-(4-aminophenyl)-substituted triazolopyrazine **30** [22] (1.0 mmol), ethyl 2-bromoacetate (4.0 mmol) and Et_3N (2.0 mmol) in anhydrous THF (15 mL) was heated under microwave irradiation at 120 °C for 1h and 30 min. The solvent was eliminated at reduced pressure and the resulting solid was rinsed with water (5 mL), collected by filtration, washed with Et_2O (10 mL) and recrystallized from CH_3CN. Yield 72%; mp 237-239 °C; ^{1}H NMR (DMSO-d_6) 8.08 (d, 2H, ar, J = 8.0 Hz), 7.71 (d, 2H, ar, J = 8.6 Hz,), 7.56 (t, 2H, ar, J = 7.9 Hz), 7.51 (s, 1H, ar), 7.44 (br s, 2H, NH_2), 7.35 (t, 1H, ar, J = 7.4 Hz), 6.60 (d, 2H, ar, J = 8.6 Hz), 6.20 (t, 1H, NH, J = 6.3 Hz), 4.14 (q, 2H, CH_2, J = 7.1 Hz,), 3.94 (d, 2H, CH_2, J = 6.3 Hz), 1.21 (t, 3H, CH_3, J = 7.1 Hz). ^{13}C-NMR (DMSO-d_6) 171.64, 148.69, 147.59, 138.04, 136.72, 131.52, 129.62, 126.86, 126.68, 124.97, 119.86, 112.45, 99.06, 60.78, 45.15, 14.61. Anal.$C_{21}H_{20}N_6O_3$ (C, H, N).

*4.1.3. (4-(8-Amino-3-oxo-2-phenyl-2,3-dihydro-1,2,4-triazolo[4,3-a]pyrazin-6-yl)phenyl)glycine (**5a**).*

1N sodium hydroxide (0.75 mmol) was added to a suspension of the ethyl ester **5** (0.25 mmol) in EtOH (4 mL), and the mixture was heated at 30 °C for about 1h and 30 min. The solvent was concentrated at reduced pressure and the resulting mixture was diluted with water (10 mL) and acidified with 6N HCl to pH = 2. The resulting solid was collected by filtration, washed with Et_2O (20 ml) and dried. It was not possible to purify the obtained acid because it was unstable upon recrystallization (EtOH) and on silica gel. Yield 64% (crude compound); ^{1}H NMR (DMSO-d_6) 8.53 (br s, 1H, OH), 8.06 (d, 2H, ar, J = 7.8 Hz), 7.67 (d, 2H, ar, J = 8.3 Hz), 7.63-7.53 (m, 4H,2H ar + NH_2), 7.38 (t, 1H, ar, J = 7.2 Hz), 6.64 (d, 2H, ar, J = 8.4 Hz), 3.87 (s, 1H, CH_2).

*4.1.4. 4-((4-(8-Amino-3-oxo-2-phenyl-2,3-dihydro-1,2,4-triazolo[4,3-a]pyrazin-6-yl)phenyl)amino)-4-oxobutanoic acid (**6**).*

A mixture of the 6-(4-aminophenyl)-triazolopyrazine derivative **30** [22] (1.0 mmol) and succinic anhydride (1.0 mmol) in anhydrous THF (15 mL) was refluxed for about 8-10 h. The mixture was cooled at rt, the suspended solid was collected by filtration, washed with Et_2O (about 5-10 mL), dried and recrystallized from MeOH. Yield 77%; mp 260-263 °C; ^{1}H NMR (DMSO-d_6) 12.03 (br s, 1H, OH), 10.07 (s, 1H, NH), 8.08 (d, 2H, ar, J = 7.7 Hz), 7.91 (d, 2H, ar, J = 8.7 Hz), 7.70 (s, 1H, H-5), 7.64 (d, 2H, ar, J = 8.7 Hz), 7.62-7.52 (m, 4H, 2 ar + NH_2), 7.36 (t, 1H, ar, J = 7.4 Hz), 2.63-2.54 (m, 4H, 2 CH_2). ^{13}C-NMR (DMSO-d_6) 174.27, 170.60, 147.80, 147.62, 139.66, 137.98, 135.78, 131.57, 131.38, 129.65, 126.75, 126.34, 119.89, 119.23, 101.00, 31.58, 29.32. Anal.$C_{21}H_{18}N_6O_4$ (C, H, N).

*4.1.5. General procedure for the synthesis of methoxy-substituted N-(4-(8-amino-3-oxo-2-phenyl-2,3-dihydro-1,2,4-triazolo[4,3-a]pyrazin-6-yl)phenyl)-benzamides **7** and **8**.*

A mixture of the 6-(4-aminophenyl)-triazolopyrazine derivative **30** [22] (0.79 mmol), the suitably substituted benzoic acid (0.95 mmol), 1-(3-(dimethylamino)-propyl))-3-ethylcarbodiimide hydrochloride (1.57 mmol), Et_3N (1.98 mmol) and 1-hydroxybenzotriazole (1.57 mmol), in anhydrous DMF (3 mL) was stirred for about 24h at rt, under nitrogen atmosphere. The mixture was diluted with water (20 mL) and the solid was collected by filtration, rinsed with water (3 mL), Et_2O (10 mL) and dried. The crude compounds were purified by column chromatography.

*4.1.5.1. N-(4-(8-Amino-3-oxo-2-phenyl-2,3-dihydro-1,2,4-triazolo[4,3-a]pyrazin-6-yl)phenyl)-4-methoxybenzamide (**7**).*

Yield 40%; eluent $CHCl_3$ 9.7/MeOH 0.3; mp 286-288 °C; ^{1}H NMR (DMSO-d_6) 10.17 (s, 1H, NH), 8.08 (d, 2H, ar, J = 7.7 Hz), 8.04-7.91 (m, 4H, ar), 7.85 (d, 2H, ar, J = 8.8 Hz), 7.74 (s, 1H, H-5), 7.62.7.50 (m, 4H, 2ar + NH_2), 7.36 (t, 1H, ar, J = 7.4 Hz), 7.08 (d, 2H, ar, J = 8.8 Hz), 3.85 (s, 3H, CH_3). Anal.$C_{25}H_{20}N_6O_3$ (C, H, N).

*4.1.5.2. N-(4-(8-Amino-3-oxo-2-phenyl-2,3-dihydro-1,2,4-triazolo[4,3-a]pyrazin-6-yl)phenyl)-3,4-dimethoxybenzamide (**8**).*

Yield 45%; eluent $CHCl_3$ 9.7/MeOH 0.3; mp 256-259 °C; ^{1}H NMR (DMSO-d_6) 10.16 (s, 1H, NH), 8.08 (d, 2H, ar, J = 7.8 Hz), 7.98 (d, 2H, ar, J = 8.6 Hz), 7.84 (d, 2H, ar, J = 8.6 Hz), 7.75 (s, 1H, ar), 7.65 (d, 1H, ar, J = 8.4 Hz), 7.62-7.50 (m, 5H, 2ar + H-5 + NH_2), 7.36 (t, 1H, ar, J = 7.3 Hz), 7.10 (d, 1H, ar, J = 8.5 Hz), 3.86 (s, 3H, CH_3), 3.85 (s, 3H, CH_3). ^{13}C-NMR (DMSO-d_6) 165.34, 152.17, 148.81, 147.80, 147.62, 139.68, 137.96, 135.76, 131.87, 131.58, 129.64, 127.43, 126.74, 126.18, 121.56, 120.68, 119.88, 111.61, 111.46, 101.14, 56.16. Anal.$C_{26}H_{22}N_6O_4$ (C, H, N).

*4.1.6. General procedure for the synthesis of hydroxy-substituted N-(4-(8-amino-3-oxo-2-phenyl-2,3-dihydro-1,2,4-triazolo[4,3-a]pyrazin-6-yl)phenyl)-benzamides **9** and **10**.*

1M BBr_3 solution in CH_2Cl_2 (2 mL) was slowly added at 0 °C, under nitrogen atmosphere, to a suspension of the methoxy-substituted derivatives **7** or **8** (0.37 mmol) in anhydrous CH_2Cl_2 (20

mL). The mixture was stirred at rt until the disappearance of the starting material (TLC monitoring, 16-48 h). Then the suspension was diluted with water (10 mL) and neutralized with a $NaHCO_3$ saturated solution. Most of the organic solvent was removed by evaporation at reduced pressure and the obtained solid was collected by filtration. The crude derivatives were dried and purified by column chromatography (**9**) or by recrystallization (**10**).

*4.1.6.1. N-(4-(8-Ammino-3-oxo-2-phenyl-2,3-dihydro-1,2,4-triazolo[4,3-a]pyrazin-6-yl)phenyl)-4-hydroxybenzamide (**9**).*

Yield 65%; eluent $CHCl_3$ 9.5/MeOH 0.5; mp >300 °C; ^{1}H NMR (DMSO-d_6) 10.10 (s, 1H, NH), 10.07 (s, 1H, OH), 8.08 (d, 2H, ar, J = 7.9 Hz), 7.95 (d, 2H, ar, J = 8.4 Hz), 7.91-7.79 (m, 4H, ar), 7.73 (s, 1H, H-5), 7.64-7.51 (m, 4H, 2ar + NH_2), 7.40-7.32 (m,1H, ar), 6.87 (d, 2H, J = 8.3 Hz). Anal.$C_{24}H_{18}N_6O_3$ (C, H, N).

*4.1.6.2. N-(4-(8-Ammino-3-oxo-2-phenyl-2,3-dihydro-1,2,4-triazolo[4,3-a]pyrazin-6-yl)phenyl)-3,4-dihydroxybenzamide (**10**).*

Yield 42%; mp 300 °C dec (MeOH); ^{1}H NMR (DMSO-d_6) 10.01 (s, 1H, NH), 9.60 (s, 1H, OH), 9.22 (s, 1H, OH), 8.09 (d, 2H, ar, J = 7.9 Hz), 7.94 (d, 2H, ar, J = 8.5 Hz), 7.83 (d, 2H, ar, J = 8.6 Hz), 7.72 (s, 1H, H-5), 7.63-7.50 (m, 4H, 2ar + NH_2), 7.47–7.31 (m, 3H, 2ar + H-5), 6.84 (d, 1H, ar, J = 8.2 Hz). ^{13}C-NMR (DMSO-d_6) 165.72, 149.39, 148.63, 147.81, 147.64, 145.44, 139.94, 137.98, 135.83, 131.59, 129.65, 126.74, 126.36, 126.14, 120.42, 120.13, 119.89, 115.93, 115.38, 101.04. Anal.$C_{24}H_{18}N_6O_4$ (C, H, N).

*4.1.7. Ethyl 4-((4-(8-amino-3-oxo-2-phenyl-2,3-dihydro-1,2,4-triazolo[4,3-a]pyrazin-6-yl)phenyl)carbamoyl)benzoate (**11**).*

A mixture of the 6-(4-aminophenyl)-substituted triazolopyrazine derivative **30** [22] (0.62 mmol), 4-(ethoxycarbonyl)benzoic acid [30] (1.57 mmol), 1-(3-(dimethylamino)-propyl))-3-ethylcarbodiimide hydrochloride (2.37 mmol), Et_3N (2.77 mmol) and 1-hydroxybenzotriazole (2.37 mmol), in anhydrous DMF (3 mL), was stirred for about 6h, at rt and under nitrogen atmosphere.

The mixture was diluted with water (20 mL) and the obtained solid was collected by filtration, washed with water (3 mL), Et_2O (10 mL), dried and recrystallized from a mixture of nitromethane/MeOH. Yield 30%; mp 296-298 °C; ^{1}H NMR (DMSO-d_6) 10.52 (s, 1H, NH), 8.21-8.06 (m, 6H, ar), 7.99 (d, 1H, J = 8.7 Hz), 7.86 (d, 2H, ar, J = 8.7 Hz), 7.75 (s, 1H, H-5), 7.64-7.51 (m, 4H, 2ar + NH_2), 7.36 (t, 1H, ar, J = 7.4 Hz), 4.37 (q, 3H, CH_3, J = 7.0 Hz), 1.36 (t, 3H, CH_3, J = 7.1 Hz). ^{13}C-NMR (DMSO-d_6) 65.65, 165.10, 147.82, 147.62, 139.39, 139.26, 137.98, 135.68, 132.80, 132.37, 131.57, 129.62, 129.57, 128.51, 126.73, 126.25, 120.69, 119.86, 101.30, 61.56, 14.59. Anal.$C_{27}H_{22}N_6O_4$ (C, H, N).

*4.1.8. 4-((4-(8-Amino-2-phenyl-2,3-dihydro-1,2,4-triazolo[4,3-a]pyrazin-6-yl)phenyl)carbamoyl)benzoic acid (**12**).*

1N Sodium hydroxide (1.86 mmol) was added to a suspension of the ethyl ester **11** (0.62 mmol) in EtOH (30 mL) and the mixture was refluxed for about 1.5 h. The solvent was eliminated at reduced pressure and the resulting solid was rinsed with water (20 ml), collected by filtration, washed and recrystallized from MeOH/EtOH/$CHCl_3$. Yield 62%; mp >300 °C; ^{1}H NMR (DMSO-d_6) 13.25 (br s, 1H, COOH), 10.50 (s, 1H, NH), 8.13-8.00 (d, 6H, ar, J = 5.9 Hz), 7.99 (d, 2H, ar, J = 8.5 Hz), 7.86 (d, 2H, ar, J = 8.5 Hz), 7.75 (s, 1H, H-5), 7.63-7.51 (m, 4H, 2ar + NH_2), 7.36 (t, 1H, ar, J = 7.3 Hz). Anal.$C_{25}H_{18}N_6O_4$ (C, H, N).

*4.1.9. N^1-(4-(8-Amino-3-oxo-2-phenyl-2,3-dihydro-1,2,4-triazolo[4,3-a]pyrazin-6-yl)phenyl)-N^4-hydroxytereftalamide (**13**).*

1M BBr_3 solution in CH_2Cl_2 (0.87 mL) was slowly added at 0 °C, under nitrogen atmosphere, to a suspension of derivative **31** (0.17 mmol) in anhydrous CH_2Cl_2 (15 mL). The mixture was stirred at rt for 2h and the excess of BBr_3 was neutralized with methanol (10 ml). The solvent was removed at reduced pressure and the resulting solid was collected by filtration, rinsed with water (20 ml) and purified by recrystallization from 2-methoxyethanol. Yield 62%; mp 275 °C dec ; ^{1}H NMR

(DMSO-d_6) 11.40 (br s, 1H), 10.44 (br s, 1H, NH), 9.17 (br s, 1H, OH), 8.14-7.93 (m, 7H, ar), 7.94-7.82 (m, 3H, ar), 7.75 (s, 1H, H-5), 7.63-7.50 (m, 4H, 2ar + NH_2), 7.36 (t, 1H, J = 7.3 Hz). Anal.$C_{25}H_{19}N_7O_4$ (C, H, N).

*4.1.10. General procedure for the synthesis of N-(4-(8-amino-3-oxo-2-phenyl-2,3-dihydro-1,2,4-triazolo[4,3-a]pyrazin-6-yl)phenyl)-sulfamoylbenzamides **14** and **15**.*

A mixture of the 6-(4-aminophenyl)-substituted triazolopyrazine **30** [22] (1.0 mmol), the suitable sulfamoylbenzoic acid (2.4 mmol), 1-(3-(dimethylamino)-propyl))-3-ethylcarbodiimide hydrochloride (2.4 mmol), Et_3N (2.9 mmol) and 1-hydroxybenzotriazole (2.4 mmol), in anhydrous DMF (3 mL), was stirred for about 48h, at rt and under nitrogen atmosphere. The mixture was diluted with water (20 mL) and the obtained solid was collected by filtration, rinsed with water (10 mL), Et_2O (10 mL), dried and purified by column chromatography (**14**) or by recrystallization (**15**).

*4.1.10.1. N-(4-(8-Amino-3-oxo-2-phenyl-2,3-dihydro-1,2,4-triazolo[4,3-a]pyrazin-6-yl)phenyl)-4-sulfamoylbenzamide (**14**).*

Yield 20%; mp >300 °C (acetone); ^{1}H NMR (DMSO-d_6) 10.52 (br s, 1H, NH), 8.14-8.08 (m, 4H, ar), 7.99 (t, 4H, ar, J = 9.9 Hz), 7.86 (d, 2H, ar, J = 8.4 Hz), 7.76 (s, 1H, ar), 7.57-7.54 (m, 4H, ar), 7.54 (br s, 2H, NH_2), 7.36 (t, 1H, ar, J = 7.2 Hz). ^{13}C-NMR (DMSO-d_6) 164.95, 147.83, 147.63, 147.01, 139.23, 138.27, 137.97, 135.62, 132.38, 131.57, 129.65, 128.85, 126.75, 126.28, 126.15, 120.62, 119.85, 101.33. IR 1717, 1684, 1647, 1558, 1541. Anal.$C_{24}H_{19}N_7O_4S$ (C, H, N).

*4.1.10.2. N-(4-(8-Amino-3-oxo-2-phenyl-2,3-dihydro-1,2,4-triazolo[4,3-a]pyrazin-6-yl)phenyl)-3-sulfamoylbenzamide (**15**).* Yield 18%; eluent $CHCl_3$ 9.5/MeOH 0.1; mp >300 °C; ^{1}H NMR (DMSO-d_6) 10.59 (br s, 1H, NH), 8.41 (s, 1H, ar), 8.21 (d, 1H, ar, J = 7.7 Hz), 8.10-7.94 (m, 5H, ar), 7.86 (d, 2H, ar, J = 8.6 Hz), 7.83-7.72 (m, 2H, ar), 7.62-7.52 (m, 4H, 2ar + NH_2), 7.50 (br s, 2H, SO_2NH_2), 7.36 (t, 1H, ar, J = 7.3 Hz). Anal.$C_{24}H_{19}N_7O_4S$ (C, H, N).

*4.4.11. 4-(((4-(8-Amino-3-oxo-2-phenyl-2,3-dihydro-1,2,4-triazolo[4,3-a]pyrazin-6-yl)phenyl)amino)methyl)benzenesulfonamide (**16**).*

4-(Bromomethyl)benzenesulfonamide [31] (2.0 mmol) was added to a suspension of the 6-(4-aminophenyl)-substituted triazolopyrazine **30 [**22] (1.6 mmol) and K_2CO_3 (3.0 mmol) in anhydrous THF (15 mL) and the mixture was heated at reflux. After 5h and 24h, other two portions of 4-(bromomethyl)benzenesulfonamide were added (2.0 mmol and 1.0 mmol, respectively). The heating was maintained for further 24h, then the solvent was evaporated at reduced pressure. The resulting solid was treated with water (20 ml), collected by filtration, washed with Et_2O (10 mL) and recrystallized from nitromethane. Yield 93%; mp > 300 °C; ^{1}H NMR (DMSO-d_6) 8.07 (d, 2H, ar, J = 7.7 Hz), 7.78 (d, 2H, ar, J = 8.3 Hz), 7.67 (d, 2H, ar, J = 8.6 Hz), 7.55 (m, 4H, ar), 7.47 (s, 1H, ar), 7.42 (br s, 2H, NH_2), 7.34 (t, 1H, ar, J = 7.4 Hz), 7.27 (br s, 2H, NH_2), 6.67-6.60 (m, 3H, 1ar + NH_2), 4.42-4.40 (m, 2H, CH_2). ^{13}C-NMR (DMSO-d_6) 148.89, 147.55, 144.98, 142.98, 138.02, 136.73, 135.15, 131.49, 129.63, 127.88, 126.92, 126.69, 126.20, 124.62, 119.85, 112.62, 98.94, 46.36. IR 3368, 1695, 1647, 1541, 1520, 1457. Anal.$C_{24}H_{21}N_7O_3S$ (C, H, N).

*4.1.12. 4-((4-(8-Amino-3-oxo-2-phenyl-2,3-dihydro-1,2,4-triazolo[4,3-a]pyrazin-6-il)phenyl)glicyl)benzensulfonamide (**17**).*

A mixture of 6-(4-aminophenyl)-substituted triazolopyrazine **30** [22] (0.31 mmol), 4-(2-bromoacetyl)benzenesulfonamide [29] (0.62 mmol) and K_2CO_3 (0.62 mmol) in anhydrous THF (15 mL) was refluxed for about 28h. The solvent was evaporated at reduced pressure and the resulting solid was suspended in water (10 mL). The suspension was acidified with 1N HCl until pH= 4 and the obtained solid was collected by filtration, washed with water (20 ml) and Et_2O and recrystallized from acetone. Yield 23%; mp 235-237 °C dec; ^{1}H NMR (DMSO-d_6) 8.25 (d, 2H, ar, J = 8.2 Hz), 8.08 (d, 2H, ar, J = 8.0 Hz), 7.99 (d, 2H, ar, J = 8.3 Hz), 7.72 (d, 2H, ar, J = 8.4 Hz), 7.60–7.50 (m, 5H, 3ar + SO_2NH_2), 7.44 (br s, 2H, NH_2), 7.35 (t, 1H, ar, J = 7.3 Hz), 6.75 (d, 2H, ar, J = 8.5 Hz), 6.16-6.10 (m, 1H, NH), 4.79 (d, 2H, CH_2, J = 5.2 Hz). Anal.$C_{25}H_{21}N_7O_4S$ (C, H, N).

*4.1.13. N-(4-(8-Amino-3-oxo-2-phenyl-2,3-dihydro-1,2,4-triazolo[4,3-a]pyrazin-6-yl)phenyl)-3-((4-sulfamoylphenethyl)amino)propanamide (**18**).* A mixture the 6-(4-acrylamidophenyl)-substituted derivative **31** [24] (6.0 mmol) and 4-(2-aminoethyl)benzensulfonamide [32] (36.0 mmol) in anhydrous THF (15 mL) was refluxed for about 24h. The solvent was eliminated at reduced pressure and the resulting solid was rinsed with EtOH (5-10 mL), collected by filtration, and recrystallized from nitromethane. Yield 69%; mp 228-230 °C; ^{1}H NMR (DMSO-d_6) 10.15 (br s, 1H, NH), 8.08 (d, 2H, ar, J = 7.7 Hz), 7.90 (d, 2H, ar, J = 8.7 Hz), 7.73 (d, 2H, ar, J = 8.2 Hz), 7.69 (s, 1H, H-5), 7.62-7.54 (m, 6H, 4ar + NH_2), 7.42 (d, 2H, ar, J = 8.3 Hz), 7.36 (t, 1H, ar, J = 7.4 Hz), 7.28 (s, 2H, SO_2NH_2), 2.85 (t, 2H, CH_2, J = 6.6 Hz), 2.80 (br s, 4H, $2CH_2$), 2.46 (t, 2H, CH_2, J = 6.5 Hz). ^{13}C-NMR (DMSO-d_6) 170.95, 147.80, 147.62, 145.24, 142.29, 139.58, 137.98, 135.78, 131.56, 131.44, 129.65, 129.52, 126.75, 126.34, 126.09, 119.87, 119.32, 101.01, 50.76, 45.69, 37.36, 35.96. IR 3327, 3310, 1699, 1539, 1506, 1456. Anal.$C_{28}H_{28}N_8O_4S$ (C, H, N).

*4.1.14. N-(4-(8-Amino-3-oxo-2-phenyl-2,3-dihydro-1,2,4-triazolo[4,3-a]pyrazin-6-yl)phenyl)-3-((4-sulfamoylbenzyl)amino)propanamide (**19**).* A mixture of the 6-(4-(3-aminopropanamido)phenyl derivative **32** (1.00 mmol), prepared from derivative **31** as previously reported [24], 4-(bromomethyl)benzenesulfonamide [31] (0.5 mmol) and K_2CO_3 (2.00 mmol) in anhydrous THF (15 mL) was refluxed. After 5h and 11h, other two portions of 4-(bromomethyl)benzenesulfonamide were added (0.5 mmol and 0.2 mmol, respectively). The heating was maintained for further 13h. The solvent was eliminated at reduced pressure and the resulting solid suspended in water (10 mL). The suspension was acidified with HCl 1N until pH= 4 and the obtained solid was collected by filtration, washed with water (20 ml) and Et_2O (10 mL) and purified by column chromatography. Yield 20%; eluent $CHCl_3$ 9.0/MeOH 1.0; mp 256-258 °C; ^{1}H NMR (DMSO-d_6) 10.14 (br s, 1H, NH), 8.08 (d, 2H, ar, J = 7.7 Hz), 7.91 (d, 2H, ar, J = 8.7 Hz), 7.78 (d, 2H, ar, J = 8.3 Hz), 7.70 (s, 1H, H-5), 7.64 (m, 2H, ar), 7.58-7.52 (m, 6H, ar + NH_2), 7.35 (t, 1H, ar, J = 7.4 Hz), 7.30 (br s, 2H,

SO_2NH_2), 3.82 (s, 2H, CH_2), 2.81 (t, 2H, CH_2, J = 6.7 Hz), 2.53-2.51 (m, 2H, CH_2). ^{13}C-NMR (DMSO-d_6) 170.84, 147.79, 147.62, 145.24, 142.94, 139.59, 137.97, 135.74, 131.56, 131.45, 129.65, 128.73, 126.74, 126.33, 126.02, 119.85, 119.35, 101.01, 52.50, 45.14, 37.26. IR 3352, 3335, 3308, 3296, 1682, 1506. Anal.$C_{27}H_{26}N_8O_4S$ (C, H, N).

4.1.15. General procedure for the synthesis of sulfamoyl-substituted N-(3-((4-(8-amino-3-oxo-2-phenyl-2,3-dihydro-1,2,4-triazolo[4,3-a]pyrazin-6-yl)phenyl)amino)-3-oxopropyl)-benzamides ***20*** *and* ***21****.*

A mixture of the 6-(4-(3-aminopropanamido)-phenyl derivative **32** [24] (1.0 mmol), the suitable sulfamoylbenzoic acid (1.1 mmol), 1-(3-(dimethylamino)-propyl))-3-ethylcarbodiimide hydrochloride (1.1 mmol), triethylamine (1.1 mmol) and 1-hydroxybenzotriazole (1.1 mmol), in anhydrous DMF (3 mL), was stirred for about 2h, at rt and under nitrogen atmosphere. The mixture was diluted with water (20 mL) and the obtained solid was collected by filtration, rinsed with water (10 mL), Et_2O (10 mL), dried and purified by recrystallization (**20**) or by column chromatography (**21**).

*4.1.15.1. N-(3-((4-(8-Amino-3-oxo-2-phenyl-2,3-dihydro-1,2,4-triazolo[4,3-a]pyrazin-6-yl)phenyl)amino)-3-oxopropyl)-4-sulfamoylbenzamide (****20****).*

Yield 75%; mp 298-300 °C (nitromethane); ^{1}H NMR (DMSO-d_6) 10.09 (br s, 1H, NH), 8.81 (br s, 1H, NH), 8.08 (d, 2H, ar, J = 8.1 Hz), 8.00 (d, 2H, ar, J = 8.4 Hz), 7.93-7.89 (m, 4H, ar), 7.70-7.66 (m, 3H, ar), 7.58-7.55 (m, 2H, ar), 7.56 (br s, 2H, NH_2), 7.55 (br s, 2H, NH_2), 7.36 (t, 1H, ar, J = 7.1 Hz), 3.59 (t, 2H, CH_2, J = 6.9 Hz), 2.67 (t, 2H, CH_2, J = 6.8 Hz). ^{13}C-NMR (DMSO-d_6) 169.91, 165.82, 147.80, 147.62, 146.68, 139.55, 137.97, 137.83, 135.72, 131.56, 129.65, 128.30, 126.75, 126.32, 126.08, 119.85, 119.88, 119.40, 101.01, 36.74, 36.53. IR 3365.78, 3282.84, 1683.86, 1647.21, 1558.48, 1521.84. Anal.$C_{27}H_{24}N_8O_5S$ (C, H, N).

*4.1.15.2. N-(3-((4-(8-Amino-3-oxo-2-phenyl-2,3-dihydro-1,2,4-triazolo[4,3-a]pyrazin-6-yl)phenyl)amino)-3-oxopropyl)-3-sulfamoylbenzamide (**21**).* Yield 24%; eluent $CHCl_3$ 9/MeOH 1; mp 272-274 °C. ^{1}H NMR (DMSO-d_6) 10.09 (br s, 1H, NH), 8.87 (br t, 1H, NH, J = 5.43 Hz), 8.32 (s, 1H, ar), 8.08-8.04 (m, 3H, ar), 7.96 (d, 1H, ar, J = 7.9 Hz), 7.91 (d, 2H, ar, J = 8.7 Hz), 7.69-7.65 (m, 4H, ar), 7.58-7.54 (m, 4H, 2ar + NH_2), 7.44 (s, 2H, SO_2NH_2), 7.35 (t, 1H, ar, J= 7.4 Hz), 3.62-3.57 (m, 2H, CH_2), 2.67 (t, 2H, CH_2, J = 6.8 Hz). ^{13}C-NMR (DMSO-d_6) 169.92, 165.63, 148.00, 147.61, 144.87, 139.55, 131.97, 135.73, 135.60, 131.56, 130.61, 129.66, 129.59, 128.57, 126.75, 126.32, 125.19, 119.86, 119.41, 101.03, 36.71, 36.54. Anal.$C_{27}H_{24}N_8O_5S$ (C, H, N).

*4.1.16. 4-(2-((2-(4-(8-Amino-3-oxo-2-phenyl-2,3-dihydro-1,2,4-triazolo[4,3-a]pyrazin-6-yl)phenoxy)ethyl)amino)ethyl)benzensulfonamide (**22**).*

A mixture of the 6-(4-(2-aminoethoxy)phenyl)triazolopyrazine **33** [24] (1 mmol), 4-(2-bromomethyl)benzenesulfonamide [31] (4 mmol) and K_2CO_3 (4 mmol) in anhydrous THF (15 mL) was refluxed for about 48h. The solvent was evaporated at reduced pressure and the obtained solid was collected by filtration, washed with water (20 mL) and Et_2O (10 mL) and purified by column chromatography. Yield 26%; eluent (CH_2Cl_2 9.5/MeOH 0.5); mp 239-241 °C; ^{1}H NMR (DMSO-d_6) 8.08 (d, 2H, ar, J = 7.7 Hz), 7.90 (d, 2H, ar, J = 8.8 Hz), 7.74 (d, 2H, ar, J = 8.3 Hz), 7.65 (s, 1H, H-5), 7.58-7.53 (m, 4H, ar + NH_2), 7.43 (d, 2H, ar, J = 8.3 Hz), 7.36 (t, 1H, ar, J = 7.4 Hz), 7.27 (br s, 2H, NH_2), 6.98 (d, 2H, ar, J = 8.9 Hz), 4.06 (t, 2H, CH_2, J = 5.6 Hz), 2.93 (t, 2H, CH_2, J = 5.6 Hz), 2.86-2.82 (m, 4H). ^{13}C-NMR (DMSO-d_6) 158.06, 147.77, 147.65, 145.71, 142.48, 137.99, 135.83, 131.82, 129.66, 129.57, 129.46, 127.31, 126.75, 126.15, 119.87, 114.93, 100,61, 50.47, 48.05, 35.18, 30,37. IR 3325, 1715, 1700, 1541, 1506, 1457. Anal.$C_{27}H_{27}N_7O_4S$ (C, H, N).

*4.1.17. N-(2-(4-(8-Amino-3-oxo-2-phenyl-2,3-dihydro-1,2,4-triazolo[4,3-a]pyrazin-6-yl)phenoxy)ethyl)-4-sulfamoylbenzamide (**23**).*

A mixture of the 6-(4-(2-aminoethoxy)phenyl)triazolopyrazine **33** [24] (0.55 mmol), 4-sulfamoylbenzoic acid (0.61 mmol), 1-(3-(dimethylamino)-propyl))-3-ethylcarbodiimide hydrochloride (0.63 mmol), triethylamine (0.93 mmol) and 1-hydroxybenzotriazole (0.63 mmol), in anhydrous DMF (3 mL), was stirred for about 2h, at rt and under nitrogen atmosphere. The mixture was diluted with water (20 mL) and the obtained solid was collected by filtration, rinsed with water (10 mL), Et_2O (10 mL), dried and purified by column chromatography. Yield 30%; eluent CH_2Cl_2 9.5/MeOH 0.5; mp 178-182 °C; ^{1}H NMR (DMSO-d_6) 8.93 (m, 1H, NH), 8.07 (d, 2H, ar, J = 7.8 Hz), 8.03 (d, 2H, ar, J = 8.4 Hz), 7.95-7.87 (m, 4H, ar), 7.67 (s, 1H, H-5), 7.72-7.55 (m, 4H, 2ar + NH_2), 7.50 (s, 2H, $SONH_2$), 7.35 (t, 1H, ar, J = 7.4 Hz), 7.02 (d, 2H, ar, J = 8.8 Hz), 4.19 (t, 2H, CH_2, J = 5.5 Hz), 3.72-3.64 (m, 2H, CH_2). ^{13}C-NMR (DMSO-d_6) 166.01, 158.92, 147.77, 147.61, 146.77, 137.98, 137.60, 135.78, 131.53, 129.66, 129.46, 128.38, 127.32, 126.75, 126.11, 119.85, 114.92, 100.61, 66.45, 65.38. Anal.$C_{26}H_{23}N_7O_5S$ (C, H, N).

*4.1.18. Ethyl 5-oxo-4-(2-oxo-2-(4-sulfamoylphenyl)ethyl)-1-phenyl-4,5-dihydro-1H-1,2,4-triazolo-3-carboxylate (**26**).*

4-(2-Bromoacetyl)benzenesulfonamide **25** [29] (1.2 mmol) was added dropwise to a mixture of ethyl 1,2,4-triazole-3-carboxylate derivative **24** [28] (1.0 mmol) and potassium carbonate (2.0 mmol) in DMF/CH_3CN (1:9, 10 mL). The suspension was stirred at rt for 4h. The solvent removed at reduced pressure and the residue was treated with water (20 mL). The resulting precipitate was collected by filtration, washed with water (30 mL) and Et_2O (20 mL). This intermediate was pure enough (NMR, TLC) to be used for the next step without further purification. Yield 91%; ^{1}H NMR (DMSO-d_6) 8.29 (d, 2H, ar, J = 8.3 Hz), 8.03 (d, 2H, ar, J = 8.4 Hz), 7.94 (d, 2H, ar, J = 8.1 Hz), 7.63 (br s, 2H, $SONH_2$), 7.56 (t, 1H, ar, J = 7.9 Hz), 7.37 (t, 1H, ar, J = 7.4 Hz), 5.63 (s, 2H, CH_2), 4.29 (q, 2H, CH_2, J = 7.1 Hz), 1.20 (t, 3H, CH_3, J = 7.1 Hz).

*4.1.19. 3,8-Dioxo-2-phenyl-2,3,7,8-tetrahydro-1,2,4-triazolo[4,3-a]pyrazine-6-sulfonamide (**27**).* A mixture of the ethyl 1,2,4-triazole-3-carboxylate derivative **26** (1 mmol) and anhydrous ammonium acetate (7 mmol) was heated in a sealed tube at 140 °C for 4h. The residue was taken up with EtOH (1 mL) and Et_2O (5 mL), collected by filtration, washed with water (20 mL) and recrystallized from 2-methoxyethanol. Yield 60%; ^{1}H NMR (DMSO-d_6) 11.74 (s, 1H, NH), 8.02 (d, 2H, ar, J = 7.9 Hz), 7.95-7.85 (m, 4H, ar), 7.57 (t, 2H, ar, J = 7.9 Hz), 7.52-7.43 (m, 3H, H-5 + $SONH_2$), 7.37 (t, 1H, ar, J = 7.4 Hz). ^{13}C-NMR (DMSO-d_6) 153.49, 147.77, 144.83, 137.65, 135.98, 134.54, 129.81, 127.38, 127.13, 126.99, 126.43, 119.58, 101.81. Anal. Calcd. for $C_{17}H_{13}N_5O_4S$ (C, H, N).

*4.1.20. N^1-((3,8-Dioxo-2-phenyl-2,3,7,8-tetrahydro-1,2,4-triazolo[4,3-a]pyrazin-6-yl)sulfonyl)-N,N-dimethylformimidamide (**28**).* N,N-dimethylformamide dimethylacetal (2 mmol) was added dropwise to a mixture of the benzensulfonamide derivative **27** (1 mmol) in DMF (2 mL) at 0 °C. The mixture was stirred at rt for 20 min, then treated with water (15 mL) and extracted with CH_2Cl_2 (15 mL x 3). The organic phase was washed with water (20 mL x 3) and anhydrified (Na_2SO_4). The solvent was eliminated at reduced pressure and the resulting solid was collected by filtration and dried. This intermediate was pure enough (NMR, TLC) to be used for the next step without further purification. Yield 70%; ^{1}H NMR (DMSO-d_6) 11.71 (s, 1H, NH), 8.27 (s, 1H, CH), 8.01 (d, 2H, J = 7.7 Hz), 7.85 (q, 4H, ar, J = 8.7 Hz), 7.57 (t, 2H, ar, J = 8.0 Hz), 7.44 (s, 1H, H-5), 7.37 (t, 1H, ar, J = 7.4 Hz), 3.17 (s, 3H, CH_3), 2.93 (s, 3H, CH_3). ^{13}C-NMR (DMSO-d_6) 160.42, 153.45, 147.75, 143.79, 137.64, 135.96, 134.46, 129.81, 127.48, 127.10, 126.99, 126.76, 119.57, 101.84, 41.43, 40.60, 40.40, 40.19, 39.98, 39.77, 39.56, 39.35, 35.59.

*4.1.21. N^1-((8-Chloro-3-oxo-2-phenyl-2,3-dihydro-1,2,4-triazolo[4,3-a]pyrazin-6-yl)sulfonyl)-N,N-dimethylformimidamide (**29**).*

A suspension of the 3,8-dioxo-triazolopyrazine derivative **28** (1 mmol) in phosphorus oxychloride (2 mL) was heated in a sealed tube at 160 °C for 1h. The excess of phosphorus oxychloride was

distilled off and the residue was treated with cyclohexane. The obtained solid was collected by filtration, washed with abundant water and dried. This intermediate was pure enough (NMR, TLC) to be used for the next step without further purification. Yield 85%; ^{1}H NMR (DMSO-d_6) 8.78 (s, 1H, CH), 8.26 (s, 1H, H_5), 8.20 (d, 2H, ar, J = 8.4 Hz), 8.06 (d, 2H, ar, J = 7.9 Hz), 7.86 (d, 2H, ar, J = 8.4 Hz), 7.60 (t, 2H, ar, J = 7.8 Hz), 7.41 (t, 1H, ar, J = 7.4 Hz), 3.17 (s, 3H, CH_3), 2.93 (s, 3H, CH_3).

*4.1.22. N^1-(4-(8-Amino-3-oxo-2-phenyl-2,3-dihydro-1,2,4-triazolo[4,3-a]pyrazin-6-yl)phenyl)-N^4-(benzyloxy)tereftalamide (**31**).* Et_3N (0,21 mmol) was added to a solution of O-benzylhydroxylamine HCl (0.21 mmol) in anhydrous DMF (3 mL) and the mixture was stirred at rt. After 15 min, the carboxylic acid **12** (0.21 mmol), 1-(3-(dimethylamino)-propyl))-3-ethylcarbodiimide hydrochloride (0.42 mmol), Et_3N (0.52 mmol) and 1-hydroxybenzotriazole (0.42 mmol) were added and the suspension was stirred at rt for 3h. The mixture was diluted with water (20 mL) and the obtained solid was collected by filtration, rinsed with water (3 mL), Et_2O (10 mL), dried and used for the next step without further purification. Yield 62%; ^{1}H NMR (DMSO-d_6) 11.85 (br s, 1H, NH), 10.45 (br s, 1H, NH), 8.17-7.9 (m, 5H, ar), 7.92-7.82 (m, 4H, ar), 7.75 (s, 1H, H-5), 7.65-7.50 (m, 5H, ar), 7.49-7.44 (m, 2H, ar), 7.43-7.31 (m, 4H, ar), 4.97 (s, 2H, CH_2).

4.2. Molecular Modeling at ARs.

4.2.1. Refinement of the hA_{2A} AR Structures. The crystal structure of the hA_{2A} AR in complex with ZM241385 was retrieved from the Protein Data Bank (http://www.rcsb.org; pdb code: 5NM4; 1.7-Å resolution [33]) and added of all hydrogen atoms within MOE (Molecular Operating Environment 2014.09) [34].

4.5.2. Molecular docking analysis. All compound structures were docked into the binding site of the AR structures using the Induced Fit docking protocol of MOE and the genetic algorithm docking

tool of CCDC Gold [33,34]. The Induced Fit docking protocol of MOE is divided into a number of stages: *Conformational Analysis of ligands*. The algorithm generated conformations from a single 3D conformation by conducting a systematic search. In this way, all combinations of angles were created for each ligand. *Placement*. A collection of poses was generated from the pool of ligand conformations using Alpha Triangle placement method. Poses were generated by superposition of ligand atom triplets and triplet points in the receptor binding site. The receptor site points are alpha sphere centers which represent locations of tight packing. At each iteration, a random conformation was selected, a random triplet of ligand atoms and a random triplet of alpha sphere centers were used to determine the pose. *Scoring*. Poses generated by the placement methodology were scored using the *Alpha HB* scoring function, which combines a term measuring the geometric fit of the ligand to the binding site and a term measuring hydrogen bonding effect. *Induced Fit*. The generated docking conformations were subjected to energy minimization within the binding site and the protein sidechains are included in the refinement stage. In detail, the protein backbone is set as rigid while the side chains are not set to "free to move" but are set to "tethered", where an atom tether is a distance restraint that restrains the distance not between two atoms but between an atom and a fixed point in space. *Rescoring*. Complexes generated by the Induced Fit methodology stage were scored using the *Alpha HB* scoring function. Gold tool was used with default efficiency settings through MOE interface, by selecting ChemScore as scoring function.

4.3. Molecular Modeling at CAs.

The crystal structure of hCA II (PDB 5LJT) [36], hCA IX (PDB 5FL4) [37] and XII (pdb JLD0) [38] were prepared using the Protein Preparation Wizard tool implemented in Maestro - Schrödinger suite, assigning bond orders, adding hydrogens, deleting water molecules, and optimizing H-bonding networks [39]. Energy minimization protocol with a root mean square deviation (RMSD) value of 0.30 was applied using an Optimized Potentials for Liquid Simulation (OPLS3e) force field. 3D ligand structures were prepared by Maestro [39a] and evaluated for their

ionization states at pH 7.4 with Epik [39b]. OPLS3e force field in Macromodel [39e] was used for energy minimization for a maximum number of 2500 conjugate gradient iteration and setting a convergence criterion of 0.05 kcal $mol^{-1}Å^{-1}$. The docking grid was centered on the center of mass of the co-crystallized ligands and Glide used with default settings. Ligands were docked with the standard precision mode (SP) of Glide [39f] and the best 5 poses of each molecule retained as output. The best pose for each compound, evaluated in terms of coordination, hydrogen bond interactions and hydrophobic contacts, was refined with Prime [39d] with a VSGB solvation model considering the target flexible within 3Å around the ligand [40-42].

4.4. Pharmacology

4.4.1. Binding Assay at ARs.

4.4.1.1 Membrane preparation.

Membranes for radioligand binding were prepared as described earlier [24]. In brief, after homogenization of CHO (Chinese Hamster Ovary) cells, stably transfected with hARs, membranes were prepared in a two-step procedure. A first low-speed step (1000 g), where cell fragments and nuclei were removed, was followed by a high-speed centrifugation (100 000g) to sediment the crude membrane fraction. The resulting membrane pellets were resuspended in the buffer used for the respective binding experiments (hA_1 ARs: 50 mM Tris/HCl buffer pH 7.4; hA_{2A} ARs: 50 mM Tris/HCl, 50 mM $MgCl_2$ pH 7.4; hA_3 ARs: 50 mM Tris/HCl, 10 mM $MgCl_2$, 1 mM EDTA, pH 8.25), frozen in liquid nitrogen, and stored in aliquots at −80 °C.

4.4.1.2. Radioligand binding.

The affinity of compounds **1**–**23** for the hAR subtypes, hA_1, hA_{2A}, hA_3, was determined with radioligand competition experiments in CHO cells that were stably transfected with the individual receptor subtypes. The radioligands used were 1.0 nM [^{3}H]CCPA for hA_1, 10 nM [^{3}H]NECA for hA_{2A} and 1.0 nM [^{3}H]HEMADO for hA_3 receptors. Results were expressed as K_i values

(dissociation constants), which were calculated with the program GraphPad (GraphPAD Software, San Diego, CA, USA). Each concentration was tested three-five times in triplicate and the values are given as the mean ± standard error (S.E.).

The potency of antagonists at the hA_{2B} receptor (expressed on CHO cells) was determined by inhibition of NECA- stimulated adenylyl cyclase activity.

4.4.2. GloSensor cAMP Assay.

Functional A_{2A} and A_{2B} activity was determined as described earlier [43,44]. Briefly, cells stably expressing the hA_{2A} or hA_{2B} AR and transiently the biosensor, were harvested and incubated in equilibration medium containing a 3% v/v GloSensor cAMP reagent stock solution, 10% FBS, and 87% CO_2 independent medium. After 2h of incubation at rt, cells were dispensed in the wells of a 384-well plate and NECA reference agonist or the understudy compounds, at different concentrations, were added. When compounds were unable to stimulate the cAMP production they were studied as antagonists. In particular, the antagonist profile was evaluated by assessing the ability of these compounds to counteract NECA-induced increase of cAMP accumulation.

Responses were expressed as percentage of the maximal relative luminescence units (RLU). Concentration–response curves were fitted by a nonlinear regression with the Prism programme. The antagonist profile of the compounds was expressed as IC_{50}, which is the concentration of antagonists that produces 50% inhibition of the agonist effect. Each concentration was tested three-five times in triplicate and the values are given as the mean ± S.E. [45].

4.5. CA inhibition Assay

An applied photophysics stopped-flow instrument has been used for assaying the hCA catalyzed CO_2 hydration activity [46]. Phenol red (at a concentration of 0.2 mM) has been used as indicator, working at the absorbance maximum of 557 nm, with 20 mM Hepes (pH 7.4) as buffer, and 20 mM Na_2SO_4

for maintaining constant the ionic strength (this anion is not inhibitory and has a K_i> 200mM against these enzymes), following the initial rates of the CA-catalyzed CO_2 hydration reaction for a period of 10–100 s. The CO_2 concentrations ranged from 1.7 to 17 mM for the determination of the kinetic parameters and inhibition constants. For each measurement three traces of the initial 5–10% of the reaction have been used for determining the initial velocity (which was the mean of the three traces), working with 10-fold decreasing inhibitor concentrations ranging between 0.1nM and 10–100 mM (depending on the inhibitor potency, but at least five points at different inhibitor concentrations were employed for determining the inhibition constants). The uncatalyzed rates were determined in the same manner and subtracted from the total observed rates. Stock solutions of inhibitor (0.1 mM) were prepared in distilled-deionized water with 10% DMSO and dilutions up to 0.1 nM were done thereafter with the assay buffer. Inhibitor and enzyme solutions were preincubated together for 15 min at room temperature prior to assay, in order to allow for the formation of the E-I complex. The inhibition constants were obtained by non-linear least-squares methods using the Cheng–Prusoff equation, and represent the mean from three independent experiments. All human isoforms were recombinant enzymes produced as described earlier in our laboratory [47-49].

Funding. The work was financially supported by the University of Florence (Fondi Ateneo Ricerca 2018).

Declaration of interests

The authors declare that they have no known competing financial interests or personal relationships that could have appeared to influence the work reported in this paper.

References

1. V. Ivasiv, C. Albertini, A.E. Goncalves, M. Rossi, M.L. Bolognesi, Molecular Hybridization as a Tool for Designing Multitarget Drug Candidates for Complex Diseases, Curr. Top. Med. Chem. 19 (2019) 1694-1711.
2. L. Antonioli, C. Blandizzi, P. Pacher, G. Haskò, Immunity, inflammation and cancer: a leading role for adenosine, Nature 13 (2013) 842-865.
3. P.A. Borea, S. Gessi, S. Merighi, F. Vincenzi, K. Varani, Pathological Overproduction: the Bad Side of Adenosine, Br. J. Pharmacol. 174 (2017) 1945−1960.
4. B. Allard, P.A Beavis, P.K. Darcy, J. Stagg. Immunosuppressive activities of adenosine in cancer, Curr. Opin. Pharmacol. 29 (2016) 7-16.
5. R.D. Leone, A.E. Leisha, Targeting adenosine for cancer immunotherapy, J. Immunother. Cancer 6 (2018) 6, 57.
6. D. Neri, C.T. Supuran, Interfering with pH regulation in tumors as a therapeutic strategy, Nat Rev. Drug Discovery 2011, 10, 767-777.
7. C.T. Supuran, Carbonic anhydrases: Novel therapeutic applications for inhibitors and activators. Nat. Rev. Drug Discovery 7 (2008) 168−181.
8. C.T. Supuran, Carbonic Anhydrase Inhibition and the Management of Hypoxic Tumors, Metabolites 7 (2017) 48.
9. C.T. Supuran, Carbonic anhydrase inhibitors as emerging agents for the treatment and imaging hypoxic tumors, Exp. Opin. Invest. Drugs 27 (2018) 963–970.
10. J. Stagg, M.J. Smyth, Extracellular adenosine triphosphate and adenosine in cancer, Oncogene 29 (2010) 5346-5358.
11. S. Merighi, E. Battistello, L. Giacomelli, K. Varani, F. Vincenzi, P.A. Borea, S. Gessi, Targeting A_3 and A_{2A} adenosine receptors in the fight against cancer, Exp. Opin. Ther. Targets, 23 (2019) 669-678.

12. S. Gessi, S. Bencivenni, E. Battistello, F. Vincenzi, V. Colotta, D. Catarzi, F. Varano, S. Merighi, P.A. Borea, K. Varani, Inhibition of A_{2A} Adenosine Receptor Signaling in Cancer Cells Proliferation by the Novel Antagonist TP455. Front. Pharmacol. 8 (2017) 888.
13. L. Fong, A. Hotson, J.D. Powderly, M. Sznol, R S. Heist, T.K. Choueiri, S. George, B.G.M. Hughes, M.D. Hellmann, D.R. Shepard, B.I. Rini, S. Kummar, A.M. Weise, M.J. Riese, B. Markman, L.A. Emens, D. Mahadevan, J.J. Luke, G. Laport, J.D. Brody, L. Hernandez-Aya, P. Bonomi, J.W. Goldman, L. Berim, D.J. Renouf, R.A. Goodwin, B. Munneke, P.Y. Ho, J. Hsieh, I. McCaffery, L. Kwei, S.B. Willingham, R.A. Miller, Adenosine A_{2A} Receptor Blockade as an Immunotherapy for Treatment-Refractory Renal Cell Cancer, Cancer Discov. 2019. doi: 10.1158/2159-8290.
14. C.T. Supuran, Advances in structure-based drug discovery of carbonic anhydrase inhibitors, Exp. Opin. Drug Discovery, 12 (2017) 61-88.
15. F. Varano, D. Catarzi, F. Vincenzi, M. Betti, M. Falsini, A. Ravani, P.A. Borea, V. Colotta, K. Varani, Design, Synthesis, and Pharmacological Characterization of 2‑(2-Furanyl)thiazolo[5,4-*d*]pyrimidine-5,7-diamine derivatives: new highly potent A_{2A} adenosine receptor inverse agonists with antinociceptive activity, J. Med. Chem. 59 (2016) 10564-10576.
16. D. Poli, M. Falsini, F. Varano, M. Betti, K. Varani, F. Vincenzi, A.M. Pugliese, F. Pedata, D. Dal Ben, A. Thomas, I. Palchetti, F. Bettazzi, D. Catarzi, V. Colotta. Imidazo[1,2-a]pyrazin-8-amine core for the design of new adenosine receptor antagonists: Structural exploration to target the A_3 and A_{2A} subtypes, Eur. J. Med. Chem, 125 (2017) 611-628.
17. L. Squarcialupi, M. Betti, D. Catarzi, F. Varano, M. Falsini, A. Ravani, S. Pasquini, F. Vincenzi, V. Salmaso, M. Sturlese, K. Varani, S. Moro, V Colotta. The role of 5-arylalkylamino- and 5-piperazino- moieties on the 7-aminopyrazolo[4,3-*d*]pyrimidine core in affecting adenosine A_1 and A_{2A} receptor affinity and selectivity Profiles, J. Enz. Inhib. Med. Chem. 32 (2017) 248-263.

18. M. Falsini, L. Squarcialupi, D. Catarzi, F. Varano, M. Betti, D. Dal Ben, G. Marucci, M. Buccioni, R. Volpini, T. De Vita, A. Cavalli, V. Colotta, The 1,2,4-triazolo[4,3-a]pyrazin-3-one as a versatile scaffold for the design of potent adenosine human receptor antagonists. Structural investigations to target the A_{2A} Receptor, J. Med. Chem. 60 (2017) 5772-5790.
19. F. Varano, D. Catarzi, M. Falsini, F. Vincenzi, S. Pasquini, K. Varani, V. Colotta, Identification of novel thiazolo[5,4-d]pyrimidine derivatives as human A_1 and A_{2A} adenosine receptor antagonists/inverse agonists, Bioorg. Med. Chem. 26 (2018) 3688-3695.
20. F. Varano, D. Catarzi, F. Vincenzi, M. Falsini, S. Pasquini, P.A. Borea, V. Colotta, K. Varani, Structure-activity relationship studies and pharmacological characterization of N5-heteroarylalkyl-substituted-2-(2-furanyl)thiazolo[5,4-d]pyrimidine-5,7-diamine-based derivatives as inverse agonists at human A_{2A} adenosine receptor, Eur. J. Med. Chem. 155 (2018) 552-561.
21. F. Varano, D. Catarzi, M. Falsini, D. Dal Ben, M. Buccioni, G. Marucci, R. Volpini, V. Colotta, Novel human adenosine receptor antagonists based on the 7-amino-thiazolo[5,4-d]pyrimidine scaffold. Structural investigations at the 2-, 5- and 7-positions to enhance affinity and tune selectivity, Bioorg. Med. Chem. Lett. 29 (2019) 563-569.
22. M. Falsini, D. Catarzi, F. Varano, D. Dal Ben, G. Marucci, M. Buccioni, R. Volpini, L. Di Cesare Mannelli, C. Ghelardini, V. Colotta, Novel 8-amino-1,2,4-triazolo[4,3-a]pyrazin-3-one derivatives as potent human adenosine A_1 and A_{2A} receptor antagonists. Evaluation of their protective effect against □-amyloid-induced neurotoxicity in SH-SY5Y cells, Bioorg. Chem. 87 (2019) 380-394.
23. M. Betti, D. Catarzi, F. Varano, M. Falsini, K. Varani, F. Vincenzi, S. Pasquini, L. Di Cesare Mannelli, C. Ghelardini, E. Lucarini, D. Dal Ben, A. Spinaci, G. Bartolucci, M. Menicatti, V. Colotta, Modifications on the amino-3,5-dicyanopyridine core to obtain multifaceted adenosine receptor ligands with antineuropathic activity, J. Med. Chem. 62 (2019) 6894-6912.

24. M. Falsini, D. Catarzi, F. Varano, C. Ceni, D. Dal Ben, G. Marucci, M. Buccioni, R. Volpini, L. Di Cesare Mannelli, E. Lucarini, C. Ghelardini, G. Bartolucci, M. Menicatti, V. Colotta, Antioxidant-conjugated 1,2,4-triazolo[4,3-a]pyrazin-3-one derivatives: highly potent and selective human A_{2A} adenosine receptor antagonists possessing protective efficacy in neuropathic pain, J. Med. Chem. 62 (2019) 8511-8531.
25. A. Bonardi, M. Falsini, D. Catarzi, F. Varano, L. Di Cesare Mannelli, B. Tenci, C. Ghelardini, A. Angeli C.T. Supuran, V. Colotta, Structural investigations on coumarins leading to chromeno[4,3-c]pyrazol-4-ones and pyrano[4,3-c]pyrazol-4-ones: new scaffolds for the design of the tumor-associated carbonic anhydrase isoforms IX and XII, Eur. J. Med. Chem. 146 (2018) 47-59.
26. M. Falsini, L. Squarcialupi, D. Catarzi, F. Varano, M. Betti, L. Di Cesare Mannelli, B. Tenci, C. Ghelardini, M. Tanc, A. Angeli, C.T. Supuran, V. Colotta, 3-Hydroxy-1H-quinazoline-2,4-dione as a new scaffold to develop potent and selective inhibitors of the tumor-associated carbonic anhydrases IX and XII, J. Med. Chem. 60 (2017) 6428-6439.
27. A. Karioti, F. Carta, C.T. Supuran, Phenol and poliphenols as carbonic anhydrases inhibitors, Molecules, 21 (2016) 1649.
28. V.S. Matiychuk, M.A. Potopnyk, R. Luboradzki, M.D. Obushak, A New method for the synthesis of 1-aryl-1,2,4-triazole derivatives, Synthesis 11 (2011) 1799–1803.
29. M. Scobie, O. Wallner, T. Koolmeister, K.S.A. Vallin, C.M. Henriksson, S. Jacques, E. Homan, T. Helleday, Diaminopyrimidines as MTH-1 inhibitors for treatment of cancer and their preparation, WO 2015187088, A1 20151210
30. E.-D. Chenot, D. Bernardi, A. Comel, G. Kirsch, Preparation of monoalkyl terephthalates: an overview, Synth. Comm. 37 (2007) 483-490.
31. R. Guillon, F. Pagniez, F. Giraud, D. Crepin, C. Picot, M. LeBorgne, F. Morio, M. Duflos, C. Loge, P. LePape, Design, synthesis, and in vitro antifungal activity of 1-[(4-Substituted-

benzyl)methylamino]-2-(2,4-difluorophenyl)-3-(1H-1,2,4-triazol-1-yl)propan-2-ols, Chem.Med.Chem, 6 (2011) 816-825.

32. G.W. Hardy, L.A. Lowe, G. Mills, P.Y. Sang, D.S.A. Simpkin, R.L. Follenfant, C. Shankley, T.W. Smith, Peripherally acting enkephalin analogues. 2. Polar tri- and tetrapeptides, J. Med. Chem. 32 (1989) 1108-1118.
33. T. Weinert, N. Olieric, R. Cheng, S. Brunle, D. James, D. Ozerov, D. Gashi, L. Vera, M. Marsh, K. Jaeger, F. Dworkowski, E. Panepucci, S. Basu, P. Skopintsev, A.S. Dore, T. Geng, R.M. Cooke, M. Liang, A.E. Prota, V. Panneels, P. Nogly, U. Ermler, G. Schertler, M. Hennig, M.O. Steinmetz, M. Wang, J. Standfuss, Serial millisecond crystallography for routine room-temperature structure determination at synchrotrons, Nat. Commun. 8 (2017) 542.
34. Molecular Operating Environment, C.C.G., Inc., 1255 University St., Suite 1600, Montreal, Quebec, Canada, H3B 3X3.
35. G. Jones, P. Willett, R.C. Glen, A.R. Leach, R. Taylor, Development and validation of a genetic algorithm for flexible docking, J. Mol. Biol. 267 (1997) 727-748.
36. A. Nocentini, M. Ferraroni, F. Carta, M. Ceruso, P. Gratteri, C. Lanzi, E. Masini, C.T. Supuran, Benzenesulfonamides incorporating flexible triazole moieties are highly effective carbonic anhydrase inhibitors: synthesis and kinetic, crystallographic, computational, and intraocular pressure lowering investigations, J. Med. Chem. 59 (2016) 10692e10704.
37. J. Leitans, A. Kazaks, A. Balode, J. Ivanova, R. Zalubovskis, C.T. Supuran, K. Tars, Efficient expression and crystallization system of cancer-associated carbonic anhydrase isoform IX, J. Med. Chem. 58 (2015) 9004e9009.
38. D.A. Whittington, A. Waheed, B. Ulmasov, G.N. Shah, J.H. Grubb, W.S. Sly, D.W. Christianson. Crystal structure of the dimeric extracellular domain of human carbonic anhydrase XII, a bitopic membrane protein overexpressed in certain cancer tumor cells. Proc. Natl. Acad. Sci. U S A. 2001; 98:9545-50.

39. Schrödinger Suite Release 2019-1, Schrödinger, LLC, New York, NY, 2018: (a) Maestro v.11.9; (b) Epik, v.4.7; (c) Impact, v.8.2; (d) Prime, v.5.5; (e) Macromodel v.12.3. (f) Glide, v.8.2.

40. A. Nocentini, P. Gratteri. C.T. Supuran, Phosphorus versus Sulfur: Discovery of Benzenephosphonamidates as Versatile Sulfonamide-Mimic Chemotypes Acting as Carbonic Anhydrase Inhibitors, Chemistry 25 (2019) 1188-1192.

41. S. Bua, L. Lucarini, L. Micheli, M. Menicatti, G. Bartolucci, S. Selleri, L. Di Cesare Mannelli, C. Ghelardini, E. Masini, F. Carta, P. Gratteri, A. Nocentini, C.T. Supuran, Bioisosteric Development of Multi-target Nonsteroidal Anti-inflammatory Drug - Carbonic Anhydrases Inhibitor Hybrids for the Management of Rheumatoid Arthritis, J. Med. Chem. 2019, doi: 10.1021/acs.jmedchem.9b01130.

42. A. Nocentini, F. Carta, M. Tanc, S. Selleri, C.T. Supuran. C. Bazzicalupi, P. Gratteri, Deciphering the Mechanism of Human Carbonic Anhydrases Inhibition with Sulfocoumarins: Computational and Experimental Studies, Chemistry 24 (2018) 7840-7844.

43. A. Thomas, M. Buccioni, D. Dal Ben, C. Lambertucci, G. Marucci, C. Santinelli, A. Spinaci, S. Kachler, K.-N. Klotz, R. Volpini, The length and flexibility of the 2-substituent of 9-ethyladenine derivatives modulate affinity and selectivity for the human A_{2A} adenosine receptor, Chem. Med. Chem. 11 (2016) 1829-1839.

44. M. Buccioni, C. Santinelli, P. Angeli, D. Dal Ben, C. Lambertucci, A. Thomas, R. Volpini, G. Marucci, Overview on Radiolabel-Free in vitro Assays for GPCRs. Mini Rev. Med. Chem. 17 (2017) 3-14.

45. M. Buccioni, G. Marucci, D. Dal Ben, D. Giacobbe, C. Lambertucci, L. Soverchia, A. Thomas, R. Volpini, G. Cristalli, Innovative functional cAMP assay for studying G protein-coupled receptors: application to the pharmacological characterization of GPR17, Purinerg. Signal. 7 (2011) 463-468.

46. R.G. Khalifah, The carbon dioxide hydration activity of carbonic anhydrase. I. Stop-flow kinetic studies on the native human isoenzymes B and C, J. Biol. Chem. 246 (1971) 2561-2567.
47. M. Ferraroni, F. Carta, A. Scozzafava, C.T. Supuran, Thioxocoumarins show an alternative carbonic anhydrase inhibition mechanism compared to coumarins, J. Med. Chem. 59 (2016) 462-473.
48. A. Scozzafava, F. Briganti, G. Mincione, L. Menabuoni, F. Mincione, C. T. Supuran, Carbonic anhydrase inhibitors: synthesis of water-soluble, aminoacyl/dipeptidyl sulfonamides possessing long-lasting intraocular pressure-lowering properties via the topical route, J. Med. Chem. 42 (1999) 3690-3700.
49. F. Carta, L. Di Cesare Mannelli, M. Pinard, C. Ghelardini, A. Scozzafava, R. McKenna, C. T. Supuran, A class of sulfonamide carbonic anhydrase inhibitors with neuropathic pain modulating effects, Bioorg. Med. Chem. 23 (2015) 1828-1840.